ATTACHMENT A

Responses to the NRC Request for Additional Information

U.S. Department of Energy
National Nuclear Security Administration
Docket No. 71-9355, TAC No. L24741
Certificate of Compliance No. 71-9355
Model No. 435-B

By letter dated November 21, 2013, the NRC requested additional information on the stated application. The requested information, followed by the NNSA response, is supplied below.

Materials Evaluation

RAI - 1 Describe the "metallic structures" and "polymeric foam" materials used for blocking/dunnage. Also, describe the functionality of these materials.

Section 1.2.2.2, "Shielded Devices," page 1.2-8 of the SAR states, "Blocking/dunnage materials are metallic structures or polymeric foam." These materials are not listed in the "Bill of Materials," these are only referred to in a general sense in SAR.

This information is needed to ensure compliance with 10 CFR 71.33(a)(5).

Response: As stated in Section 7.1.2.2, Step 7a, the blocking/dunnage material: "...shall be structural metal such as aluminum, stainless steel, or carbon steel in a welded or bolted configuration, or it may be made from blocks of polymeric foam. Polymeric foam dunnage shall be rigid, closed-cell, and have a decomposition temperature greater than or equal to 400 °F." The purpose of the blocking/dunnage is to locate the shielded device inside the inner container (IC) during transport and to prevent unwanted movement due to transport vehicle accelerations. The blocking/dunnage does not have a safety function. Structurally, the 435-B package containment function is not dependent on blocking/dunnage performance. As demonstrated during certification testing and illustrated in Figure 2.12.3-37, in which a maximum weight dummy shielded device impacted and cut the inner container wall but did not damage the containment boundary, the primary means of ensuring the integrity of containment against damage from the shielded device is the inner container structure, not the blocking/dunnage. Further, the integrity of the shielded devices against the impacts resulting from the HAC free drop is evaluated in Section 2.7.1.6, where it is shown that the sources will remain securely located within the shielded shipping position. Thermally, the blocking/dunnage does not have a significant impact on temperatures. However, behavior of foam dunnage is important to the pressurization in the HAC fire event. Since the thermal analysis of maximum pressure assumes a specific offgassing behavior, the blocking/dunnage, if made of foam, will be required to be of the same type as that analyzed, General Plastics polyurethane foam FR3700. From a shielding perspective, blocking/dunnage is not needed to maintain package external dose rates. As stated in Section 7.1.2.2.1 and Section 7.1.2.2.2, the devices are required to have a dose rate on the surface and at one meter which is no higher than that required by regulation for the package. Since the device is inside the package, the package dose rates are automatically met. Therefore, since the blocking/dunnage material is not safety related, it does not need to be detailed in the Bill of Materials.

To clarify the purpose of the blocking/dunnage material, several changes to the SAR have been made:

- The second paragraph of Section 1.2.2.2 has been revised to read: "All shielded devices are placed into the inner container for shipment in the 435-B, described in Section 1.2.1.7, *Inner Container*, and blocked in position using dunnage materials. Blocking/dunnage materials are metallic structures or polyurethane foam, and are described in Section 7.1.2.2, *Loading the Inner Container (IC)*. The blocking/dunnage is used to prevent unwanted motion during normal transport, and does not provide a safety function. Cabinets, stands, or unnecessary appurtenances are not transported. Prior to loading, movable sources are placed in the safe shipping position, the structural integrity is evaluated, and a radiation survey is performed. More information is provided in Section 7.1.2.2, *Loading the Inner Container (IC)*."

- Step 7(a) of Section 7.1.2.2 has been revised to read: "Prepare the blocking/dunnage. Dunnage shall be structural metal such as aluminum, stainless steel, or carbon steel in a welded or bolted configuration, or it may be made from blocks of Series FR3700 polyurethane foam, manufactured by General Plastics Manufacturing Company, Tacoma, WA. Polyurethane foam dunnage shall be rigid, closed-cell, and have a decomposition temperature greater than or equal to 435 °F. The total weight of all dunnage material must be less than or equal to 500 lb." (Note: the increase of the foam decomposition temperature from 400 °F to 435 °F is discussed in the response to RAI-18.)

- Step 7(d)(iii) of Section 7.1.2.2 has been revised to read: "If using polyurethane foam as dunnage,..."

- The last sentence of the second paragraph of Section 3.1.1.2 has been revised to read: "Acceptable blocking/dunnage materials are metallic structures or polyurethane foam as defined in Section 7.1.2.2, *Loading the Inner Container (IC)*."

- The following text has been added to the end of the last paragraph of Section 5.5.3.3.1: "Prior to transport, each device will be surveyed. Only devices with a surface dose rate of 200 mrem/hr, or less, and a dose rate at a distance of one meter from the surface of 10 mrem/hr, or less, will be transported."

RAI - 2 Provide the specifications of the cast iron shell that surrounds the shielding material.

Section 1.2.2.2, "Shielded Devices," page 1.2-7 of the SAR states, "Each such [shielded] device includes a sealed source (or group of sources), shielding material, and a steel or cast iron shell to surround the shielding material and provide structure. Nevertheless, the specifications of the cast iron shell are not provided.

This information is needed to ensure compliance with 10 CFR 71.33(a)(5).

Response: Cast iron material is used for a portion of the GC-40 (Group 3) device. With reference to SAR Figure 2.7-2, the GC-40 consists of an inner, 3-inch diameter tube which contains the source drawer, an outer cylindrical shell made of 0.38-inch thick carbon steel, two flat ends made of 1-inch thick carbon steel, and, on a transverse axis, inner and outer conical shells. The inner conical shell is clearly shown in Figure 2.7-2, and is cast in one piece with the large flange (shown in the figure as having a diameter of 24.7 inches). The outer conical shell is not clearly shown in Figure 2.7-2, but is shown in the photograph of Figure 1.2-16. The outer conical shell is made of 0.38-thick carbon steel. Thus, only the inner conical shell and associated flange are made of cast iron, and the rest is carbon steel. The GC-40 has been designed and manufactured by a third party, and the specification of the cast iron is not available. Section 2.7.1.6.2 has been revised to discuss the effect of the HAC free drop on the integrity of the GC-40 shells. In addition, Section 1.2.2.2 and Section 2.7.1.6 have been revised to clarify the incidence of cast iron in the devices.

- The following has been added after the last paragraph of Section 2.7.1.6.2: "As noted in Section 1.2.2.2, a limited portion of the shell of the GC-40 is made from cast iron. With reference to Figure 2.7-2, the shells of the GC-40 consist of an outer cylindrical shell made of 0.38-inch thick carbon steel, two flat ends made of 1-inch thick carbon steel, and, on a transverse axis, inner and outer conical shells. The inner conical shell is clearly shown in Figure 2.7-2, and is cast in one piece with the large flange (shown in the figure as having a diameter of 24.7 inches). The outer conical shell is partially shown in Figure 2.7-2, but is more clearly shown in the photograph of Figure 1.2-16. The outer conical shell is made of 0.38-thick carbon steel. Thus, only the inner conical shell and associated flange are made of cast iron, and the rest is carbon steel. In the shipping position, the source is located in the cylindrical shell portion of the device. The device is well protected by the blocking/dunnage, the inner container, and the 435-B package. In the unlikely event of a non-ductile response of the cast portion of the shell to an HAC free drop, the carbon steel in the remainder of the shell will keep the device intact, and shielding of the source will be unaffected."

- The second sentence of Section 1.2.2.2 has been revised to read: "Each such device includes a sealed source (or a group of sources), shielding material, and a steel shell to surround the shielding material and provide structure (a limited portion of the GC-40 shell includes cast iron)."

- The fifth sentence of Section 2.7.1.6 has been revised to read: "The main structural members of the devices are made of carbon steel, stainless steel, or, in the case of the GC-40, a limited portion of cast iron."

RAI - 3 Explain and discuss Figure 1.1-3, "435-B Package with Shielded Device," on page 1.1-4 of the SAR. Include a description of the shielded device.

Based on Figure 1.1-3, describe the following in detail:

1. loading process of the,
    a. shielded device into the inner container, and
    b. "blocking/dunnage" material and fitting into the inner container,
2. positioning the shielded device in the inner container, and
3. the configuration of the shielded device unit.

This information is needed to ensure compliance with 10 CFR 71.33(a)(5).

Response: Figure 1.1-3 is meant to represent all of the shielded devices inside the inner container inside the 435-B packaging. The figure represents schematically the generalized arrangement of blocking/dunnage and the shielded device contents. Since several different shielded devices may be shipped in the package and different blocking/dunnage arrangements may be used, the figure must be schematic. The shielded devices are described in detail in Section 1.2.2.2 and Table 1.2-2.

1. The process of loading the shielded device into the inner container is discussed in Section 7.1.2.2, Step 7. This includes the loading of any blocking or dunnage that may be needed. Precise construction of the blocking/dunnage is not specified, since the blocking/dunnage is not a safety-related material as stated in the response to RAI – 1.
2. The lateral and axial positioning of the shielded device and the orientation of its axis is discussed in Step 7d of Section 7.1.2.2.
3. The shipping configuration of each device is discussed in Sections 7.1.2.2.1 and 7.1.2.2.2.

RAI - 4 Discuss and describe the following materials in the context of the SAR, Drawing 1916-01-01-SAR:

	Material	SAR Reference
a.	Nuclear grade duct tape	Note 27 of Drawing 1916-01-01-SAR, sheet 1 of 7 of the SAR states, "A weather seal or *nuclear grade duct tape* may be used to cover joints as shown."
b.	Silicone adhesive	Note 35 of Drawing 1916-01-01-SAR, sheet 2 of 7 of the SAR states, "Attach I/N 18 (insulation sheet) to impact limiter shell using *silicone adhesive.*"
c.	Approved tape	Note 41 of Drawing 1916-01-01-SAR, sheet 2 of 7 of the SAR states, "*Approved tape* may be used during installation."

This information is needed to ensure compliance with 10 CFR 71.33(a)(5).

Response: A discussion of the listed items follows:

a. Nuclear Grade Duct Tape is obtained from 3M Company. It is intended for applications on stainless steel in the nuclear industry. The critical characteristic for the 435-B is a low level of leachable halides and sulfur for protection against corrosion. To better define this material, Note 27 of Drawing 1916-01-01-SAR has been revised to read: "A weather seal or nuclear grade duct tape (3M Company Part No. 8979N or equivalent tape meeting MIL-STD-2041D(SH), Notice 2) may be used to cover joints as shown."

b. The silicone adhesive is used to adhere the item 18 insulation sheet to the bottom inside surface of the external impact limiter prior to installation of the polyurethane foam, which helps to ensure proper placement of the sheet until the foam has solidified. Once the foam has solidified, the silicone adhesive has no function. Thus, the silicone adhesive has no safety function, and does not require a detailed specification. To clarify the requirement for the silicone adhesive, Note 35 of Drawing 1916-01-01-SAR has been revised to read: "Attach I/N 18 (insulation sheet) to impact limiter shell using commercial silicone adhesive."

c. Note 41 identifies that tape may be used to hold the insulation pieces in place while installing the protective shell, item 26. Once the item 26 shell is in place, the tape has no function. Hence, the tape has no safety function, and does not require a detailed specification. To clarify the requirement for the tape, Note 41 of Drawing 1916-01-01-SAR has been revised to read: "Item 18 may be supplied in up to 3 pieces. Commercial adhesive tape may be used to hold item 18 in place while installing items 18 and 26."

RAI - 5 Define "or equivalent."

Item 18, Specification of Drawing 1916-01-01-SAR, sheet 1 of 7, and Item 10

Specification of Drawing 1916-01-03-SAR, sheet 1 of 2, of SAR state, "Lytherm Grade 1530-L *or equivalent.*" Item 33 Specification of Drawing 1916-01-01-SAR, sheet 2 of 7, of SAR states, "Wedge Products, Inc. *or equivalent.*" Note 7 of Drawing 1916-01-02-SAR, sheet 1 of 2, of SAR states, "...Loctite 30537 contact adhesive *or equivalent.*"

This information is needed to ensure compliance with 10 CFR 71.33(a)(5).

Response: In each case, the words "or equivalent" have been supplemented by a drawing note which specifies the minimum requirements of the equivalent material or part. Specifically:

- Item 18 of Drawing 1916-01-01-SAR and item 10 of Drawing 1916-01-03-SAR identify ¼" thick Lytherm paper. Flag notes (51 and 14, respectively) have been added to the item line in each case which states: "Equivalent material must be a refractory material made primarily from alumina silica fibers with a minimum melting point of 2000 °F."

- Item 33 of Drawing 1916-01-01-SAR identifies a small cup made of stainless steel that closes off the bolt holes in the lower flange and the alignment pin holes in the upper flange. Flag note 52 has been added to item 33 which states: "Equivalent item must be made of austenitic stainless steel with a nominal inside diameter of 1.66 inches and a nominal inside depth of 13/16 inches."

- Flag note 7 of Drawing 1916-01-02-SAR identifies an adhesive for use in affixing the neoprene sheet parts (I/N 13) to the lodgment. Flag note 7 has been revised to read: "Attach neoprene items to weldment using Loctite 30537 or other air-drying contact adhesive designed to adhere rubber to metal."

RAI - 6 Discuss the fabrication or construction of vent or seal test port insulation cylinder, include joint design and method of assembly.

a. Discuss how Item 36 wire is welded to Item 25.
b. Discuss how Item 25 is welded to Item 35.
c. Discuss if degradation of Item 37 wool is a concern due to heat from welding.

The *Vent and Seal Test Port Insulation Cylinder (A5)* depicted on Drawing 1916-01-01-SAR, sheet 6 of 7, of SAR shows Item 36 welded as part of the cylinder fabrication.

This information is needed to ensure compliance with 10 CFR 71.33(a)(5).

Response:

a. Item 36 wire is inserted through two holes in the upper item 25 and welded to the underside of item 25 using an all-around fillet weld before installing item 25 into the assembly. The minimum fillet size, per note 26, is the smaller of the thicknesses of item 25 or item 36, which is 1/16 inch.

b. Item 25 is set into item 35 at the top and the bottom by a small amount to permit the specified fillet weld to be made around the inside surface of item 35.

c. The amount of heat deposited in the components by these small welds is negligible. Furthermore, mineral wool is both heat resistant and a poor conductor of heat. An effect on the material (if any) due to the welding would be only very local, since the heat would not travel any appreciable distance into the wool.

To clarify the construction of the cylinder, the following text has been inserted before the last sentence of the third paragraph of Section 1.2.1.3: "The port insulation cylinder is made from a 2-inch diameter, 0.06-inch wall thickness stainless steel tube, closed at both ends with a 0.06-inch thick disk of stainless steel, and filled with mineral wool. Each disk is attached using a 1/16-inch all-around fillet weld. A 1/8-inch diameter wire loop is fillet welded to the top disk for handling."

RAI - 7 Explain whether Section Y-Y weld symbol is used correctly.

Section Y-Y of Drawing 1916-01-01-SAR, sheet 7 of 7, of the SAR shows Item 12 welded to Item 31 using 1/16-inch fillet weld, 1/2-inch long, 2-inch on center *and* "all around."

This information is needed to ensure compliance with 10 CFR 71.33(a)(5).

Response: According to AWS D2.4, this is a correct weld symbol. The symbol requires an intermittent weld around the inside circumference of the tube. The tube ID is nominally $2.0 - 2 \times 0.035 = 1.93$ inches, or a circumference of $1.93\pi = 6.06$ inches. Thus, there will be three, ½-inch long welds, equally spaced around the circumference. The all-around circle does not imply a continuous weld, but only that the required weld (intermittent in this case) is a closed loop.

RAI - 8 Discuss the pouring method of polyurethane foam (15 pounds per cubic feet (lb/ft^3), Item 19 of Drawing 1916-01-01-SAR, Section E-E, on sheet 4 of 7) into the external impact limiter. Include the following in your discussion:

a. the process to ensure uniform density throughout the polyurethane foam material once it is poured;
b. explain if the foam expands once it is poured;
c. the pour capped off process and explain if a weld is used for closure of the external impact limiter; and
d. explain if the heat, due to the weld, is a possible issue for the degradation of the polyurethane foam material.

Section 1.2.1.2, page 1.2-2, of the SAR states that "...The cavity of the limiter is filled with 15 lb/ft^3 polyurethane foam. The foam is rigid, closed-cell, and is *poured in place.*"

This information is needed to ensure compliance with 10 CFR 71.33(a)(5).

Response: a. Polyurethane foam is created by mixing liquid constituents along with a blowing agent. The liquid foam is poured into the impact limiter shell, and the chemical reaction with the blowing agent creates the bubbles as the material expands and hardens into the final product. Chemicals are mixed using a controlled procedure to ensure complete liquid uniformity. The test specimens are taken from the same stream that is filling the shell. The test specimens are used to confirm that the foam density and crush strength are within specified limits. More than one pour, or 'lift', may be used to fill an impact limiter shell. Each such pour has its own data set, which must meet the specification described in Chapter 8 of the SAR. Much more detail about the process and the required properties of the polyurethane foam is provided in Section 8.1.5.1, *Polyurethane Foam.*

b. Polyurethane foam expands after pouring due to chemical reactions within the liquid foam, and it fills the entire impact limiter shell.

c. The foam is poured and visually monitored through three, 5-inch diameter holes in the bottom of the external impact limiter (the shell of the limiter is inverted for foam installation). Once the foam has hardened, a small amount of excess foam is cut away from the pouring holes such that a flat closure plate can be set in place on top of a backing ring which is present around the hole's perimeter. As shown on SAR Drawing 1916-01-01-SAR, sheet 4, zone A-7, a CJP weld to the main bottom sheet, and against the backing ring, secures the closure plate.

d. Experience over many years of use of poured-in-place polyurethane foam has shown that adjacent to a weld bead (for welds performed after foam installation), a small zone of darkened foam shows the effect of weld heat. However, the darkening is superficial and the zone of darkening is small (typically less than one inch on either side of the weld), and actual damage, if any, is limited to a region essentially the size of the weld bead. The thermal conductivity of the material is very low (essentially the same as that of still air), which limits the heat flow into the material. The material is flame-retardant, preventing any propagation of local heat damage. Furthermore, post-pour welding is only done on the closure plates, not on any of the other seams in the shell, which limits the extent of the phenomenon to a very small area. This method of closing off the foam installation holes has been used successfully for nearly 30 years, starting with the 125-B (NRC Docket 71-9200) and the TRUPACT-II (NRC Docket 71-9218), and more recently, the MFFP (NRC Docket 71-9295) and the BEA Research Reactor Package (NRC Docket 71-9341).

RAI - 9 Describe where the fifth row of tubes, consisting of 22 tubes, is located in Drawing 1916-01-01-SAR, sheet 7 of 7.

Section 1.2.1.4, page 1.2-4, of the SAR states that "...The fifth row of tubes (consisting of 22 tubes at a radius of 12.5 inches) is slightly longer than the other rows..."

This information is needed to ensure compliance with 10 CFR 71.33(a)(5).

Response: Detail V and Note 44 on drawing 1916-01-01-SAR indicate the fifth concentric row. The open ends of the whole array of tubes forms a spherical surface which corresponds to the internal spherical surface of the torispherical heads. The fifth concentric row at a radius of 12.5 inches extends slightly above the other rows of tubes, and thus, forms the load path from the payload, through the lower internal impact limiter, and into the lower torispherical head under normal operating conditions. The other rows of tubes normally do not contact the lower head. This can be seen in the isometric view in the referenced Detail V. To clarify this, Section 1.2.1.4 has been revised to read: "The fifth concentric row of tubes extends slightly above the adjacent rows of tubes, thus supporting the payload under normal operation."

RAI - 10 Explain how Items 6 and 13 (neoprene sheets) of Drawing 1916-01-02-SAR, sheet 1 of 2, are used in the LTSS Lodgment (A1). Include the following in your explanation:

a. the purpose of these neoprene sheets;
b. location of the neoprene sheets in the LTSS Lodgment - Referring to Note 7 of the drawing, "Attach neoprene items to weldment..."; and
c. the steps for attaching the neoprene items (e.g., cut-to-fit).

View B-B and Section D-D of Drawing 1916-01-02-SAR, sheet 2 of 2, show neoprene sheets being used.

This information is needed to ensure compliance with 10 CFR 71.33(a)(5).

Response:

a. The purpose of the neoprene sheets is to provide a resilient surface between the LTSS and the lodgment to protect the LTSS from handling damage. The neoprene sheets do not have any safety function. To improve clarity, the sentence in Section 1.2.1.5 which reads in Revision 0, "Rubber is also used on the tapered edges of the lower ribs, but there is nominally no contact between lodgment ribs and the LTSS." has been revised to read, "Rubber is also used on the angled edges of the upper and lower ribs to protect the surface of the LTSS, but there is nominally no contact between lodgment ribs and the LTSS. The neoprene rubber has no safety function."

b. The neoprene sheets are not subject to any welding heat or other potentially degrading environment since they are applied to the weldment as a last step.

c. The neoprene is cut to fit and glued in place using the stated adhesive in Note 7 of 1916-01-01-SAR.

RAI - 11 Discuss "Bill of Materials" for LTSS. Provide reasoning for not listing the "Bill of Materials" in any of the drawings for the LTSS and LTSS Source Drawers.

The materials used for the LTSS are mentioned in the SAR text, Section 1.2.1.6, page 1.2-5. However, specifications are not referenced on the stainless steel or lead used in the LTSS. Additionally, specifications are not used for drawer materials: cap screws, lead, brass, tungsten, and depleted uranium.

This information is needed to ensure compliance with 10 CFR 71.33(a)(5).

Response: A materials list for the LTSS has been added to Figure 1.2-9, and a materials list for the large source drawer has been added to Figure 1.2-10. The T80/T780 source drawer (Figure 1.2-11) design drawings and material specifications are not available. However, a specimen of this drawer was sectioned down the mid-plane, and the data was used in the shielding calculation. As stated in the response to RAI-12, the T80 and T780 drawers are dimensionally identical, but where the T80 drawer only uses lead shielding, the T780 drawer may optionally use tungsten or depleted uranium instead of lead. As stated in the last paragraph of Section 5.3.1, the shielding analysis conservatively used lead, since tungsten or depleted uranium are better shielding materials. To clarify the modeling of the various shielding materials used in the payloads, the last paragraph of Section 5.3.2 has been revised to read: "The T80 and T780 source drawers have the same dimensions. The T80 uses lead, while the T780 may use lead, tungsten, or depleted uranium. Since the density of tungsten (17 g/cm^3) and of depleted uranium (18.95 g/cm^3) are greater than the density of lead (11.35 g/cm^3), lead is conservatively used in the analysis. The T80/T780 drawer tube is modeled as brass with a density of 8.07 g/cm^3, and the composition of brass is provided in Table 5.3-9 [7]."

Structurally, the T80/T780 source drawers are held inside the barrel of the LTSS, which does not deform in the HAC free drop. Since the cavity in the barrel is only slightly larger than the source drawer, the drawer cannot reconfigure due to impact, and the shielding function of the drawer is not affected.

RAI - 12 Clarify the differences between the T80 and T780 Source Drawer. Explain if the T780 can be qualified as a T80 drawer, since it also uses lead as a shielding material.

Section 1.2.1.6, page 1.2-6 states, "The T80 and T780 drawers are physically identical...For the T80 drawer, the shielding on each side of the source is 9.2 inches of lead. For the T780 drawer, the shielding may be either *lead*, tungsten, or depleted uranium." If the T80 and T780 drawers are physically identical, the only difference being the side shielding materials.

This information is needed to ensure compliance with 10 CFR 71.33(a)(5).

Response: To clarify the SAR, the statement in Section 1.2.1.6 and in the last paragraph of Section 5.3.1 which reads: "The T80 and T780 drawers are physically identical..." has been changed to read: "The T80 and T780 drawers are dimensionally identical...". In addition, Figure 1.2-11 has been revised to indicate that tungsten and depleted uranium may be optionally used in the T780 drawer.

RAI - 13 Clarify if a neutron shielding material is used in the LTSS to transport a neutron source. If a neutron source is transported in the LTSS, describe the shielding material used in this case.

Section 1.1, page 1.1-1 of the SAR states, "The LTSS may transport gamma sources (the majority of the sources in the LTSS), beta sources, *and very small neutron sources.*"

This information is needed to ensure compliance with 10 CFR 71.33(a)(5).

Response: As stated in SAR Section 1.2.1.14, "Biological shielding of gamma radiation is provided by lead located in the LTSS or in the shielded devices. No other components whose primary purpose is shielding are included in the 435-B." Thus, the 435-B package does not contain any material whose principal purpose is neutron shielding. The neutron shielding dose rates calculated in Chapter 5 of the SAR are based on the natural attenuation of neutrons as they pass through the metallic materials of construction and by distance from the source. Since these materials do not have a significant effect on neutrons, the allowable activity of any neutron sources in the package is relatively low. However, some attenuation of neutrons does occur as stated, which makes it possible to transport very small neutron sources while dose rates remain below regulatory limits. The limiting values for neutron sources are defined in Table 1.2-1.

Structural Evaluation

RAI - 14 Provide a margin of safety for the remaining torque on the closure bolts in the cold condition.

The applicant provides calculations showing a reduction in closure bolt preload under the cold condition and states that a large positive preload exists under normal conditions of transport. The applicant did not provide a comparison to demonstrate that this large preload was sufficient when compared with an allowable value.

This information is necessary to determine compliance with 10 CFR 71.71(c)(2).

Response: A margin of safety calculation has been added which shows that the remaining bolt preload at cold temperature is sufficient to retain the seal compression against the maximum vibration loading.

The last sentence of Section 2.6.2 has been deleted. A new paragraph has been added to the end of Section 2.6.2 as follows: "As shown in Section 2.6.5, *Vibration*, a loading in the vertical (i.e., axial) direction of ± 2g can result from transportation vibration. From Table 2.1-2, the weight of the upper body assembly (bell) is 2,670 lb. Thus, to keep the bell seated on the lower flange (and the containment seal properly compressed), the sum of preload forces in the closure bolts must be at least equal to the upward vertical vibration load on the bell of 2,670 × 2 = 5,340 lb. Since there are 24 closure bolts, each bolt needs to have a minimum preload of 5,340 / 24 = 222.5 lb. Since the remaining preload in the -40 °F case is 9,640 lb per bolt, the margin of safety is:

$$(9{,}640/222.5 - 1) = +42.3$$

Thus the remaining preload force per bolt is adequate to maintain the joint and containment seal in a closed and leak tight configuration for the 10 CFR §71.71(c)(2) Cold condition."

RAI - 15 Clarify if the package penetration test was performed. If it was not performed, provide further justification demonstrating why the test was not necessary. Also, the language in the safety analysis report (SAR) should be revised to clearly state if this test was performed or not.

The applicant states the following in its SAR:

"The impact of a 1.25-inch diameter, hemispherically ended, 13-pound steel bar, per 10 CFR §71.71 (c)(10), dropped vertically from a height of 40 inches, has no significant effect on the 435-B package. Slight denting of the thermal shield on the outside of the cask <u>can</u> occur, but the bar cannot penetrate or rip into the shield, and <u>cannot</u> harm the impact limiter nor damage the ½-inch rain shield attachment bolts. Therefore, this test has no significant effect on the package."

This information is necessary to determine compliance with 10 CFR 71.71(c)(10).

Response: The package penetration test was not physically performed. Section 2.6.10 has been revised to read: "Section 10 CFR §71.71(c)(10) requires the impact of the hemispherical end of a vertical steel cylinder having a 1.25-inch diameter and 13 lb mass, dropped from a height of 40 inches onto the exposed surface of the package that is expected to be most vulnerable to puncture. This test was not performed in lieu of the much more demanding HAC puncture tests which were performed as documented in Appendix 2.12.3, *Certification Test Results*. In the HAC puncture tests, a far greater amount of energy was applied to the package, based on the package weight compared to the 13 lb cylinder. The radius of the HAC puncture bar (0.25 inches maximum) is also significantly more damaging than the 0.63-inch radius of the penetration test bar. As documented in Appendix 2.12.3, HAC puncture tests were performed on the package side, the package upper head, the impact limiter shell, and on the rain shield. Subsequent to all of these tests, the containment boundary was shown by test to remain leak tight per ANSI N14.5. The penetration bar of 10 CFR §71.71(c)(10) could impart only a very small fraction of the damage that was imparted by the HAC puncture test. This same demonstration approach has been used in other safety analysis reports, including the TRUPACT-II (NRC Docket 71-9218) and the MFFP (NRC Docket 71-9295). Therefore, the penetration test has no significant effect on the package."

Thermal Evaluation

RAI - 16 Provide the maximum temperature for neoprene in Table 3.1-1, "Maximum NCT and HAC Temperatures with LTSS Payload," of the application.

Page 3.2-4 of the application states that the appropriate temperature range for neoprene is -40°F to 200°F for normal conditions of transport (NCT) and maintaining neoprene below 500°F will prevent significant off-gassing and eliminate any possibility for auto ignition of the material, but the maximum temperature for neoprene during NCT and hypothetical accident conditions (HAC) was not specifically provided in the application.

This information is needed to determine compliance with 10 CFR 71.71 and 71.73.

Response: Neoprene is used only on the LTSS Lodgment. Table 3.1-1, Section 3.3.1.1, Table 3.3-1, Section 3.4.3.1, Table 3.4-1, and Table 3.4-2 have been revised to specifically state the peak neoprene temperatures achieved under NCT and HAC. As seen from these results, the peak temperature achieved by the neoprene is within the allowable long and short-term temperature limits of 200°F and 500°F, respectively.

RAI - 17 Clarify if the maximum normal operating pressure (MNOP) and hypothetical accident conditions pressures in Table 3.1-3, "Summary of Maximum Pressures," of the application capture the gas temperature within the upper and lower internal impact limiters cavity volumes.

The upper and lower internal impact limiter cavity volumes are within the containment boundary and include void spaces filled with air. It appears that the pressure calculations presented in Sections 3.3.2, "Maximum Normal Operating Pressure," and 3.4.3.2, "Maximum HAC Pressures," of the application are based on the cask cavity temperature, which may not bound the upper and lower internal impact limiter gas temperature.

This information is needed to determine compliance with 10 CFR 71.43(c) and (f).

Response: The upper and lower internal impact limiter cavity volumes are included in the determination of the bulk average gas temperature. Section 3.5.3.5, *Bulk Average Gas Temperature*, has been added to the SAR and provides an overview of how the cavity volumes within the upper and lower internal impact limiter are included in the determination of the bulk average gas temperature.

RAI - 18 For the fire initial condition, clarify the assumptions of an initial temperature distribution equivalent to the package at steady state conditions with a 100°F ambient temperature and no insolation.

In Section 3.4.1, "Initial Conditions," page 3.4-2, of the SAR, the applicant assumes, for a fire initial condition, an initial temperature distribution equivalent to the package at steady state conditions, a 100°F ambient temperature, and no insolation. The applicant also states that this assumption complies with the requirement of 10 CFR 71.73(b). This initial condition may be unrealistic. The initial package temperatures at the start of the fire should be higher than 100°F due to solar heating considering that the initial temperature distribution will be a function of the ambient temperature and insolation.

This information is needed to determine compliance with 10 CFR 71.73.

Response: The initial test conditions specified in 10 CFR 71.73(b) addresses only the ambient temperature and is silent on the level of insolation. The NRC has adopted the view that the effects of insolation may be ignored prior to and during the fire (see attached excerpt from the 10 CFR Part 71 Compatibility with the International Atomic Energy Agency Final Rule as published in the Federal Register, Sept. 28, 1995). Paragraph 3.5.5.1 of NUREG-1609 reflects this position by stating that the initial conditions for HAC is "An ambient temperature between 29°C (-20°F) and 38°C (100°F) with no insolation." Therefore, the initial condition evaluated in the SAR is in compliance with both 10 CFR 71 and NUREG-1609. Insolation is considered for the post-fire thermal response of the package.

The appropriateness of the assumed starting condition is further supported by the low thermal mass of the package sidewall which minimizes the HAC impact of higher initial component temperatures due to insolation. As seen from Tables 3.3-1 and 3.3-2, consideration of the maximum insolation loading raises the packaging contents (lodgment and IC and their contents) temperatures by approximately 20°F above the levels resulting from the 100°F ambient assumed by the HAC evaluation. While the outer components, such as the shell and thermal shield temperatures, exhibit a 30 to 80°F temperature difference between the two conditions, the thermal response curves presented in Figures 3.4-1 and 3.4-6 demonstrate that the fire condition recovers the temperature difference for the outer components within the first few moments of fire exposure. Further, since all interior package components exhibit thermal margins much greater than 20°F, the inclusion of insolation effects prior to the fire event would not have impacted the safety basis for the design.

The upper limit for dunnage foam temperature (interior to the IC) has been changed to a value of 435 °F, in order to be consistent with the temperature level given in the third bullet in Section 3.5.4 of the SAR. This change has been made to Section 3.2.2, Table 3.1-2, Section 3.4.3.3, Table 3.4-3, and Section 7.1.2.2. Section 3.4.3 and Table 3.1-3 of the SAR have been revised to include the above discussion of insolation effects in the subsequent evaluation of the safety basis for the design, as recommended by the NRC and IAEA. In addition, the second bullet of Section 3.5.4 has been clarified, and Section 2.7.4.1 and Section 2.7.4.3 have been updated for the slight increase in pressure calculated in Section 3.4.3.4.

RAI - 19 Discuss the impact of modeling internal convection on the maximum temperatures of the containment boundary upper torispherical head during HAC, as well as the impact on the maximum allowable surface temperature without insolation during NCT.

In Section 3.5.3.2, "LTSS and LTSS Lodgment Thermal Model," of the SAR, the applicant discusses the results of a sensitivity study where maximum component temperatures were compared with and without modeling convection between the LTSS and LTSS lodgement. While the impact on the maximum temperature of the source capsule and LTSS lead shielding was discussed, the impact on the maximum temperature of components with less margin, such as the containment boundary upper torispherical head during HAC, and the maximum allowable surface temperature without insolation during NCT should also be addressed.

This information is needed to determine compliance with 10 CFR 71.43(g) and 71.73.

Response: The thermal modeling of convection for the safety evaluation is based on a combination of physics and conservatism. In some cases, a combination of package orientation and heat loading will physically prevent the formation of a convection cell, while in other cases ignoring the potential presence of convection will yield bounding package component temperatures. SAR Section 3.5.3.2 has been revised to clarify the impact of convection on the presented component temperatures. The following paragraphs summarize the added clarification.

The thermal modeling ignores convection heat transfer within the void volume encompassed by the containment's upper torispherical head during both NCT or HAC. This is done for two reasons: one, to most accurately model the real heat transfer in the head, and two, to maximize payload temperatures under NCT and package shell temperatures under HAC. Peak NCT temperatures occur with the upper torispherical head hotter than either the bulk average gas temperature or the upper internal impact limiter. As such, there is no buoyant force to drive convection. Under HAC, the potential contribution of convection within the containment's upper torispherical head void volume depends on the orientation of the package following the pre-fire drop event. However, the assumption of no convection within the containment's upper torispherical head void volume yields the upper torispherical head's peak temperature in either case. Inclusion of convection where it could occur would serve to accelerate heat removal from the torispherical head and lower the SAR predicted peak temperature with little to no change for the payload components.

The sensitivity study conducted without convection between the LTSS and LTSS lodgement was for the NCT condition without insolation. Examination of the results showed that the maximum allowable surface temperature without insolation during NCT did rise 4°F to 121°F. However, as pointed out in SAR Section 3.3.1.1, the peak accessible surface temperature occurs in a very narrow band at the base of the side thermal shields where the closeout welds provide a direct thermal path to the package shell. Beyond this narrow band the accessible surface temperatures are significantly lower. Furthermore, the size of the open areas within the package payload cavity makes a 'no convection' situation a thermal impossibility.

RAI - 20 Clarify how the side drop damage for the shielded device payload described in Section 3.4.3.1, "Side Drop Damage with Shielded Device Payload," of the application produces bounding temperatures for HAC.

The applicant provided HAC temperatures for the shielded device payload based on side drop damage. The applicant did not address how these results would bound the head down drop damage.

This information is needed to determine compliance with 10 CFR 71.73.

Response: As discussed in Section 3.4.3.3, the thermal performance of the 435-B packaging with the shielded device payload under HAC conditions is bounded by those for the LTSS payload due to the higher decay loading of the LTSS payload. Further, as seen by the results for the LTSS payload, the side drop damage scenario results in the highest payload component temperatures over those achieved under the head down drop damage. As such, a separate analysis for the head down drop damage with the shielded device payload is not required to establish either the peak packaging or the peak shielded device payload temperatures under HAC. The text in Section 3.4.3.3 has been revised to include this explanation.

RAI - 21 Provide and include a description of a temperature survey in Section 7.1.3, "Preparation of the 435-B Package for Transport," of the application to verify that the limits specified in 71.43(g) are not exceeded.

In Section 7.1.3, the applicant did not describe a temperature survey to verify that the limits specified in 71.43(g) would not be exceeded.

This information is needed to determine compliance with 10 CFR 71.87(k).

Response: 10 CFR §71.87(k) requires the licensee to ensure that the accessible surface temperature will not exceed the limits of 10 CFR §71.43(g) at any time during shipment. This is best done using the analysis of accessible surface temperature provided in Chapter 3 of the 435-B SAR. The evaluation presented in Chapter 3 is based on well-established heat transfer properties and methodologies. The peak accessible temperature is reported in Table 3.1-1 as 117 °F. This temperature represents only 77% of the temperature difference available to reject the payload decay heat under non-exclusive use (i.e., (117 – 100)/(122 – 100) × 100 = 77%), and occurs over a small region at the base of the side thermal shield. The calculated peak temperature takes into account the maximum decay heat, a steady ambient temperature of 100 °F, and applies to the fully equilibrated condition. Thus, the licensee can rely on the conservative thermal analysis for the fulfilment of the requirement of 10 CFR §71.87(k), and a physical temperature survey is not necessary.

Performing a physical temperature survey is fraught with difficulties. At the time of the survey, the ambient temperature could be less than 100 °F, but could rise during transport, invalidating the initial measurement. In addition, a considerable length of time (days) would be needed before the package would reach thermal equilibrium. During this time, the ambient temperature would be varying through a day-night cycle, and could be changing due to weather conditions. If it is necessary to store the package outdoors, varying solar conditions would come into play. Thus, it would be nearly impossible to take a measurement from the accessible surface of the package that relates in a meaningful way to the requirement of 10 CFR §71.87(k). The only practical way to determine that the requirement of 10 CFR §71.43(g) is met is by the analysis presented in Chapter 3 and by following the loading procedure prescribed in Chapter 7.

RAI - 22 Provide justification for the impact limiter and thermal shield components quality categories given in Table 9.2-2, "QA Categories for Design and Procurement of 435-B Subcomponents," of the application.

The impact limiters (upper, lower, and internal) provide the properties of the materials used for energy absorption are important to the proper function of the impact limiter. The impact limiters and thermal shield are also required to control temperature under accident conditions. NUREG/CR-6407, "Classification of Transportation Packaging and Dry Spent Fuel Storage System Components According to Importance to Safety," provides guidance that the impact limiters and temperature control components should be Category A items.

This information is needed to determine compliance with 10 CFR 71.107(a).

Response: Table 2 of NUREG/CR-6407 gives descriptions of the various classification categories, based on Appendix A of Reg. Guide 7.10. Category A items are those for which "failure of a single item could cause loss [of containment, shielding, or criticality control]." Category B items are those "whose failure or malfunction could indirectly result in a condition adversely affecting public health and safety. The failure of a Category B item, in conjunction with the failure of an additional item, could result in an unsafe condition." Appendix A of Reg. Guide 7.10 adds, "However, an unsafe condition could result only if the primary event occurs in conjunction with a secondary event or other failure or environmental occurrence." It is clear that the failure of the additional item or the occurrence of the secondary event are independent of the primary event, and not a consequence of it, or else there would be no Category B items at all.

For example, the outer shell of a lead-shielded cask does not directly provide containment, shielding, or criticality control, although it is indirectly associated with all of these functions. It is classified, appropriately, as a Category B item in Table 2 of the NUREG. It requires a failure of a second component, such as breach of the containment boundary, for example, to achieve actual loss of containment. In a similar manner, the impact limiter material or thermal shield components of the 435-B have an indirect effect on containment, shielding, and criticality control, and should also be classified as Category B. Their listing as Category A in Table 2 of the NUREG is, in our view, inconsistent with the principle established in Reg. Guide 7.10.

Thus, the classification of the 435-B's impact limiters and thermal shield components as Category B is appropriate. Even though these components are important to the proper functioning of the package, failure of a second component is required before loss of containment or shielding can occur.

Operating Procedures

RAI - 23 Revise the SAR to clearly state compliance with 10 CFR 71.85(a).

Section 7.1.2.2.1, "Preparing Group 1 Devices for Transport," and Section 7.1.2.2.2, "Preparing Group 3 Devices for Transport," state... "Identify any cracks, voids, or corrosion that is significantly deeper than the surface... Any
flaws <u>of this kind</u> disqualify the device for transport." Identifying pinholes and "other defects that could significantly reduce the effectiveness of the package," as specified in 10 CFR 71.85(a), are not included in the types of "flaws" that disqualify the package for transport.

Section 8.1, "Acceptance Tests," states that "Per the requirements of 10 CFR §71.85, this section discusses the inspections and tests to be performed prior to first use of the 435-B packaging." Nevertheless, inspections as specified in 10 CFR 71.85(a) are not clearly discussed.

This information is necessary to determine compliance with 10 CFR 71.85(a).

Response: It is agreed that the shielded devices should comply with 10 CFR 71.85(a). However, it would not be appropriate to apply 10 CFR 71.85(a) *in toto* to the devices by invoking that section by reference. For example, the prohibition of "pinholes" in §71.85(a) is associated with containment, which is not related to any function of the shielded devices. Since the 435-B packaging provides all containment, pinholes should not disqualify a device for transport. Further, since the shielded devices are payloads being transported for storage and disposal, in §71.85 the words "first use" and "packaging" may cause confusion for the package user if applied to the devices. To provide the necessary clarification, the subject operational steps have been revised to use the language of §71.85(a) and to apply it in an appropriate manner to the shielded devices, as follows:

> Section 7.1.2.2.1, Step 5 has been revised to read: "Inspect the device for damage to the body assembly and to structural components that contain the lead shielding or retain the source in a safe position. Visually inspect the weld that retains the shield plug. Any cracks, voids, damage, corrosion that is significantly deeper than the surface, or other defects that could significantly reduce the structural or shielding integrity of the device disqualifies the device for transport."
>
> Section 7.1.2.2.2, Step 5 has been revised to read: "Disassemble the upper head from the sample chamber. Inspect the device for damage to the body assembly and to structural components that contain the lead shielding or retain the source in a safe position. Any cracks, voids, damage, corrosion that is significantly deeper than the surface, or other defects that could significantly reduce the structural or shielding integrity of the device disqualifies the device for transport."
>
> Section 7.1.2.2.2, Step 13 has been revised to read: "Inspect the device for damage to the body assembly and to structural components that contain the lead shielding or retain the source in a safe position. Any cracks, voids, damage, corrosion that is significantly deeper than the surface, or other defects that could significantly reduce the structural or shielding integrity of the device disqualifies the device for transport."

The acceptance tests described in Section 8.1 ensure that the requirements of 10 CFR §71.85(a) are met. These include visual inspections and measurements (discussed in Section 8.1.1), weld inspections (Section 8.1.2), structural and pressure tests (Section 8.1.3), leakage rate tests (Section 8.1.4), and component tests for the polyurethane foam and the containment seal elastomer O-ring (Section 8.1.5). The sole purpose of these inspections and tests is to ensure that the requirements of 10 CFR §71.85(a) are met. To clarify this point, the first two sentences of Section 8.1 has been revised to read: "Per the requirements of 10 CFR §71.85, this section discusses the inspections and tests to be performed prior to first use of the 435-B packaging. Successful completion of these tests will ensure that the requirements of 10 CFR §71.85(a) have been met."

RAI - 24 Revise the SAR to ensure that the torques described in Chapter 7 are reflected in the drawings for the Model No. 435-B, and vice versa.

For example, Section 7.1.4.3, "Loading Drawers into the LTSS," step number 9, mentions a torque ranging from 60 – 70 Newton-meter (44 – 52 feet-pound). Nevertheless, this specific torque cannot be found in the drawings provided in the SAR.

This information is necessary to determine compliance with 10 CFR 71.107(a) and 71.111.

Response: To ensure that the application of the bolt torque value specified in Section 7.1.4.3 Step 9 is clearly understood by the package user, a figure of the LTSS has been added to the end of Section 7.1.4.3 to illustrate the correct application of the specified torque value. All of the remaining tightening torque values used on the packaging are specified both in the SAR drawing notes and in the text of the operating procedure.

Note: The changes made to Section 2.12.3 that were supplied in response to the Request for Supplementary Information dated July 1, 2013, have been included verbatim in Revision 1 of the SAR. (This required an update to one section reference in Section 2.12.4, also included).

Additional Change: Exclusion of americium by air. The following additional change has been made to the 435-B SAR:

In order to comply with the TS-R-1 paragraph 433(c) limit for a Type B package of $3,000A_2$ when transporting by air, americium has been excluded from air transport. Currently, plutonium and greater than 200 Ci of americium are excluded from air transport. The SAR has been revised to exclude both plutonium and americium sources from air transport. The revision will affect SAR Section 1.2.2.1, Section 5.4.5 Step 3 and Examples 2 and 4, Section 7.1.4.1 Step 3, and Section 7.5.1, Examples 2 and 4.

ATTACHMENT B
Delete and Insert Instructions
for
Updating 435-B Package Safety Analysis Report
Docket Number 71–9355

SAR Section	Delete Rev. 0	Insert Rev. 1
Cover and Spine	Cover Page and Spine	Cover Page and Spine
Table of Contents	Pages i to vi	Pages i to vi
Chapter 1	Chapter 1 (complete)	Chapter 1 (complete)
General Arrangement Drawings	1916-01-01-SAR, Rev. 1 1916-01-02-SAR, Rev. 0 1916-01-03-SAR, Rev. 0	1916-01-01-SAR, Rev. 2 1916-01-02-SAR, Rev. 1 1916-01-03-SAR, Rev. 1
2.6	Pages 2.6-5 – 2.6-9	Pages 2.6-5 – 2.6-9
2.7	Pages 2.7-7 – 2.7-18	Pages 2.7-7 – 2.7-18
2.12.3	Section 2.12.3 (complete)	Section 2.12.3 (complete)
2.12.4	Page 2.12.4-10	Page 2.12.4-10
Chapter 3	Chapter 3 (complete)	Chapter 3 (complete)
5.3	Page 5.3-3	Page 5.3-3
5.4	Pages 5.4-4 – 5.4-6	Pages 5.4-4 – 5.4-6
5.5.3	Page 5.5.3-4	Page 5.5.3-4
7.1	Pages 7.1-4 – 7.1-11	Pages 7.1-4 – 7.1-11
7.5	Pages 7.5-1 – 7.5-2	Pages 7.5-1 – 7.5-2
8.1	Page 8.1-1	Page 8.1-1

AREVA

DOCKET 71–9355

435-B

TRANSPORT PACKAGE

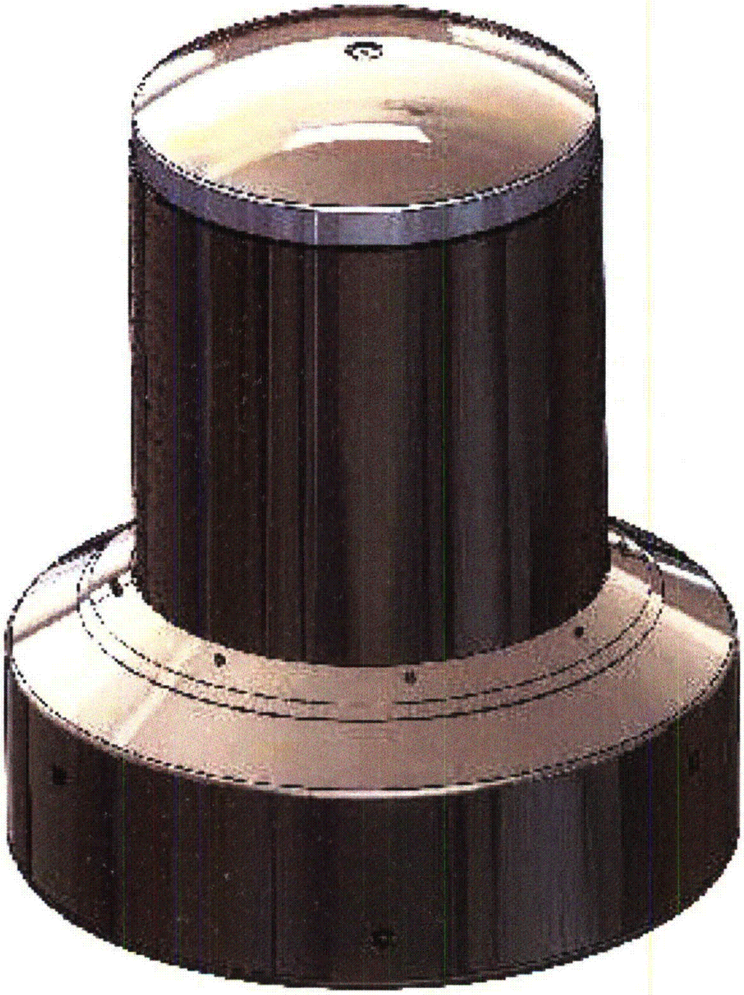

Safety Analysis Report

Revision 1

AREVA Federal Services LLC

February 2014

AREVA

435-B

TRANSPORT PACKAGE

Safety Analysis Report
Docket 71–9355

Revision 1
February 2014

AREVA

DOCKET 71–9355

435-B

TRANSPORT PACKAGE

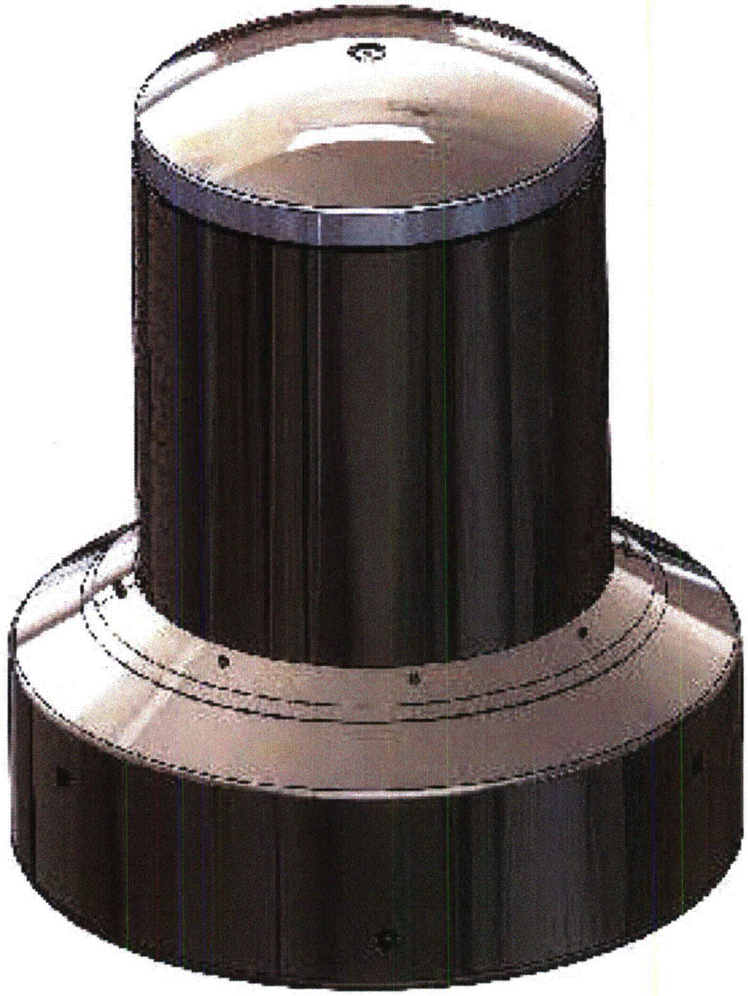

Safety Analysis Report

Revision 1

February 2014

AREVA Federal Services LLC

TABLE OF CONTENTS

1.0 GENERAL INFORMATION

This section presents a general introduction and description of the 435-B package. The 435-B package is used to transport radioactive sources in the Long Term Storage Shield (LTSS) or shielded devices containing their sources. This application seeks authorization of the 435-B package as a Type B(U)–96 shipping container in accordance with the provisions of Title 10, Part 71 of the Code of Federal Regulations [1]. The packaging also meets the requirements of TS-R-1 [2].

The major components comprising the package are discussed in Section 1.2.1, *Packaging*, and illustrated in Figure 1.2-1 through Figure 1.2-8. A glossary of terms is presented in Appendix 1.3.2, *Glossary of Terms and Acronyms*. Detailed drawings of the package design are presented in Appendix 1.3.3, *Packaging General Arrangement Drawings*.

1.1 Introduction

The **Model No. 435-B** package has been developed to transport radioactive sealed sources in the LTSS, as well as shielded irradiation devices (shielded devices) containing sources. The LTSS may transport gamma sources (the majority of sources in the LTSS), beta sources, and very small neutron sources. Fissile materials such as Pu-239 are limited to quantities of less than 15 grams. Thus the payload is fissile exempt per the provisions of §71.15(b) [1]. All shielded devices contain gamma sources only. The 435-B package does not supply significant biological shielding. The primary shielding is provided by the lead shielding in the LTSS or in the shielded devices. All sources are sealed. The 435-B package provides leaktight containment of the radioactive contents under all NCT and HAC.[1]

The packaging consists of a base, a bell cover which is bolted to the base, and an internal lodgment which supports the LTSS. Shielded devices are placed in an inner container for shipment. The package uses conventional materials and metalworking techniques. When loaded and prepared for transport, the 435-B package is 83 inches tall, 70 inches in diameter (over the lower impact limiter), and weighs a maximum of 10,100 lb. The package is designed to be transported singly, with its longitudinal axis vertical, by ground, air, or by water in non-exclusive use.

Since all payloads transported in the 435-B are either non-fissile or fissile-exempt, the criticality safety index does not apply.

An isometric view of the 435-B packaging is shown in Figure 1.1-1. Cross sectional views of the package configured with a LTSS payload and a shielded device payload are shown in Figure 1.1-2 and 1.1-3, respectively.

[1] Leaktight is defined as a maximum of 1×10^{-7} reference–cm^3/sec, air leakage per ANSI N14.5–1997 [3].

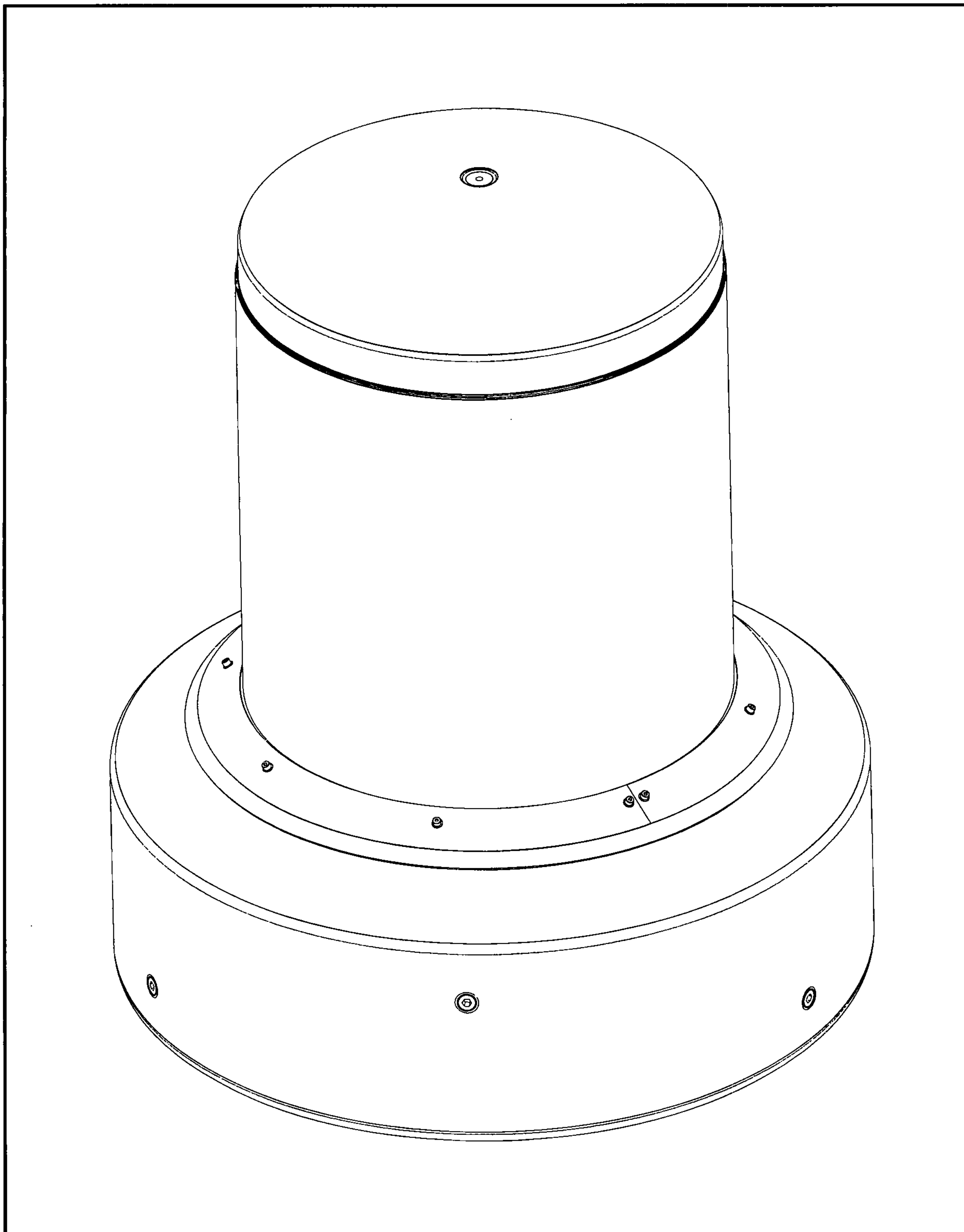

Figure 1.1-1 – 435-B Packaging

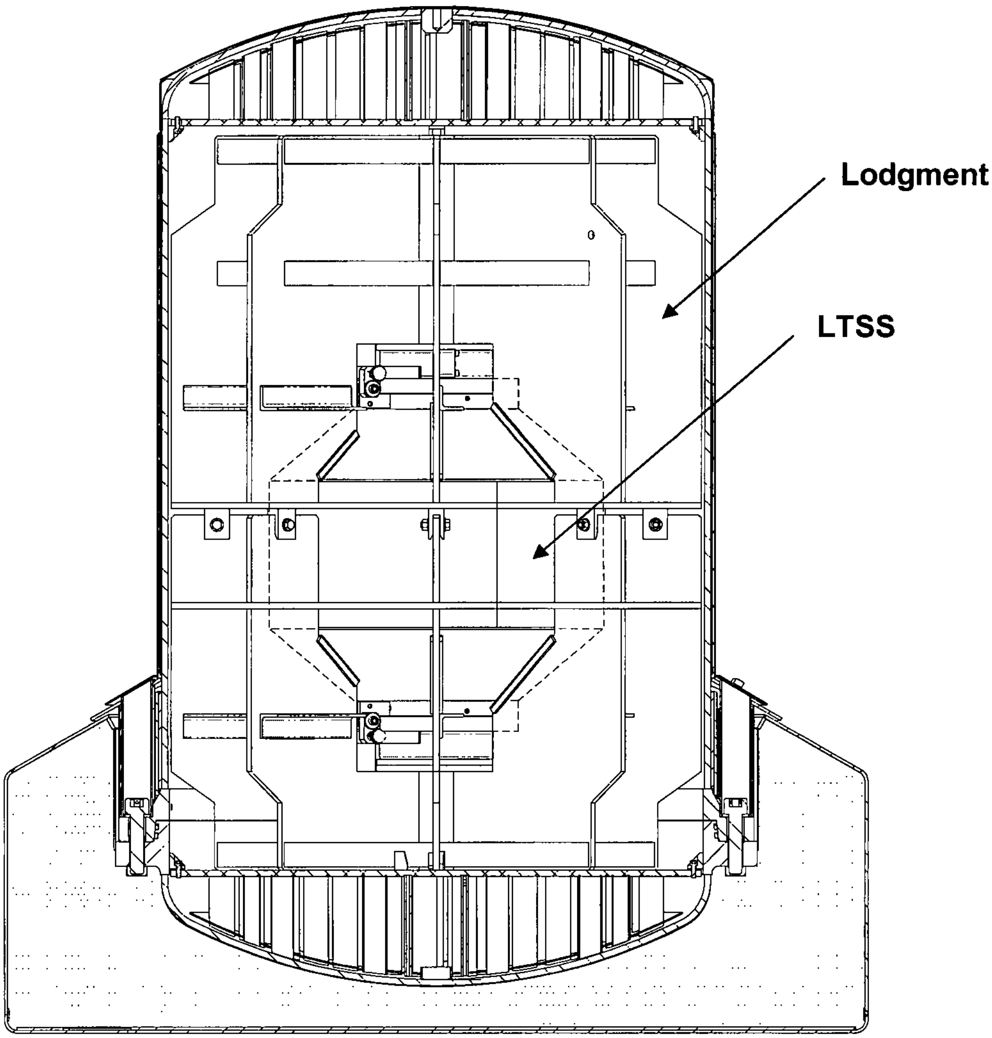

Figure 1.1-2 – 435-B Package With LTSS

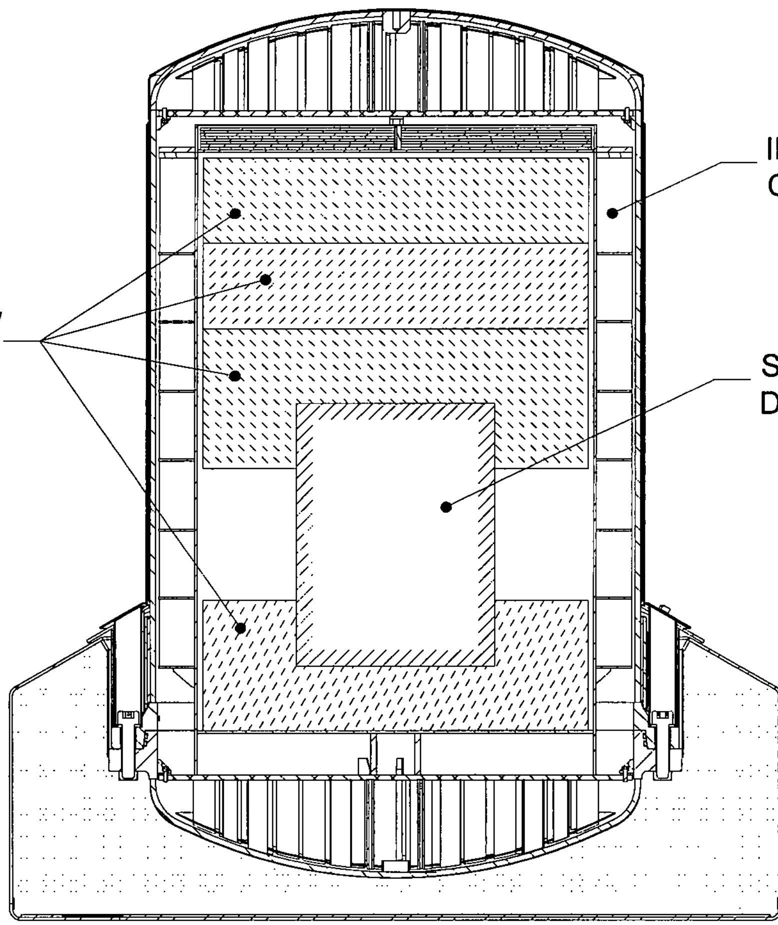

Figure 1.1-3 – 435-B Package With Shielded Device

1.2 Package Description

This section presents a basic description of the 435-B package components and construction. In the following, drawing references are to the general arrangement drawings provided in Appendix 1.3.3, *Packaging General Arrangement Drawings*.

1.2.1 Packaging

The 435-B package (drawing 1916-01-01-SAR) consists of a lower body assembly or base, including the impact limiter containing polyurethane foam, an upper body assembly or bell, two internal impact limiter assemblies, 24 closure bolts, the LTSS payload with a lodgment (drawing 1916-01-02-SAR) to support the LTSS within the package, or a shielded device payload inside an inner container (drawing 1916-01-03-SAR). The package is primarily of welded construction, using Type 304 austenitic stainless steel. The lodgment is made from welded structural aluminum. The LTSS is made from Type 304 stainless steel and lead. The inner container is made of Type 304 stainless steel. These components will now be discussed in detail.

1.2.1.1 Containment Vessel

The 435-B containment vessel consists of a cylindrical body shell with an inner diameter of 43.5 inches and two torispherical heads, all ½ inches thick. The torispherical inner radius is equal to 43.5 inches, and the knuckle radius is equal to 3.5 inches. The vessel is made from ASTM Type 304 stainless steel and includes a brass vent port plug. The upper and lower portions of the vessel connect at a heavy flange joint, located at the lower end of the cylindrical shell. The flanges are 2 inches thick and are connected using 24, 1-1/4-7 UNC bolts made of ASTM A320, L43 material. Each of these components (not including the bolts) may be made from separate pieces of material and joined using full penetration welds. All butt welds in the containment boundary are full-penetration and radiograph inspected.

The closure seal is a 3/8-inch cross-sectional diameter O-ring made of butyl rubber. A vent port, sealed with a butyl sealing washer and threaded brass plug, is located in a block welded to the upper flange (see Section M-M on sheet 6). The block is attached using a circumferential 3/16-inch (non-containment) fillet weld, and the containment is made by a circumferential 1/8-inch fillet weld. The machined opening on the lower flange face (containment) is closed using a full depth groove weld of minimum 0.25-inch thickness. Both of these containment welds are liquid penetrant inspected on the final pass. The seal test port block (not part of containment) is identically configured. The elastomer material of the containment seal and test seal O-rings, and the vent port and seal test port sealing washers, is made from Rainier Rubber R-0405-70, and subject to the tests given in Section 8.1.5.2, *Butyl Rubber O-rings*. The 435-B containment boundary consists of the following components:

- The upper torispherical head and upper body assembly lifting boss
- The cylindrical side shell
- The upper flange (attached to the upper body assembly)
- The lower flange (attached to the lower body assembly)
- The lower torispherical head
- The containment elastomer O-ring seal

- The vent port block in the upper flange including brass plug and elastomer sealing washer

A sketch of the containment vessel is shown in Figure 1.2-1. Additional detail on the containment vessel and other packaging components is given below, and depicted in Figure 1.2-2 through Figure 1.2-7.

1.2.1.2 Lower Body Assembly (Base)

The lower body assembly consists of the lower torispherical head, lower flange, lower internal impact limiter, and integral external impact limiter, and is depicted as Assembly A2 on drawing 1916-01-01-SAR. All material conforms to ASTM A240, Type 304 stainless steel unless otherwise specified.

The lower torispherical head is formed from ½-inch thick plate, and is connected to the lower flange using a full penetration weld. The lower flange is made from ASTM A182, Grade F304 forging, or ASTM A240, Type 304 plate material. The flange has an inner diameter of 43-1/4 inches, an outer diameter of 52.0 inches, and is 2.0 inches thick. An extension of the flange supports the containment closure and test O-ring grooves. The O-rings are arranged on a 5° taper, are bore-type seals, and interface with a recess in the upper flange.

The external impact limiter is integral with, and permanently connected to the lower body. The inner cylindrical shell of the impact limiter is 0.12 inches thick and is welded to the outer edge of the lower flange. The outer shell (tapered top, outer cylinder, and flat bottom) is ¼ inches thick. The top plate of the impact limiter is tapered at 30° from the horizontal, and includes a short lead-in chamfer to guide the upper body assembly into place. The outer cylindrical shell is 70 inches in diameter and approximately 21 inches tall and features six fire-consumable plastic plugs designed to relieve pressure in the HAC fire event. The inside surface of the bottom shell is covered with a ¼-inch thick layer of refractory insulation paper to reduce heat flow into the flat bottom from the HAC fire event. The cavity of the limiter is filled with 15 lb/ft^3 polyurethane foam. The foam is rigid, closed–cell, and is poured in place.

The lower flange features threaded holes for the closure bolts and two alignment pins. These holes may be optionally fitted with alloy steel thread inserts or helically coiled stainless steel thread inserts. On the underside (foam side) of the flange, each hole is covered with a thin cross-section stainless steel cup, tack welded in place and sealed using RTV sealant. The cups provide clearance for the ends of the closure bolts and seal the foam cavity.

The lower internal impact limiter is described in Section 1.2.1.4, *Internal Impact Limiters*.

1.2.1.3 Upper Body Assembly (Bell)

The upper body assembly consists of the upper torispherical head, cylindrical shell, upper flange, vent and test port blocks, upper internal impact limiter, dual side thermal shield, head thermal shield, and the closure bolt access tube structure, and is depicted as Assembly A3 on drawing 1916-01-01-SAR. All material conforms to ASTM A240, Type 304 stainless steel unless otherwise specified.

The upper torispherical head and cylindrical shell are formed from ½-inch thick plate, having a minimum yield strength of 40 ksi and a minimum ultimate tensile strength of 80 ksi. The upper flange is made from ASTM A182, Grade F304 forging, or ASTM A240, Type 304 plate material. The flange has an inner diameter of 43-1/4 inches, an outer diameter of 51.5 inches, and is 2.0 inches thick. The inner diameter of the cylindrical shell is 43.5 inches. A 2.5-inch diameter, 2-inch thick lifting boss, containing a 3/4-10 UNC threaded hole, is located in the center of the torispherical head. This hole may be optionally fitted with an alloy steel thread insert or with a helically coiled stainless steel thread insert. The head, lifting boss, cylindrical shell, and flange are connected using full penetration welds. The vent and test port blocks are made from A276 or A479, Type 304 stainless steel. Their configuration is discussed in Section 1.2.1.1, *Containment Vessel.*

At the lower end of the upper body assembly is a structure consisting of tubes and shells which provides access to the closure bolts and the vent port and seal test port while also protecting these components from HAC puncture bar impact or excessive heat input from the HAC fire event. A detail view of this area is shown in Detail D, Section B-B, and Section C-C on sheet 6. An isometric cut-away view is given on sheet 7. There are 24 evenly spaced, 2.5-inch O.D. × 0.12-inch wall thickness bolt access tubes made from ASTM A249 or A269, Type TP304 stainless steel. In addition, there are two more tubes, 90° apart, and located halfway between bolt access tubes, which provide access to the vent port and seal test port. Both ports are closed with threaded plugs made of ASTM B16 brass and sealed with butyl rubber sealing washers. A port insulation cylinder (Assembly A5 on sheet 6) is used in each port access tube to prevent excessive heat input from the HAC fire event. The port insulation cylinder is made from a 2-inch diameter, 0.06-inch wall thickness stainless steel tube, closed at both ends with a 0.06-inch thick disk of stainless steel, and filled with mineral wool. Each disk is attached using a 1/16-inch all-around fillet weld. A 1/8-inch diameter wire loop is fillet welded to the top disk for handling. Detail views of the vent port and test port are given in Section M-M and Section N-N, respectively, on sheet 6.

The top ends of the tubes are held in place by a ¼-inch thick tube sheet, oriented at a slope to match the upper surface of the external impact limiter. The outside edge of the tube sheet forms a skirt to cover the gap between the upper and lower body assemblies. This prevents the entry of precipitation and, in the HAC fire event, the entry of excessive heat. The tubes pass through the tube sheet and are fillet welded to the sheet all around each tube. The lower ends of the tubes are partially welded to the flange, and the remaining joint which is inaccessible for welding is sealed with RTV sealant. The upper end of the sloped tube sheet is connected to the cylindrical side wall of the package using a partial penetration weld as shown in Detail U on sheet 5. The outer shell of the tube region consists of a 0.12-inch thick sheet, welded to the outer top edge of the flange on the lower end, and to the underside of the tube sheet on the upper end. The area of the containment wall adjacent to the tubes is covered with two, ¼-inch thick layers of refractory insulation paper. The paper is retained using a formed sheet of 0.048-inch thick stainless steel, which is held in place using tack welds. Machined blocks of 30 lb/ft^3 polyurethane foam are located between the tubes.

The top openings of the tubes are covered by a 0.12-inch thick stainless steel rain shield cover. The rain shield is formed in two halves and attached to bolting bosses located in the tube sheet using 5, ½-13 UNC stainless steel bolts (total of 10 bolts). These holes may be optionally fitted with alloy steel thread inserts or helically coiled stainless steel thread inserts. The rain shield also retains the port insulation cylinders used in the vent and seal test ports.

Between the top of the tube sheet and approximately the location of the weld between the torispherical head and sidewall, is located a dual side thermal shield consisting of two gaps and two sheets, as depicted in Detail R and Detail U on sheet 5. The inner sheet is 0.060 inches thick, and the outer sheet is 0.105 inches thick. The gaps are formed by a spiral wrap of stainless steel wire, 0.105 inches in nominal diameter, wrapped on a 3-inch pitch and tack welded in place. At each end of the shield, small spacer strips are used to locate the sheets, which are fully welded in place to seal the gaps. Covering the upper torispherical head is a single thermal shield, 0.105 inches thick, using

0.105-inch nominal diameter wire, spiral wrapped on a 3-inch pitch, as depicted in Detail T on sheet 6. The inner edge of the head thermal shield is welded to a circular spacer strip, and the lower edge is welded to the top end of the side shield. In order to maintain a low thermal emissivity across the shields, the outer surface of the ½-inch thick containment shell, the inner and outer faces of the 0.060-inch thick sheet, and the inner surface of the 0.105-inch thick sheet are brightened per flag note 42 on sheet 2.

The upper body and lower body assemblies are connected using 24, 1-1/4-7 UNC bolts made of ASTM A320, L43 material, with hardened stainless steel washers. The bolts are plated with electroless nickel per SAE-AMS 2404, Revision F, Class 1, or MIL-DTL-26074 Rev. F Class 1 Grade B, and tightened to a torque of 300 ± 30 ft-lb.

The upper internal impact limiter is described in Section 1.2.1.4, *Internal Impact Limiters*.

1.2.1.4 Internal Impact Limiters

The internal impact limiters located at each end of the payload cavity are depicted as Assembly A4 on drawing 1916-01-01-SAR, sheet 7. They are made from an array of 130, 2-inch diameter × 0.035-inch wall thickness, ASTM A249 or A269, Type TP304 stainless steel tubes. The limiters are curved on one side to match the inside of the torispherical head, and flat on the other, so that when fully assembled, the payload cavity is a right circular cylinder 60.3 inches long.

The flat side of the impact limiters is made from a ½-inch thick, ASTM B209, 6061-T651 aluminum plate. The tubes are located in shallow grooves machined into one side of the plate, which stabilizes one end of the tubes. The other end of the tubes is stabilized by passing through a 0.105-inch thick stainless steel tube stabilizer sheet which is spherically curved to match the torispherical heads. Each of the 130 tubes is tack welded in three places to the tube sheet. The tube array is bolted to the aluminum plate using 10, 1/4-20 stainless steel bolts as shown in Section Y-Y on sheet 7. The limiters absorb energy in an impact by crippling deformation in an axial direction. The aluminum plate of the lower impact limiter has protrusions on the top surface that aid in proper placement of the payload during package use.

The internal impact limiters are held in place using four stainless steel clips welded to the inner surface of the containment boundary in the lower and upper position. There are four square notches in the 1/2-inch thick aluminum plate that match the four clips, which allow the limiter to pass beyond the clips. Then the limiter is turned about the package axis approximately 22.5° until smaller notches in the aluminum plate align with any two opposite (180° apart) clips. A 3/8-16 UNC, ASTM A574 bolt is installed in the two clips, which prevents the limiter from rotating. The lower internal impact limiter rests directly on the lower torispherical head, and the load path of the payload is directly into the head, not the clips. To ensure stability in normal use, the load path for the payload goes through a single row of tubes. The fifth concentric row of tubes (consisting of 22 tubes at a radius of 12.5 inches) extends slightly above the adjacent rows of tubes, thus supporting the entire load under normal operation. The upper internal impact limiter rests on the upper clips.

1.2.1.5 Lodgment

The lodgment is designed to maintain the position of the LTSS within the package payload cavity during NCT and HAC, and is depicted as Assembly A1 on sheet 2 of drawing 1916-01-02-SAR. It is a weldment made from ASTM B209 or B221, 6061 T651 aluminum alloy. The LTSS is transported with its axis vertical and its lower end approximately 8 inches above the bottom surface of the lodgment. The main structural components of the lodgment are 8 equally spaced ribs running longitudinally and two circumferential ribs going around the body of the LTSS. All ribs are ½ inches thick. At the center of the longitudinal ribs is a "hub" made from MIL-P25995, 6061-T6, 4-inch, schedule 40 pipe. The longitudinal ribs are spaced and stiffened by 2-in. × 2-in. × ¼-in. thick angles made from ASTM B308, 6061-T651.

The lodgment is constructed with a lower half and an upper half. The two halves are connected using 8, ½-13 UNC bolts and nuts in double shear. When assembled, the lodgment is 42.75 inches in diameter and 59.5 inches tall. The LTSS rests on a ½-inch thick plate covered with a ½-inch thick layer of neoprene rubber. Rubber is also used on the angled edges of the upper and lower ribs to protect the surface of the LTSS, but there is nominally no contact between lodgment ribs and the LTSS. The neoprene rubber has no safety function. The top end of the LTSS is stabilized for transport using three toggle clamps which are bolted to three ribs. The lodgment is lifted using two opposite ribs. The lifting shackles may be placed in storage positions on the lodgment for transport.

1.2.1.6 LTSS

The LTSS consists of a central steel magazine, or barrel, surrounded by thick lead encased in a steel shell. All of the steel used in the LTSS is ASTM type 304 stainless steel. The barrel contains four longitudinal holes, each of which can accommodate one drawer assembly. The barrel is maintained axially in position using a support plate on each end, which is 20 mm thick and attached to the main body of the LTSS using eight, M10 socket head cap screws. A non-structural plate is attached to each support plate. Each end of the LTSS is closed using a lead-filled, hinged door which is attached using eight, M16 socket head cap screws. Four lift lugs are attached to the top lateral side for use in transporting the LTSS horizontally in a facility. On one end are located two threaded lifting blocks for upending and for transporting the LTSS with the axis vertical. Except for some minor operational differences in the support plates and index pins, and except for the axial lifting blocks, the LTSS is essentially radially symmetric and identical at each end. The LTSS is depicted in Figure 1.2-8 and Figure 1.2-9.

The drawer assemblies are 548 mm long and 63 mm in diameter. There are two types of drawer assembly. The Large Source Drawer has a cavity 508 mm long and a wall thickness of 5 mm. It contains the NLM-52 source capsule, which has an outer diameter of 52 mm, and two end shields made of tungsten having a minimum density of 17 g/cm^3. There are five different lengths of the NLM-52, as shown in the following table:

Capsule ID	Capsule Length, mm
NLM 52-74	74
NLM 52-150	150
NLM 52-200	200
NLM 52-250	250
NLM 52-325	325

Each NLM-52 source capsule may contain one or more sealed sources as described in Section 1.2.2, *Contents*. Other special form or non-special form capsules may be used that have the same length, diameter, and at least as much radiation attenuation as the NLM-52 capsule series. The Large Source Drawer is depicted in Figure 1.2-10.

The other drawer type is the T80/T780. The T80 and T780 drawers are dimensionally identical. Like the large source drawer, they are 21.5 inches long and 2.5 inches in diameter. In the center is a 1.1-inch diameter cross-drilled hole which accepts a source capsule. The drawers are made of brass with a wall thickness of 0.2 inches and a stainless steel end thickness of 0.8 inches. For the T80 drawer, the shielding on each side of the source is 9.2 inches of lead. For the T780 drawer, the shielding may be either lead, tungsten, or depleted uranium. The T80/780 drawer is depicted in Figure 1.2-11.

1.2.1.7 Inner Container

The inner container (IC) is designed to hold a shielded device and provide support for the device and the blocking materials during transport. It is depicted as Assembly A1 on sheet 2 of drawing 1916-01-03-SAR. The IC is 59.5 inches tall and 42.75 inches in outer diameter, with an interior cavity of 36.0 inches in diameter and 53.0 inches long. The IC is a weldment made from ASTM A240, Type 304 stainless steel. The lid is attached using six, 1-8UNC hex bolts with flat washers and nuts. The shell, the base, and the inner sheet of the lid are made from 1/4-inch thick material; the bolting flanges, of 1/2-inch thick material; and the grid pattern of stiffening and energy-absorbing ribs on the outside are made from 3/16-inch thick material. The base structure is 4.0 inches high and is stiffened by 8 ribs made from 1/4-inch thick material. The lid is 2.5 inches thick, with three, 1/4-inch thick ribs and three threaded blocks near the outer diameter for lifting the entire IC. The open space in the lid is filled with eight layers of 1/4-inch thick refractory insulation paper. The top of the lid is sealed with 16 GA (0.06-inch thick) sheet metal.

1.2.1.8 Gross Weight

The gross weight of the 435-B package, including the empty packaging, and lodgment and LTSS or inner container and shielded device, is 10,100 lb. The empty weight is 4,940 lb. A summary of overall component weights is shown in Table 2.1-2 and discussed in Section 2.1.3, *Weights and Centers of Gravity*.

1.2.1.9 Neutron Moderation and Absorption

Since the 435-B package transports material which is either non-fissile or fissile exempt, no moderation or absorption of neutrons is necessary to control criticality.

1.2.1.10 Receptacles, Valves, Testing and Sampling Ports

The 435-B package upper body assembly contains a vent port and a containment seal test port. There are no valves or receptacles used in the 435-B package.

1.2.1.11 Heat Dissipation

The dissipation of heat from the 435-B package is entirely passive. A thermal shield is used on the upper body assembly and upper head to limit the heat flux into the package in the HAC fire event. A more detailed description of the package thermal design is given in Chapter 3, *Thermal Evaluation*.

1.2.1.12 Lifting and Tie–down Devices

The 435-B is lifted using a shipping skid and a fork lift truck. The threaded hole on the top of the upper package assembly is used only to lift the upper package assembly component. The package is tied down using straps or hold-down structures placed over the top of the impact limiter, and which are fastened to the shipping skid or to the conveyance. Thus, there are no lifting or tie-down devices that are a structural part of the package.

1.2.1.13 Pressure Relief System

There is no pressure relief system in the 435-B package.

1.2.1.14 Shielding

Biological shielding of gamma radiation is provided by lead located in the LTSS or in the shielded devices. No other components whose primary purpose is shielding are included in the 435-B. Details of the gamma shielding in the LTSS are provided in Section 1.2.1.6, *LTSS*. Gamma shielding in the shielded devices is described and evaluated in Chapter 5, *Shielding Evaluation*.

1.2.2 Contents

The 435-B package contains two payload types: the LTSS and shielded devices. The contents of the LTSS are subdivided into Content 1 and Content 2. The shielded device category is subdivided into Group 1 and Group 3 devices.

1.2.2.1 LTSS Contents

The LTSS contains sealed sources taken from shielded devices such as industrial irradiators, medical equipment, or research facilities. The sources are sealed and may be in special form, and may be present in the T80/T780 source drawer. Content 1 and Content 2 are defined in Section 7.1.4.1, *Qualifying a Payload for Transport*. The nuclides that will be transported in the LTSS are listed in Table 1.2-1. The maximum decay heat in the package is 200W or less. The quantity of Pu-239 is less than 15g. No other fissile isotopes are transported. Fissile exemption of the payload is discussed in Chapter 6, *Criticality Evaluation*. The 435-B, when containing isotopes of plutonium or americium, will not be offered for transport by air. Allowable combinations of nuclides within a single LTSS is discussed in Chapter 5, *Shielding Evaluation*.

1.2.2.2 Shielded Devices

Shielded devices are units which were designed and manufactured to provide a safe source of radiation for industrial, medical, or research purposes. Each such device includes a sealed source (or a group of sources), shielding material, and a steel shell to surround the shielding material and provide structure (a limited portion of the GC-40 shell includes cast iron). All devices transported in the 435-B are found in the NRC Sealed Source Device Registry (SSDR). Each device was engineered to be safely used in a normally occupied environment (i.e., not requiring a hot cell environment), and was repeatedly surveyed for radiation dose over its lifetime. Conservatively, prior to transport, each device will be surveyed, with a surface dose rate limit of 200 mrem/hr and a dose rate at a distance of one meter from the surface of 10 mrem/hr. As noted in the SSDRs, the actual measured dose rate is as much as two orders of magnitude lower than this.

All shielded devices are placed into the inner container for shipment in the 435-B, described in Section 1.2.1.7, *Inner Container*, and blocked in position using dunnage materials. Blocking/dunnage materials are metallic structures or polymeric foam, and are described in Section 7.1.2.2, *Loading the Inner Container (IC)*. The blocking/dunnage is used to prevent unwanted motion during normal transport, and does not provide a safety function. Cabinets, stands, or unnecessary appurtenances are not transported. Prior to loading, movable sources are placed in the safe shipping position, the structural integrity is evaluated, and a radiation survey is performed. More information is provided in Section 7.1.2.2, *Loading the Inner Container (IC)*.

Group 1 shielded devices were manufactured by Radiation Machinery Corporation, Isomedix, Atomic Energy of Canada Limited, MDS Nordion, and Best Theratronics. All of the Group 1 devices feature a fixed-source design, that is, the source capsule(s) are located in a fixed position within the device, and the sample was moved (typically rotated) into or out of position using a shielded specimen holder. All Group 1 devices use Cs-137, with a maximum activity of 3,840 Ci and have a weight of approximately 3,300 lb. All of the devices are shielded with lead, which is contained within a thick steel shell weldment. The model types included in Group 1 are listed in Table 1.2-2. Photographs of the Group 1 devices are provided in Figure 1.2-12 through Figure 1.2-15.

Group 3 consists of the Gammacell-40 (a.k.a. GC-40 and Exactor), formerly manufactured by Atomic Energy of Canada Limited and MDS Nordion, and currently by Best Theratronics. The GC-40 features a telescoping source design, in which the source is contained in a source drawer which is moved along its axis through the shield. In the active position, the source is exposed to a lateral opening in the shield. In the storage position, the source is located near the center of the shield. The drawer contains shielding on each end of the source. All shielding material is lead. The GC-40 has two essentially identical shielded units (upper and lower). Each unit is transported singly. The maximum activity in any one unit is 2,250 Ci of Cs-137. The weight is approximately 2,650 lb. A figure of the GC-40 is provided in Figure 1.2-16.

1.2.3 Special Requirement for Plutonium

The 435-B package may contain plutonium in excess of 20 Ci, which is in solid form.

1.2.4 Operational Features

The 435-B package is of conventional design and is not complex to operate. Operational features are depicted on the drawings provided in Appendix 1.3.3, *Packaging General Arrangement Drawings*. Operating procedures and instructions for loading, unloading, and preparing an empty package for transport are provided in Chapter 7, *Package Operations*.

Table 1.2-1 – LTSS Payload Source Nuclides

Nuclide	Maximum Activity
Co-60	12,970 Ci
Cs-137	14,000 Ci
Sr-90	1,000 Ci
Ra-226 (no Be)[5]	20 Ci
Ra-226Be[5]	1.3 Ci
Am-241 (no Be)[6]	1000 Ci
Am-241Be[6]	6.6 Ci
Pu-238 (no Be)[7]	75 g Pu
Pu-239 (no Be)[7]	15 g Pu
Pu-239Be[7]	15 g Pu
Ir-192	200 Ci
Se-75	80 Ci

Notes:

1. Physical form of all nuclides is solid material in a sealed capsule.
2. The maximum decay heat limit for the 435-B package is 200W.
3. The maximum activity listed is the maximum for a single nuclide in the LTSS. For combinations of different nuclides, lower activity limits apply as discussed in Chapter 5, *Shielding Evaluation*.
4. The total activity in this table is 86,732 A_2. This value exceeds the maximum number of A_2 that could be transported.
5. Impurities may include oxygen, carbon, sulfur, bromine, and chlorine (hydrous and anhydrous).
6. Impurities may include oxygen and chlorine.
7. Impurities may include oxygen.

Table 1.2-2 – Shielded Devices

Model Name/Type	**Maximum Activity, Ci**	**Weight, lb**	**SSDR No.**[3]
Group 1 Devices			
Gammator 50B, B, B34, G-50-B	420	1800	NR-0880-D-802-S
Gammator M34	1,920	1,850	NR-0880-D-806-S
Gammator M38	3,840	2,250	NR-0880-D-806-S
Gammacell 1000 (GC-1000) -Models A through D -Elite A through D, Type I and Type II	3,840 (bounding value)	2,800	NR-0880-D-808-S, NR-1307-D-102-S
Gammacell 3000 (GC-3000) -Elan A through C, Type I and Type II[2]	3,048	3,300	NR-1307-D-102-S
Group 3 Devices			
Gammacell-40 (GC-40, Exactor)	2,250[4]	2,650	NR-1307-D-101-S

Notes:

1. Radionuclide in all cases is Cs-137.
2. Gammacell 3000 external secondary shielding is not credited in the shielding analysis.
3. Consult SSDR for design and safety features of each model.
4. Gammacell-40 activity is given for one of the two device components that make up a complete Gammacell-40. Only one device component may be shipped at one time.

Security Related Information
Withheld Under 10 CFR 2.390

Figure 1.2-1 – 435-B Containment Boundary

Security Related Information
Figure Withheld Under 10 CFR 2.390

Figure 1.2-2 – 435-B Cross Sectional View

Security Related Information
Figure Withheld Under 10 CFR 2.390

Figure 1.2-3 – Exploded View

Security Related Information
Figure Withheld Under 10 CFR 2.390

Figure 1.2-4 – Detail View of Flange Area

Security Related Information
Figure Withheld Under 10 CFR 2.390

Figure 1.2-5 –Internal Impact Limiter

Security Related Information
Figure Withheld Under 10 CFR 2.390

Figure 1.2-6 – LTSS Lodgment

Security Related Information
Figure Withheld Under 10 CFR 2.390

Figure 1.2-7 – Inner Container

Security Related Information
Figure Withheld Under 10 CFR 2.390

Figure 1.2-8 – LTSS Overview

Security Related Information
Figure Withheld Under 10 CFR 2.390

Material List:

- Shell: 304 Stainless Steel, EN 10088.2-95, 1.4307
- Liner Tube: 304S31 Stainless Steel, Hollow Bar, BS 970
- Liner Tube Flange: 304L Stainless Steel, EN 10088.3-95, 1.4307
- Shielded Flange: 304L Stainless Steel, EN 10088.3-95, 1.4301
- Drawer Barrel: ASTM A276 or A479, Type 304 Stainless Steel
- Pivot and Security Plates: ASTM A240, Type 304 Stainless Steel
- Lead: ASTM B29
- Shielded Flange, Pivot Plate, and Security Plate Fasteners: ASTM Type 302 Stainless Steel

Millimeters

Figure 1.2-9 – LTSS Section View

Security Related Information
Figure Withheld Under 10 CFR 2.390

Material List:
Body and Closed End: 303S31 Stainless Steel, EN 10088.3-95, 1.4305
End Piece: 304L Stainless Steel, EN 10088.3-95, 1.4301
Tungsten End Shield: Tungsten, minimum density 17 g/cm^3
Special Form Capsule: AISI 316L Stainless Steel

Millimeters

Figure 1.2-10 – LTSS Large Source Drawer

Security Related Information
Figure Withheld Under 10 CFR 2.390

T80 Source Drawer shown. T780 Source Drawer identical except shielding may be lead, tungsten, or depleted uranium.

Figure 1.2-11 – T80/780 Source Drawer (inches)

Figure 1.2-12 – Gammator G-50-B Shielded Device

Figure 1.2-13 – Gammator M38 Shielded Device

Figure 1.2-14 – Gammacell 1000 Shielded Device

Figure 1.2-15 – Gammacell 3000 Shielded Device

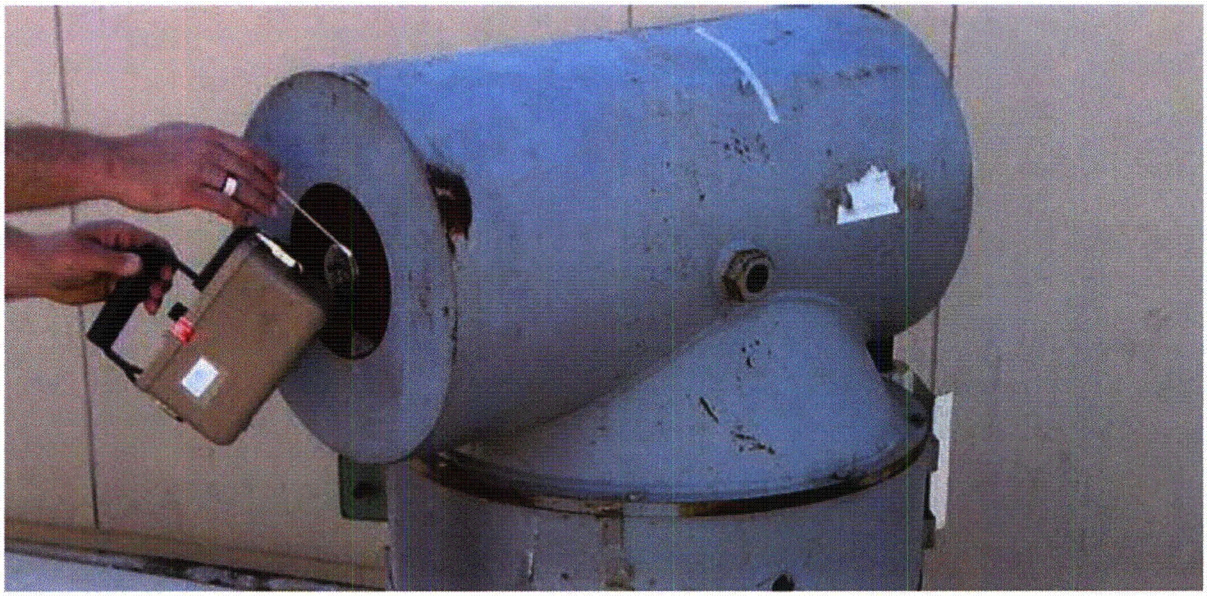

Figure 1.2-16 – Gammacell-40 Shielded Device (Upper Head Shown)

1.3 Appendices

1.3.1 References

1. Title 10, Code of Federal Regulations, Part 71 (10 CFR 71), *Packaging and Transportation of Radioactive Material*, 01–01–11 Edition.
2. International Atomic Energy Agency, *Regulations for the Safe Transport of Radioactive Material*, TS-R-1.
3. ANSI N14.5–1997, *American National Standard for Radioactive Materials – Leakage Tests on Packages for Shipment*, American National Standards Institute (ANSI), Inc.

1.3.2 Glossary of Terms and Acronyms

ANSI –	American National Standards Institute.
ASME B&PV Code –	American Society of Mechanical Engineers Boiler and Pressure Vessel Code.
ASTM –	American Society for Testing and Materials.
AWS –	American Welding Society.
Base –	See *Lower Body Assembly.*
Bell –	See *Upper Body Assembly.*
Clip –	Eight brackets (four top and four bottom), welded to the inside of the containment boundary, supports and retains the *Internal Impact Limiters* in place.
Closure Bolts –	Fasteners that secure the *Upper Body Assembly* to the *Lower Body Assembly.* Includes washers.
Closure Bolt Access Tube –	24, 2-¼ -inch inner diameter tubes that permit access to the *Closure Bolt* heads. See also *Port Access Tube.*
Containment O–ring Seal –	Upper elastomeric seal, retained by the lower flange, which forms part of the containment boundary.
Crush Tubes –	Tubes used with the *Internal Impact Limiter* to absorb free drop energy.
HAC –	Hypothetical Accident Conditions.
Head Thermal Shield –	Assembly of a sheet and a wire wrap attached to the outside of the upper torispherical head, forming a thin air gap that inhibits heat transfer into the package during the HAC fire event.
Inner Container –	Steel container with a bolted lid used to house *Shielded Devices*, interfaces with the 435-B payload cavity.
Internal Impact Limiter –	An energy absorbing component that is placed into each torispherical head. Forms flat ends for the payload cavity and absorbs payload kinetic energy in end drops.
Large Source Drawer –	Shielded drawer used with the *LTSS.*
Lodgment –	Aluminum weldment used to hold the *LTSS* inside the payload cavity.
Lower Body Assembly (Base) –	Lower part of packaging, includes the lower torispherical head, lower flange, *Internal Impact Limiter*, and external impact limiter. Interfaces with the *Upper Body Assembly.*

Long Term Storage Shield (LTSS) – Lead-shielded container which holds source capsules.

MNOP –	Maximum Normal Operating Pressure.
NCT –	Normal Conditions of Transport.

Port Access Tube –	Two, 2-¼ -inch inner diameter tubes that permit access to the *Vent Port* and *Seal Test Port* plugs. Holds the *Port Insulation Cylinder*. See also *Closure Bolt Access Tube*.
Port Insulation Cylinder –	An insulated tube that fits within each *Port Access Tube* to provide additional thermal insulation for the port *Sealing Washers*.
Rain Shield –	Sheet, 0.120-inch thick, which covers the open ends of the *Closure Bolt Access Tubes* and *Port Access Tubes*.
Seal Test Port –	Opening located in a block welded to the upper flange, used to test the leakage rate of the *Containment O–ring Seal*. Closed with the *Seal Test Port* plug.
Sealed Source –	Sealed capsule containing source material.
Sealing Washers –	Integrated metal and elastomer seals that are used with the *Vent Port* and *Seal Test Ports*.
Side Thermal Shield –	Assembly of sheets and wire wraps attached to the outside of the outer shell, forming two thin air gaps that inhibit heat transfer into the package during the HAC fire event.
Shielded Device –	Industrial, medical, or research device for use in irradiating samples. Contains the source, shielding, and surrounding structure.
Special Form Capsule –	NLM 52, a welded capsule used in the *Large Source Drawer*.
T80/T780 Drawers –	Shielded source drawers used with the *LTSS*.
Test O–ring Seal –	Lower elastomeric O-ring seal, retained by the lower flange, used to allow leakage rate testing of the *Containment O-ring Seal*.
Tube Sheet –	The ¼-inch thick plate, inclined at 30° to the horizontal, that holds the upper end of the *Closure Bolt Access Tubes* in place.
Tube Stabilizer Sheet –	Bowl-shaped, 0.105-inch thick sheet that stabilizes the *Internal Impact Limiter* tubes.
Upper Body Assembly (Bell) –	Upper part of packaging, includes the upper torispherical head, cylindrical shell, upper flange, lifting boss, bolt tube structures, vent and test port blocks, access to closure bolts, and upper inner impact limiter. Interfaces with the *Lower Body Assembly*.
Vent Port –	Opening located in a block welded to the upper flange, used to vent the cavity and to introduce helium for leakage rate testing during operations. Closed with the vent port plug.

1.3.3 Packaging General Arrangement Drawings

The packaging general arrangement drawings consist of:

- 1916–01–01–SAR, 435-B Package Assembly SAR Drawing, 7 sheets
- 1916–01–02–SAR, 435-B LTSS Lodgment SAR Drawing, 2 sheets
- 1916–01–03–SAR, 435-B Inner Container SAR Drawing, 2 sheets

DWG NO 1916-01-01-SAR REV 2 SH 1

Security Related Information
Figure Withheld Under 10 CFR 2.390

AREVA
FEB 12 2014
Records Management

REV	DESCRIPTION	DRAWN	CHECKER	VERIFIED
2	SEE ECN NO. 1916-01-01-SARR1-E1	R. LE 02/05/14	DLS 2-11-14	P. Noss 2-11-14
1	SEE ECN NO. 1916-01-01-SARR0-E1	P. PIKULIN 2/12/13	DLS 2/14/13	P. NOSS 2/22/13

REVISION HISTORY

	NAME/SIGNATURE	DATE
APPD		
APPD	R BURNHAM	6/5/12
ENGR	P NOSS	6/4/12
QA	K. KING	6/4/12
CHECK	DL STEVENSON	6-4-12
DRAWN	P. PIKULIN	06/1/12

AREVA

AREVA Federal Services LLC
Packaging Projects
Federal Way, WA 98003

DWG TITLE 435-B PACKAGE ASSEMBLY SAR DRAWING

TOLERANCES:
FRACTIONS ± 1/2
ANGLES ± 3°
3 PLACE DECIMALS AS SHOWN
2 PLACE DECIMALS ± .12
1 PLACE DECIMALS ± .4

SCALE: NOTED | WT. -
REV: 2 | SHEET 1 OF 7
DWG SIZE D | DWG NO. 1916-01-01-SAR
CADFILE: 19160101SAR2.SLDDRW
DWG-3005156-002

Security Related Information
Figure Withheld Under 10 CFR 2.390

DWG NO	REV	SH
1916-01-01-SAR	2	3

Security Related Information
Figure Withheld Under 10 CFR 2.390

REV: 2	SHEET 3 OF 7
DWG NO. 1916-01-01-SAR	

DWG NO 1916-01-01-SAR REV 2 SH 4

Security Related Information
Figure Withheld Under 10 CFR 2.390

REV: 2 SHEET 4 OF 7
DWG NO.
1916-01-01-SAR

Security Related Information
Figure Withheld Under 10 CFR 2.390

Security Related Information
Figure Withheld Under 10 CFR 2.390

Security Related Information
Figure Withheld Under 10 CFR 2.390

Security Related Information
Figure Withheld Under 10 CFR 2.390

REV	DESCRIPTION	DRAWN	CHECKER	VERIFIED
1	SEE ECN NO. 1916-01-02-SARR0-E1	R. LE 02/05/14	DLS 2-11-14	P. Noss 2-11-14

REVISION HISTORY

	NAME/SIGNATURE	DATE
APPD		
APPD	R. BURNHAM	5/21/12
ENGR	P. NOSS	5/21/12
QA	F. GRYGORCEWICZ	5/17/12
CHECK	D. STEVENSON	5/18/12
DRAWN	P. PIKULIN	05/09/12

WELD & FORMED TOLERANCES:
FRACTIONS ± 1/2 ANGLES ± 3° 3 PLACE DECIMALS AS SHOWN 2 PLACE DECIMALS ± .12 1 PLACE DECIMALS ± .4

AREVA

AREVA Federal Services LLC
Packaging Projects
Federal Way, WA 98003

DWG TITLE 435-B LTSS LODGMENT SAR DRAWING

SCALE: NOTED WT. ~
REV: 1 SHEET 1 OF 2
DWG SIZE D DWG NO. 1916-01-02-SAR
CADFILE: 19160102SAR1.SLDDRW
DWG-3005157-001

DWG NO 1916-01-02-SAR REV 1 SH 2

Security Related Information
Figure Withheld Under 10 CFR 2.390

REV: 1 SHEET 2 OF 2
DWG NO.
1916-01-02-SAR

Security Related Information
Figure Withheld Under 10 CFR 2.390

REV	DESCRIPTION	DRAWN	CHECKER	VERIFIED
1	SEE ECN NO. 1916-01-03-SARR0-E1	R. LE 02/05/14	2-11-14 DLS	P. Noss 2-11-14

REVISION HISTORY

	NAME/SIGNATURE	DATE
APPD		
APPD	R. BURNHAM	5/21/12
ENGR	P. NOSS	5/21/12
QA	F. GRYGORCEWICZ	5/17/12
CHECK	D. STEVENSON	5/18/12
DRAWN	P PIKULIN	05/09/12

AREVA Federal Services LLC
Packaging Projects
Federal Way, WA 98003

DWG TITLE 435-B INNER CONTAINER SAR DRAWING

TOLERANCES:
FRACTIONS ± 1/2
ANGLES ± 3°
3 PLACE DECIMALS AS SHOWN
2 PLACE DECIMALS ± .12
1 PLACE DECIMALS ± .4

SCALE: NOTED | WT. ~
REV: 1 | SHEET 1 OF 2
DWG SIZE D | DWG NO. 1916-01-03-SAR
CADFILE: 19160103SAR1.SLDDRW
DWG-3005261-001

Security Related Information
Figure Withheld Under 10 CFR 2.390

Thus the closure bolts are not of concern for the NCT warm condition, including the reduced external pressure load case.

2.6.2 Cold

For the cold condition, a -40 °F steady state ambient temperature is utilized per Regulatory Guide 7.8 [3], with zero insolation and zero decay heat. This results in a uniform temperature of -40 °F throughout the cask. The materials of construction for the 435-B package are not adversely affected by the -40 °F condition, including brittle fracture, which is evaluated in Section 2.1.2.3.1, *Brittle Fracture*.

Since the coefficient of thermal expansion of the flange material is slightly larger than that of the bolting material, a reduction in closure bolt preload will occur at the NCT cold condition. Using the terminology of [10], the reduction in preload is:

$$\mathrm{Fa} = \frac{\pi}{4}\mathrm{Db}^2(\mathrm{Eb})[\mathrm{al}(\mathrm{Tl}) - \mathrm{ab}(\mathrm{Tb})] = -7{,}640 \text{ lb}$$

where the bolt nominal diameter, Db = 1.25 inches, the bolt modulus of elasticity, Eb = $28.3(10^6)$ psi, the coefficient of thermal expansion of the flange material, al = $8.2(10^{-6})$ in/in/°F for Type 304 stainless steel, the coefficient of thermal expansion of the bolt material, ab = $6.2(10^{-6})$ in/in/°F for A320 L43 alloy steel, and Tl = Tb = –40 – 70 = –110 °F. The material properties are taken from Table 2.6-1. The minimum bolt preload torque is 300 ft-lb minus 30 ft-lb, or Qmin = 3,240 in-lb. The minimum bolt preload force is:

$$\mathrm{Fa\_min} = \frac{\mathrm{Qmin}}{\mathrm{K}(\mathrm{Db})} = 17{,}280 \text{ lb}$$

where Db is defined above and K = 0.15, consistent with the definition in Section 2.6.1.5, *Closure Bolts*. Accounting for differential thermal expansion, the remaining preload is 17,280 – 7,640 = 9,640 lb.

As shown in Section 2.6.5, *Vibration*, a loading in the vertical (i.e., axial) direction of ± 2g can result from transportation vibration. From Table 2.1-2, the weight of the upper body assembly (bell) is 2,670 lb. Thus, to keep the bell seated on the lower flange (and the containment seal properly compressed), the sum of preload forces in the closure bolts must be at least equal to the upward vertical vibration load on the bell of 2,670 × 2 = 5,340 lb. Since there are 24 closure bolts, each bolt needs to have a minimum preload of 5,340 / 24 = 222.5 lb. Since the remaining preload in the -40 °F case is 9,640 lb per bolt, the margin of safety is:

$$MS = \frac{9{,}640}{222.5} - 1 = +42.3$$

Thus the remaining preload force per bolt is adequate to maintain the joint and containment seal in a closed and leak tight configuration for the 10 CFR §71.71(c)(2) Cold condition.

2.6.3 Reduced External Pressure

The effect of reduced external pressure of 3.5 psia, per 10 CFR §71.71(c)(3), is considered negligible for the 435-B package compared to other design loadings. This conclusion is based on the NCT structural analyses presented in Section 2.6.1, *Heat*, demonstrating the structural integrity for a 25 psig internal design pressure. Based on the Maximum Normal Operating Pressure (MNOP) of 5 psig, the reduced external pressure conditions would cause a pressure of 16.2 psig. Therefore, the 25 psig internal design pressure analysis is conservatively bounding for the reduced external pressure case.

2.6.4 Increased External Pressure

The effect of an increased external pressure of 20 psia, per 10 CFR §71.71(c)(4), is acceptable for the 435-B package. Consistent with Regulatory Guide 7.8, this loading corresponds to an ambient temperature of -20 °F, no insolation, no decay heat, and minimum internal pressure.

As stated in Chapter 7, *Package Operations*, at the time of shipment, the package cavity is backfilled to a pressure of approximately one atmosphere, or 14.7 psia. Since the cask is closed under ambient conditions, the internal pressure in the cask at a temperature of -20 °F is

$$p_i = p_{amb} \frac{(-20 + 460)}{(70 + 460)} = 12.2 \text{ psia}$$

where p_{amb} is 14.7 psia. Therefore the net external differential gas pressure $p_o = 20 - 12.2 = 7.8$ psi. The compressive hoop stress is:

$$\sigma_\theta = p_o \frac{r_{avg}}{t} = 343 \text{ psi}$$

where the meridional radius, $r_{avg} = 22.0$ inches and the wall thickness, $t = 0.5$ inches. It is evident from this small resultant that a significant state of stress will not occur from the increased external pressure case. In addition, the package is subjected to an external pressure differential of a full atmosphere (14.7 psi) during the fabrication verification leakage rate testing (see Section 8.1.4, *Fabrication Leakage Rate Tests*) and at maintenance intervals (see Section 8.2.2, *Maintenance/Periodic Leakage Rate Tests*), without evidence of buckling or distortion. The factor of safety on buckling is therefore at least equal to 14.7/7.8 = 1.9. The actual factor of safety is much higher than 2.0 since the package is routinely subjected to a full vacuum without imminent risk of buckling. This is consistent with the factor of safety recommended in [13] for NCT. Thus, the increased external pressure load case is not of concern for the 435-B package.

2.6.5 Vibration

The effects of vibration normally incident to transport are shown to be insignificant. Draft ANSI Standard N14.23 [23] identifies peak truck trailer vibration inputs. Table 2 of [23] shows peak vibration accelerations of a trailer bed as a function of package and tiedown system natural frequency. For the frequency range 0 to 5 Hz, and conservatively assuming a light package, Table 2 gives peak accelerations (99% level) of $2g$ in the vertical direction, and $0.1g$ in both the lateral and longitudinal directions. All other frequency ranges give significantly lower acceleration levels. Due to cask symmetry, the vertical load of $\pm 2g$ governs the $\pm 0.1g$ in the lateral and longitudinal directions.

Design fatigue curves are taken from Figure I-9.2 and Table I-9.2 of [12] for the Type 304 stainless steel cask material, from which the allowable amplitude, S_a, of the alternating stress component (1/2 of the alternating stress range) as a function of number of loading cycles may be obtained. The allowable amplitude, S_a at the fatigue limit, which is used in the fatigue assessment of transportation vibration, is 13,600 psi from Table I-9.2 for Type 304 stainless steel cask material at 10^{11} cycles. This value is adjusted based on the ratio of room temperature elastic modulus of $28.3(10)^6$ psi, which is the basis for Table I-9.2, and the elastic modulus at NCT maximum temperature, as follows:

$$S_a = 13{,}600\left[\frac{27.5(10^6)}{28.3(10^6)}\right] = 13{,}216 \text{ psi}$$

where $27.5(10^6)$ psi is the elastic modulus at the bounding temperature of 200 °F from Table 2.6-1.

The 435-B package is transported vertically. In this orientation, the upper torispherical head experiences the ±2g loading as a transverse load (i.e., along the package axis). Conservatively, the head will be evaluated as a simply supported flat plate having the same mass. This representation has much less transverse stiffness and results in larger vibrational stress than would occur in the actual head. The weight of the head, including the crown, knuckle, and lifting boss, is bounded by W = 310 lb. The diameter of the plate is equal to the outside diameter of the head skirt of 44.5 inches, or a = 44.5/2 = 22.25 inches. The projected area of the plate is thus

$$A = \pi a^2 = 1{,}555.3 \text{ in}^2$$

Under a load of 2g, the maximum bending moment in the plate (at the center) is found from Table 24, Case 10a of [24], and is:

$$M = 2K_M q a^2 = 40.8 \text{ in} - \text{lb/in}$$

where the factor 2 is the vibrational load, $K_M = 0.20625$ for $r_o = 0$ from [24], the plate radius, a, is defined above, and q is the 1-g plate loading, equivalent to a pressure, found from:

$$q = \frac{W}{A} = 0.2 \text{ psi}$$

where W and A are defined above. The stress in the flat head is:

$$\sigma = \frac{6M}{t^2} = 979.2 \text{ psi}$$

where the thickness of the head, t = 0.5 inches. For the allowable amplitude, S_a, found above, equal to 13,216 psi, the margin of safety against fatigue of the torispherical head due to vibration is:

$$MS = \frac{13{,}216}{979.2} - 1 = +12.5$$

Therefore, fatigue of the 435-B package due to transportation vibration is not of concern.

2.6.6 Water Spray

The materials of construction used in the 435-B package are not affected by the water spray test identified in 10 CFR §71.71(c)(6).

2.6.7 Free Drop

Section 10 CFR §71.71(c)(7) specifies a free drop from a height of 4 ft for a package weight less than 11,000 lb. As discussed in Appendix 2.12.2, *Certification Test Plan*, each HAC, 30-ft free drop was preceded by a NCT, 4-ft free drop in the same orientation and impact location, and performed at the same worst-case temperatures as the HAC free drop. Because the NCT and HAC free drops were identical (except for the drop height), the damage resulting from any NCT free drop was similar to the corresponding HAC damage, except having a significantly lesser magnitude. The damage resulting from the bounding HAC free drops is described and illustrated by photographs in Appendix 2.12.3, *Certification Test Results*. The impact magnitudes of the NCT and HAC free drops, as recorded by active accelerometers, is given in Appendix 2.12.3. Since the packaging containment was leaktight per the requirements of [3] after each full sequence of NCT free drop, HAC free drop, and HAC puncture drop, then the packaging was leaktight following all NCT free drops. Thus, the effects of the damage resulting from the NCT free drop is demonstrated not to affect the ability of the 435-B package to meet the HAC requirements of 10 CFR §71.73.

2.6.8 Corner Drop

The 435-B package is not required to be evaluated for the corner drop condition, since 10 CFR §71.71(c)(8) applies only to rectangular fiberboard or wood packages weighing less than 110 lb or to cylindrical fiberboard or wood packages weighing less than 220 lb. The weight of the 435-B package exceeds these limits and therefore does not need to be evaluated for the NCT corner drop.

2.6.9 Compression

Section 10 CFR §71.71(c)(9) specifies, for packages weighing up to 11,000 lb, a compression loading equal to the greater of the equivalent of five times the package weight or 2 lb/in^2 over the package projected area. Since the 435-B weighs 10,100 lb, five times the package weight is W = 50,500 lb. The projected area of the head thermal shield, having an outer diameter of 44.9 inches, is A = 1,583 in^2. The resulting pressure, W/A = 31.9 psi. This is greater than 2 psi and is thus required to be used for this evaluation.

As shown in Section 2.7.6, *Immersion – All Packages*, the maximum pressure loading which may be applied to the head per ASME B&PV Code, Section III, Subsection NE-3133.4(e) (before application of the factor of 1.5 for HAC) is 92.0 psi. Since this pressure is nearly three times the bounding compression loading determined above, the compression load on the 435-B package is not of concern.

2.6.10 Penetration

Section 10 CFR §71.71(c)(10) requires the impact of the hemispherical end of a vertical steel cylinder having a 1.25-inch diameter and 13 lb mass, dropped from a height of 40 inches onto the exposed surface of the package that is expected to be most vulnerable to puncture. This test was not performed in lieu of the much more demanding HAC puncture tests which were performed as documented in Appendix 2.12.3, *Certification Test Results*. In the HAC puncture tests, a far greater amount of energy was applied to the package, based on the package weight compared to the 13 lb cylinder. The radius of the HAC puncture bar (0.25 inches maximum) is also significantly more damaging than the 0.63-inch radius of the penetration test bar. As documented in Appendix 2.12.3, HAC puncture tests were performed on the package side, the package upper head, the impact limiter shell, and on the rain shield. Subsequent to all of these tests, the containment boundary was shown by test to remain leak tight per ANSI N14.5. The penetration bar of 10 CFR §71.71(c)(10) could impart only a very small fraction of the damage that was imparted by the HAC puncture test. This same demonstration approach has been used in other safety analysis reports, including the TRUPACT-II (NRC Docket 71-9218) and the MFFP (NRC Docket 71-9295). Therefore, the penetration test has no significant effect on the package.

Table 2.6-1 – Summary of NCT Design Parameters

Parameter	Containment (Type 304)	Closure Bolts (A320, Grade L43)
NCT Hot Bounding Temperature, °F	200	200
Coefficient of Thermal Expansion, α,(in/in/°F)	8.9×10^{-6}	6.7×10^{-6}
Elastic Modulus, psi	27.5×10^{6}	27.1×10^{6}
Design Stress, S_m, psi	20,000	66,000
Yield Stress, S_y, psi	25,000	99,000
Primary Membrane Stress Intensity (P_m), psi	$S_m = 20{,}000$	n/a*
Primary Membrane + Bending Stress Intensity ($P_m + P_b$), psi	$1.5S_m = 30{,}000$	n/a*
Primary Membrane + Bending + Secondary Stress Intensity ($P_m + P_b + Q$), psi	$3.0S_m = 60{,}000$	n/a*
NCT Cold Bounding Temperature, °F	-40	-40
Coefficient of Thermal Expansion, α,(in/in/°F)	8.2×10^{-6}	6.2×10^{-6}
Elastic Modulus, psi	28.9×10^{6}	28.3×10^{6}

* Bolting allowable stresses are discussed in the sections where they are used.

$$\frac{\text{Measured test result}}{\text{Calculated test result}} = \frac{3.62}{6.25} = 0.579$$

Consequently, the expected maximum crush using prototypic, 15 lb/ft^3 foam under warm conditions is equal to $0.579 \times 6.75 = 3.91$ inches. The increase in crush due to the lower foam strength is $3.91 - 3.62 = 0.29$ inches. This value will be conservatively rounded up to 0.5 inches. Thus, the thickness of foam remaining in the worst case, based on certification test measurements and applicable to the thermal analysis, is $5.13 - 0.5 = 4.63$ inches.

2.7.1.6 Structural Evaluation of the Shielded Devices

The inner container will contain shielded devices from Group 1 and Group 3 as noted in Table 1.2-2. The devices contain the radioactive sources and provide shielding. The Sealed Source Device Registry (SSDR) number for each device is given in the table. Shielded devices are designed to be used in a normally occupied environment, and the external dose rates are small. The main structural members of the devices are made of carbon steel, stainless steel, or, in the case of the GC-40, a limited portion of cast iron. If the radioactive source is movable, it is placed into the shielded transport position and secured. To ensure safe transport of the source, it must remain in a shielded position within the device under all NCT and HAC.

As shown in Appendix 2.12.3, *Certification Test Results*, the dummy shielded device was contained within the inner container and located using wood dunnage. In the free drop events, some of the energy of the dummy device was absorbed either by the crush of the wood dunnage (see Figure 2.12.3-15) or by deformation of the inner container (see Figure 2.12.3-37). Conversely, the lodgment and LTSS responded in a more rigid manner, having only negligible damage as shown in Figure 2.12.3-20 and Figure 2.12.3-21. For this reason, the calculated acceleration of the LTSS will bound the acceleration of the shielded device. As shown in Section 2.12.4.5.2, *Slapdown Free Drop Results*, the maximum acceleration of the LTSS is 206g in the bottom down orientation, and 228g in the side orientation. In the analyses which follow, a conservative bounding value of 300g is used. This value is valid for other kinds of dunnage such as rigid polymer foams or aluminum structures.

2.7.1.6.1 Group 1 Shielded Devices

Group 1 shielded devices have fixed, pencil-shaped sources that are held in position inside the shield by a shield plug which is welded to the outer shell. The devices are shipped with their axis vertical. Figure 2.7-1, which shows the GC-3000, illustrates the plug attachment. The plug is located in the upper right of the figure. A circular butt weld between the top plate of the plug and the outer shell of the device retains the plug in position. The plug is stepped, having a larger diameter equal to 5.75 inches and a smaller diameter equal to 4.5 inches. The overall depth of the plug is 3.5 inches. To calculate a bounding weight, it will be assumed to be of a single diameter equal to 6 inches and a depth of 4 inches, and the entire volume will be assumed to be lead (no steel). The weight of this cylinder, using a density of 0.41 lb/in^3 for lead, is 46.4 lb. The source and holder can be bounded by a block of steel 13.25 inches long, 2.5 inches wide, and 0.9 inches thick, having a weight of 8.6 lb. With an impact of 300g, the force on the weld is $(46.4 + 8.6) \times 300 = 16{,}500$ lb. The circular weld has a 5.75-inch diameter on the GC-3000, but will be conservatively represented by a 5.0-inch diameter weld. A conservatively low material yield strength of 25,000 psi is assumed. The shear yield strength is therefore $0.6 \times 25{,}000 =$

15,000 psi. If the depth of penetration of the weld is *h* and the weld stress is τ, then the shear stress in the weld can be written:

$$\tau = \frac{16{,}500}{5\pi h} = 15{,}000 \text{ psi}$$

This can be solved for *h*, which is the required minimum weld penetration of 0.07 inches. Since the material thickness of the shell and the top plate of the shield plug is 3/8 inches thick, a weld penetration of 0.07 inches will be assured. (Note: full depth penetration has been confirmed during numerous device disassembly operations by a DOE contractor.) Note also that weld yield shear strength has been conservatively used instead of the ultimate shear strength. Use of ultimate strength would be justified, since the source cannot be released until the weld completely fails. In a side drop, the plug is supported by the structure of the device and no load is applied to the weld. Thus, a conservative analysis shows that the source will be retained inside the Group 1 devices in the worst-case HAC impact event.

2.7.1.6.2 Group 3 Shielded Devices

Group 3 shielded devices have a sliding source drawer. For shipping, the drawer containing the source is moved all the way to the left in Figure 2.7-2, and a shipping spacer is placed in the remaining cavity. The drawer and spacer are retained in this position by shipping retainers on each end. The retainers are made of steel, nominally 1.5 inches thick, and are retained by four, 3/8-16 UNC socket head cap screws (SHCS). The shipping retainers interlock with the body of the device on each end by means of an approximately 0.1" deep step, which prevents shear loads from being applied to the bolts. In addition, the outer edge of the retainers have a virtually full-depth taper of approximately 45°, as shown in Figure 2.7-2. This feature prevents significant side loads from being applied to the shipping retainers.

An upper bound weight which would be applied to the shipping retainer SHCS on one side in the worst case HAC drop impact can be found by assuming that the drawer is made of solid lead, 2.5 inches in diameter and 16 inches long. The drawer weight is therefore bounded by 32.2 lb. The shipping spacer is a cylinder, 11.4 inches long, 2.5 inches O.D., and ¼ inches thick, made of stainless steel. It weighs 5.8 lb. The shipping retainer can be modeled as a disk, 9 inches in diameter and 1.5 inches thick which has a bounding weight of 27.7 lb. With an impact of 300g, the load on one SHCS is:

$$F_b = 300(32.2 + 5.8 + 27.7)/4 = 4{,}928 \text{ lb}$$

The SHCS may be made of stainless steel or alloy steel. For stainless steel, ASTM standard F837 [28], Table 4, gives a minimum tensile strength for a 0.375-16 fastener made of stainless steel as 6,199 lb. For alloy steel, ASTM standard A574 [29], Table 4, gives a minimum tensile strength for the 0.375-16 fastener of 13,900 lb. The minimum margin of safety on the SHCS is for the stainless steel screw and is:

$$MS = \frac{6{,}199}{4{,}928} - 1 = +0.26$$

Thus, a conservative analysis shows that the source will be retained inside the Group 3 devices in the worst-case HAC impact event.

As noted in Section 1.2.2.2, a limited portion of the shell of the GC-40 is made from cast iron. With reference to Figure 2.7-2, the shells of the GC-40 consist of an outer cylindrical shell made of 0.38-inch thick carbon steel, two flat ends made of 1-inch thick carbon steel, and, on a transverse axis, inner and outer conical shells. The inner conical shell is clearly shown in Figure 2.7-2, and is cast in one piece with the large flange (shown in the figure as having a diameter of 24.7 inches). The outer conical shell is partially shown in Figure 2.7-2, but is more clearly shown in the photograph of Figure 1.2-16. The outer conical shell is made of 0.38-thick carbon steel. Thus, only the inner conical shell and associated flange are made of cast iron, and the rest is carbon steel. In the shipping position, the source is located in the cylindrical shell portion of the device. The device is well protected by the blocking/dunnage, the inner container, and the 435-B package. In the unlikely event of a non-ductile response of the cast portion of the shell to an HAC free drop, the carbon steel in the remainder of the shell will keep the device intact, and shielding of the source will be unaffected.

2.7.2 Crush

Since the weight of the 435-B package exceeds 1,100 lb, the crush test specified in 10 CFR §71.73(c)(2) does not apply.

2.7.3 Puncture

The 435-B package is evaluated for puncture resistance under HAC as defined in 10 CFR §71.73(c)(3). The puncture event is defined as a free drop from a height of 40 inches onto a vertical, cylindrical mild steel bar, 6 inches in diameter, in an orientation and in a location for which maximum damage is expected. The puncture event must occur subsequent to the free drop event. Seven different puncture tests were performed on the three 435-B CTUs.

2.7.3.1 Technical Basis for the Puncture Drops

Section 2.7.1.1, *Technical Basis for the Free Drops*, includes a list of the packaging components that are subject to possible damage in the HAC puncture drop event. The susceptibility of the 435-B package to puncture damage was considered and assumed to occur on undamaged areas as well as on prior free drop damage. As discussed in Section 2.12.2.3.2, *Puncture Drops*, the worst-case puncture drops are as follows (all punctures are through the CG, unless stated otherwise):

- A puncture directly on the prior CG-over-knuckle free drop damage would maximize the containment boundary strain, since it would add to the strain generated in the free drop.
- An oblique puncture on the bottom-down free drop damage could tear into the impact limiter shell and damage the lower torispherical head, or expose excessive amounts of polyurethane foam, with consequences for the containment seals in the HAC fire event.
- A puncture on the impact limiter side drop damage, generated in the warm side drop, would create the minimum remaining foam thickness (locally) and, if the shell tore, could expose excessive amounts of foam, with consequences for the containment seals in the HAC fire event.
- A puncture from the side on the rain shield/tube sheet region could impart enough deformation to compromise the vent port containment sealing washer, or make the rain shield

unable to retain the port insulation cylinder. In order to place the puncture bar impact in the most damaging location and orientation, it may not be possible to aim the bar through the CG, however, the effect will be small.

- A puncture on the side drop damage to the knuckle would be similar to the puncture on the CG-over-corner damage to the knuckle, but in a different orientation. A puncture impact directly on the side drop knuckle damage would cause little damage, due to the geometric relationship of the CG to the damage. Therefore, an impact on the head, in the thinner knuckle region, adjacent to the side drop damage, would apply further strain deformation to the prior deformation of the containment boundary.
- A puncture on the side thermal shield could cause the relatively thinner thermal shield sheet(s) to rip and expose the inner shield sheet or even the containment boundary wall to the HAC fire heat.

A more detailed discussion of the puncture drop orientations which were considered, including orientations that are not governing, is given in Section 2.12.2.3.2, *Puncture Drops*. The seven puncture drops actually performed were distributed across the three CTUs to avoid overtesting a single test unit, and in most cases were applied on, or in relation to, prior free drop damage. The tests performed and the justification for choosing them is detailed in Section 2.12.2.4, *Summary of Certification Tests*, summarized in Table 2.12.2-1, and depicted in Figure 2.12.2-2.

2.7.3.2 Summary of the Results of the Puncture Drop Tests

The damage resulting from the puncture tests is summarized below, with further details and photographs given in Appendix 2.12.3, *Certification Test Results*. None of the puncture tests compromised the leak tight condition of the containment, nor caused exposure of excessive polyurethane foam (only one puncture test exposed any foam). There was no significant damage to either the rain shield or to the external thermal shield.

2.7.3.2.1 Puncture Drop Tests P1 and P6

Puncture tests P1 and P6 were identical tests performed on CTU #1 (subsequent to free drop test D1H) and CTU #3 (subsequent to free drop test D5H), respectively. For both tests, the package orientation, impact location, and prior free drop test were identical. CTU #1 was used to test the packaging and the lodgment/LTSS payload; CTU #3 was used to test the response of the packaging to the inner container/shielded device payload. The purpose of repeating the puncture test was to maintain consistency between the two test units. Puncture test P1 made a dent 3-1/8 inches deep, and partially cut through the impact limiter shell over a portion of the bar circumference, and exposed a segment of foam approximately 1.5 inches wide. As shown in Section 3.5.4, *'Last-A-Foam' Response under HAC Conditions*, the polyurethane foam used in the impact limiter forms a char in the hypothetical fire which will tend to block this opening from direct exposure to the flame, preventing significant local temperature peaks. Of note, no other puncture drop test exposed any foam. Puncture test P6 made a dent 1-9/16 inches deep, without cutting the shell. In neither case was any damage imparted to the lower torispherical head or lower flange. More detail is given in Section 2.12.3.4.1, *Test Series D1*, and Section 2.12.3.4.2, *Test Series D5*.

2.7.3.2.2 Puncture Drop Test P2

Puncture drop test P2 was performed on CTU #1 subsequent to free drop D2H. The bar struck the upper torispherical head adjacent to the side free drop damage to the knuckle, and left a dent approximately ¾ inches deep. There was no evidence of cracking of the containment boundary. Of note, this test was conservative because the 0.105-inch thick upper thermal shield was not present on CTU #1, which would have added to the resistance to this puncture. More detail is given in Section 2.12.3.4.3, *Test Series D2.*

2.7.3.2.3 Puncture Drop Test P3

Puncture drop test P3 was performed on CTU #2 subsequent to free drop D3H. The package orientation for the puncture drop was identical to that for the free drop. The bar struck the package at a location three inches radially inboard from the outside edge of the damaged knuckle region. The bar struck in a location such that it did not receive support from the lodgment ribs inside. The resulting dent was approximately 1-3/8 inches deep relative to the flat damaged area. More detail is given in Section 2.12.3.4.4, *Test Series D3.*

2.7.3.2.4 Puncture Drop Test P4

Puncture drop test P4 was performed on CTU #2 subsequent to free drop D4H. The bar struck the damaged impact limiter surface, through the CG, and left a dent approximately 1-1/2 inches deep. The bar did not cut the impact limiter shell. More detail is given in Section 2.12.3.4.6, *Test Series D4.*

2.7.3.2.5 Puncture Drop Test P5

Puncture drop test P5 was performed on CTU #3 subsequent to free drop D6H. The bar struck the tube sheet and deformed the edge of the sheet by approximately ½ inches. Very slight deformation of the rain shield also occurred, but none of the rain shield attachment bolts were loosened, and the rain shield still covered the bolt tubes and the vent port and seal test port tubes. More detail is given in Section 2.12.3.4.5, *Test Series D6.*

2.7.3.2.6 Puncture Drop Test P7

Puncture drop test P7 was performed on CTU #3 subsequent to free drop D6H. The bar struck the side of the package on the dual thermal shield, aiming through the CG. The resulting dent was 1-7/8 inches deep. The outer, 0.105-inch thick thermal shield shell was not cut by the puncture bar. More detail is given in Section 2.12.3.4.5, *Test Series D6.*

2.7.4 Thermal

The 435-B package is designed to withstand the HAC 30 minute fire specified in 10 CFR §71.73(c)(4). The thermal evaluation is presented in Section 3.4, *Thermal Evaluation under Hypothetical Accident Conditions.*

2.7.4.1 Summary of Pressures and Temperatures

As shown in Table 3.1-3, the maximum internal pressure as a result of the HAC fire event is 9.4 psig. This is higher than the MNOP of 5 psig conservatively assumed in Section 2.6.1.1, *Summary of Pressures and Temperatures*. A value of 10 psig will be utilized in the stress calculations which follow.

From Table 3.1-1, as a result of the HAC fire event, the maximum temperature of the containment boundary occurs in the upper torispherical head and is equal to 1,269 °F. This peak temperature occurs at the end of the fire and is located in a hypothetical puncture dent, which locally compresses the head thermal shield. A peak temperature of 1,156 °F occurs at the junction between the thermal shields on the head and bell where a narrow segment of the bell is directly exposed to ambient conditions. At an alternate puncture location just above the rain shield on the side of the package, the peak temperature is 1,127 °F (see Table 3.4-1). The peak temperatures at all of these locations represent temporary excursions which exceed the continuous-duty limit for Type 304 stainless steel of 800 °F for less than one hour. The peak temperatures of the closure flanges, closure bolts, and lower torispherical head are much lower. The peak temperature of the lodgment is 449 °F and occurs at the location where the lodgment is touching the package shell at the location of the hypothetical puncture damage on the package side, as shown in Table 3.4-1 and Figure 3.4-5. At the end of the fire, this highly localized temperature rapidly falls as energy is distributed to the rest of the lodgment structure. The peak temperature of the inner container is 972 °F, which occurs in a single rib at the location of the hypothetical puncture damage on the package side, as shown in Table 3.4-3 and Figure 3.4-12. The peak temperature of the ¼-inch thick cylindrical shell of the inner container, which controls the thermal expansion, is 432 °F, from Section 3.4.3.3, *Side Drop Damage with Shielded Device Payload*.

2.7.4.2 Differential Thermal Expansion

The following calculations demonstrate a positive clearance under HAC between the 435-B payload cavity and the payload, consisting of the lodgment or inner container. The aluminum lodgment is governing due to its higher temperature (449 °F compared to 432 °F) and larger coefficient of thermal expansion. In addition, the hot rib of the inner container may locally deform under thermal expansion and have only a negligible effect on the overall length or diameter of the inner container. Thus, the clearances applicable to the lodgment bound those that would occur when using the inner container.

The payload cavity has a nominal length of 60.30 inches with a tolerance of ± 0.25 inches, giving a minimum length of 60.05 inches. The lodgment has a nominal length of 59.50 inches with a tolerance of ± 0.25 inches, giving a maximum length of 59.75 inches, for a minimum room temperature axial clearance of 0.30 inches. The maximum length of the lodgment is calculated using the peak lodgment temperature, bounded by a value of 450 °F, which occurs at the end of the HAC fire. Since the peak temperature is highly localized, this approach is very conservative. The maximum length of the lodgment is:

$$L_L = 59.75[1 + \alpha(450 - 70)] = 60.06 \text{ inches}$$

where the coefficient of thermal expansion for the aluminum lodgment at 450 °F, $\alpha = 13.8(10^{-6})$ in/in/°F from Table 2.2-4, and the reference temperature is 70 °F. The temperature of the package shell is relatively hot, but is conservatively considered to be a minimum of 100 °F, since the ambient temperature is 100 °F during the cool down period. The increased length of the package cavity is:

$$L_C = 60.05[1 + \alpha(100 - 70)] = 60.07 \text{ inches}$$

where the coefficient of thermal expansion for Type 304 at 100 °F, $\alpha = 8.6(10^{-6})$ in/in/°F from Table 2.2-1, and the reference temperature is 70 °F. The minimum axial clearance is:

$$CLR_{axial} = L_C - L_L = 0.01 \text{ inches}$$

As noted, this minimum clearance is conservatively calculated, since it considers that the localized peak temperature of the lodgment is uniform, and considers a relatively cool temperature for the package sidewall.

The payload cavity has a nominal inner diameter of 43.5 inches with a tolerance of ± 0.3 inches, giving a minimum diameter of $D_C = 43.2$ inches. The lodgment has a nominal diameter of 42.75 inches with a tolerance of ± 0.12 inches, giving a maximum diameter of 42.87 inches, for a minimum room temperature diametral clearance of 0.33 inches. The diameter of the lodgment at the bounding, uniform temperature of 450 °F is:

$$D_L = 42.87[1 + \alpha(450 - 70)] = 43.09 \text{ inches}$$

where α is defined above. The minimum diametral clearance, conservatively neglecting any expansion of the payload cavity diameter, is:

$$CLR_{diametral} = D_C - D_L = 0.11 \text{ inches}$$

Thus, positive clearance is maintained under worst case HAC.

2.7.4.3 Stress Calculations

The 435-B containment boundary is designed as a pressure vessel. As shown in Section 2.6.1.3.1, *Stresses Due to Pressure Loading*, the stress generated in the material by internal pressure is relatively small. However, for the HAC fire event, some deformation of the structure may be present. The most penalizing damage would be for the top down free drop case, since it creates a quasi-flat end on the upper end of the package, which generates higher stress than the original torispherical shape. As shown in Figure 2.12.4-76, the top down drop creates a flat approximately 38 inches in diameter, with a smooth radius connecting it to the side wall. This will be conservatively modeled using a pressurized flat plate having the full package meridional diameter of 44 inches. From [24], Table 24, Case 10b for a fixed-edge plate, the maximum bending moment in the plate is:

$$M_{ra} = \frac{qa^2}{8} = 605 \text{ in} - \text{lb/in}$$

where the pressure, q = 10 psig, and the radius, a = 22 inches. The stress (located at the plate edge) is:

$$\sigma = \frac{6M_{ra}}{t^2} = 14{,}520 \text{ psi}$$

where the thickness, t = 0.5 inches. The stress evaluation method is found in [30]. The stress rupture value is taken from Table I-14.6A at a temperature of 1,300 °F and a duration of one hour, and is equal to 23 ksi. The allowable stress is 67% of this value, or 0.67 × 23 = 15.4 ksi.

The stress from the flat plate evaluation is a bending stress, which may be designated P_b. From Article NH-3223(c), $K_t = 1.25$. Therefore:

$$P_L + P_b / K_t = 11{,}616 \text{ psi}$$

where $P_L = 0$, $P_b = 14{,}520$ psi, and K_t is defined above. The margin of safety is:

$$MS = \frac{15{,}400}{11{,}616} - 1 = +0.33$$

This evaluation is carried out with the following conservative assumptions:

1. The configuration considers a flat plate geometry which is larger than the worst case configuration calculated for the free drop impact damage. Since stress is proportional to diameter squared, this overestimates the stress by approximately 34%.
2. The rupture stress is taken at a conservative temperature (1,300 °F > 1,269 °F), which underestimates the rupture stress by approximately 8%.
3. The maximum temperature is assumed to remain constant for one hour. However, the transient temperature only peaks at 1,269 °F, and falls rapidly. In fact, the length of time for which the maximum temperature exceeds 800 °F is less than one hour.
4. The pressure of 10 psig exceeds the calculated maximum pressure of 9.4 psig, which overestimates the stress by approximately 6%. Furthermore, the peak pressure occurs at a later time than the peak temperature occurs.
5. The material of the head and sidewall of the package have a minimum yield strength of 40 ksi and minimum ultimate strength of 80 ksi, which is greater than the minimum values of 30 ksi and 75 ksi, respectively. The temperature and time to which the torispherical head is exposed is not sufficient to anneal the material (i.e., to reduce the strength to minimum). However, no adjustment was made to the ASME Code minimum rupture strength value.

Thus, it is evident that the true margin of safety is larger than 0.33. In addition, the stress must meet the Level D Service Limit in Section III, Appendix F, Article F-1331.1, of $1.5 \times 0.7 S_u = S_u$. Since S_u for Type 304 material at a temperature of 1,300 °F, from Table NH-3225-1, is 37.7 ksi, the margin of safety is:

$$MS = \frac{37{,}700}{14{,}520} - 1 = +1.60$$

Thus, stress in the HAC fire event is not of concern.

Per Regulatory Guide 7.6, paragraph C.7, the extreme range of stress must be considered. Of all the various allowable stresses corresponding to the different conditions evaluated (including fabrication stresses and normal conditions of transport), the largest allowable stress is equal to the material ultimate strength, S_u. It is therefore conservative to assume that S_u bounds all stresses actually developed in the structure. For Type 304 stainless steel, $S_u = 75{,}000$ psi at 70 °F. The maximum possible stress intensity range is twice this value, or 150,000 psi. Applying a factor of four to account for possible stress concentrations at structural discontinuities gives a total elastic stress range of 600,000 psi. The alternating component is one-half of this value, or 300,000 psi. To account for temperature effects, this value of alternating stress is factored by the ratio of modulus of elasticity. This ratio is formed between the modulus of elasticity at room temperature (at which the test data applies directly) and the modulus of elasticity at the maximum temperature, conservatively bounded by a temperature of 1300 °F for the upper torispherical head in the HAC fire event. The adjusted stress is

$$S_{alt} = 300{,}000 \frac{E_{70^\circ F}}{E_{1300^\circ F}} = 418{,}227 \text{ psi}$$

where $E_{70^\circ F} = 28.3(10^6)$ psi and $E_{1300^\circ F} = 20.3(10^6)$ psi, from Table TM-1 of the ASME Code, for Material Group G. Per Figure I-9.2 and Table I-9.2 of the ASME Code [12], the allowable value for S_{alt} at 10 cycles is 870,000 psi. The margin of safety is

$$MS = \frac{870{,}000}{418{,}227} - 1 = +1.08$$

Considering the significant conservatism used in the underlying assumptions (e.g., use of allowable stress rather than smaller actual stresses, assuming worst case stresses are fully reversing, use of the maximum factor of stress concentration), it is apparent that the actual margin of safety is larger than 1.08. Thus, the requirement of paragraph C.7 of Regulatory Guide 7.6 is met.

2.7.5 Immersion – Fissile

An immersion test for fissile material packages is required by 10 CFR §71.73(c)(5). Since the 435-B package does not transport fissile materials, this requirement does not apply.

2.7.6 Immersion – All Packages

An immersion test for all packages is required by 10 CFR §71.73(c)(6), in which a separate, undamaged specimen must be subjected an equivalent pressure of 21.7 psig. The package will be evaluated for buckling resistance of the cylindrical portion of the containment boundary using Code Case N-284-2, and the torispherical heads using ASME B&PV Code, Section III, Subsection NE-3133.4(e). Although the immersion takes place in water, the maximum NCT warm temperature of 200 °F (see Section 2.6.1.1, *Summary of Pressures and Temperatures*) is conservatively utilized.

For the cylindrical side shell, the compressive hoop stress is:

$$\sigma_\theta = p_o \frac{r_{avg}}{t} = 954.8 \text{ psi}$$

where the pressure, $p_o = 21.7$ psig, the mean shell radius, $r_{avg} = 22.0$ inches, and the thickness, $t = 0.5$ inches. The compressive axial stress is:

$$\sigma_\phi = \frac{p_o \pi r_{skirt}^2}{2\pi r_{avg} t} = 488.3 \text{ psi}$$

Where the pressure load is applied to the projected area of the top of the containment boundary, having an outer radius of $r_{skirt} = 44.5/2 = 22.25$ inches. Using Mohr's circle, the maximum shear stress is:

$$\sigma_{\phi\theta} = \frac{1}{2}\left(\sigma_\theta - \sigma_\phi\right) = 233.3 \text{ psi}$$

The possibility of buckling of the inner shell is evaluated using [13]. Consistent with Regulatory Guide 7.6, a factor of safety corresponding to ASME Code, Service Level D is employed. In this case, the applicable factor of safety is 1.34 for hypothetical accident conditions, as specified in [13]. The analysis used a modulus of elasticity of $27.5(10^6)$ psi, corresponding to 200 °F. Buckling analysis geometry and loading parameters are listed in Table 2.7-2 and results of the analysis in Table 2.7-3. As shown, all interaction parameters, including the maximum value of 0.0654, are less than unity, as required.

The buckling analysis of the torispherical head is evaluated using the technique outlined in [31]. The analysis for torispherical heads is the same as for ellipsoidal heads. Factor A is found as:

$$A = \frac{0.125}{R/T} = 0.00144$$

where the inside crown radius, R = 43.5 inches, and the head thickness, T = 0.5 inches. From ASME B&PV Code, Section II, Part D, Table HA-1, the corresponding value of factor B for a temperature of 200 °F is conservatively taken as B = 8,000. The maximum allowable external pressure is:

$$P_a = \frac{B}{(R/T)} = 92.0 \text{ psig}$$

Per Article NE-3222.2, a factor of 1.5 may be applied for Service Level D conditions, which are appropriate for HAC. The permissible external pressure is therefore 1.5 × 92.0 = 138 psig. For an external pressure of 21.7 psig, the factor of safety against buckling of the torispherical head is:

$$FS = \frac{138}{21.7} = 6.4$$

This value is significantly in excess of the minimum factor of 1.34 suggested by [13]. Therefore, the immersion test is not of concern.

2.7.7 Deep Water Immersion Test (for Type B Packages Containing More than 10^5 A_2)

For Type B packages containing an activity of more than 10^5 A_2, 10 CFR §71.61 requires that an undamaged containment system withstand an external pressure of p_o = 290 psig for a period of not less than one hour without collapse, buckling, or inleakage of water. As shown in Table 1.2-1, the payload represents a maximum activity of less than 10^5 A_2. Therefore, this requirement does not apply to the 435-B package.

2.7.8 Summary of Damage

2.7.8.1 Summary of Certification Test Damage

From the discussions presented in the foregoing sections, it is shown that the hypothetical accident sequence does not result in any adverse structural damage to the 435-B package, and that the criteria established for hypothetical accident conditions in Section 2.1.2., Design

Criteria, are satisfied. Full scale certification testing of free drop and puncture drop, including prior damage imposed by the NCT free drop, has demonstrated the resistance of the 435-B package to hypothetical accident conditions. A total of six potentially worst-case HAC sequences (consisting of a NCT free drop, followed by a HAC free drop followed by one or two puncture drops) were applied to three CTUs. After each test series (in one case, after a pair of test series), the main containment O-ring seal and the vent port sealing washer were leaktight to a level of 1×10^{-7} scc/sec, air, per [4]. After all testing was complete, the metallic containment boundary was leaktight as documented in Table 2.12.3-2. Deformations of the containment boundary were only observed in the upper half of the bell in connection with direct free drop or puncture impacts. No deformations were observed in the closure flanges or in the lower torispherical head, and gross buckling did not occur. None of the deformations compromised the leaktight barrier presented by the containment boundary.

The lodgment maintained the LTSS in essentially its original position in all cases. The LTSS did not experience any lead slump or deformations or other failures that could affect its ability to shield the radioactive sources transported. Since there were no loadings or evidence of damage to the LTSS end door closures, the radioactive sources within the LTSS could not change their position relative to the lead shielding. The inner container supported the shielded device and maintained it within the confines of the inner container. The inner container absorbed most of the potential energy of the device, and protected the packaging containment boundary, while absorbing some energy in the array of external ribs.

The fire analysis assumptions regarding the post-accident configuration of the packaging were supported. Particularly, the absence of significant exposure of foam and the integrity of the thermal shield shells was demonstrated. The vent port and seal test port insulation cylinders and the rain shield remained intact and in place, with no loosening of the rain shield attachment bolts.

2.7.8.2 Summary of Analytical Evaluation Results

Analytical evaluations support the conclusions stated above. The closure bolts, considering the worst case orientation and a conservative payload CG height and payload gap, have a margin of safety of 1.04. The retention of the radioactive source in the shielded position within the Group 1 or Group 3 shielded devices was demonstrated assuming conservatively bounding free drop accelerations. Utilizing a series of conservative assumptions, the stress in the containment boundary during and after the HAC fire event was demonstrated to have a minimum margin of safety of 0.33, and the range of stress, evaluated according to Reg. Guide 7.6, has a margin of safety of 1.08. The factor of safety for immersion of the package under water is 6.4.

Therefore, the 435-B satisfies all of the requirements of 10 CFR §71.73.

Table 2.7-1 – HAC Free Drop Impact Accelerations

Free Drop	Acceleration, g[1]		Comment[2]
D1H	768		Average of four accelerometer locations
D2H	466	249	Avg. of two upper locations/avg. of two lower locations
D3H	178		Average of four accelerometer locations
D4H	374	183	Avg. of two upper locations/avg. of two lower locations
D5H	812		Average of four accelerometer locations
D6H	411	173	Avg. of two upper locations/avg. of two lower locations

Notes:
1. Resolved perpendicular to the ground.
2. Accelerometer locations are described in Section 2.12.3.2.2, *Instrumentation.*

Table 2.7-2 – Immersion Test: Geometry and Loads

	Containment boundary shell dimensions, inches	Applied stress, psi	
Inner Dia.	43.5	σ_φ	954.8
Outer Dia.	44.5	σ_θ	488.3
Length (bounding)	60.0	$\sigma_{\varphi\theta}$	233.3

2.12.3 Certification Test Results

This appendix presents the results of the certification testing of the 435-B package that addresses the performance requirements of 10 CFR 71 [1]. This material summarizes the information presented in the certification test report [2].

2.12.3.1 Introduction

Demonstration of the compliance of the design of the 435-B package with the requirements of 10 CFR §71.73 was primarily achieved using formal certification testing. Analysis was used for all NCT events except the free drop, and for the HAC thermal case. Analysis using a model benchmarked against test results was also used to evaluate certain orientations that were not tested. The NCT and HAC free drop events and HAC puncture event were demonstrated by testing. This appendix describes the results of the free drop and puncture testing, including post-test measurements and evaluations. The testing utilized three, full-scale certification test units (CTUs). Testing was performed to a written procedure which was based on the test plan presented in Appendix 2.12.2, *Certification Test Plan.* A total of six NCT free drops, six HAC free drops, and seven HAC puncture drop tests were performed on the units. The primary success criterion was that, subsequent to all free drop and puncture testing, the CTU containment boundary, including the main containment seal and vent port seal, be leaktight per ANSI N14.5 [3]. Other supporting data, including accelerations and physical measurements, was collected as described herein.

2.12.3.2 Test Facilities and Instrumentation

2.12.3.2.1 Test Facilities

Testing was performed at Lampson International LLC in Pasco, Washington, beginning November 28, 2011. The drop pad weighed approximately 110,000 lb, including a 2-inch thick, embedded steel plate impact surface. The pad therefore represented an essentially unyielding surface for the CTUs, which weighed between approximately 9,650 and 9,775 lb. The puncture bar assembly was made of ASTM A36 steel, 6 inches in diameter, 24 inches long, with an edge radius of 0.22 to 0.25 inches. The bar was affixed to a steel baseplate and welded to the drop pad for puncture drop testing.

Eight free drops were performed with the impact limiter polyurethane foam in the cold condition. A refrigerated trailer was present onsite to chill the CTUs prior to testing. Thermocouples were inserted in 1/4-inch diameter holes in each CTU, 9 inches deep, through the plastic plugs on the side of the CTUs. Three thermocouples were used for each test article, located 120° apart. Two free drops were performed with the impact limiter foam at warm temperature. A combination of heating blankets and warm ambient air inside an enclosure were used to warm the foam. Two free drops were performed using the prevailing temperature of the CTU. All puncture tests used prevailing temperature.

2.12.3.2.2 Instrumentation

Accelerometers were used to record the impact of each free drop. Accelerations of the puncture drops were not recorded. For axial or near-axial drop orientations, the measurement axis of the accelerometers was axial. For the near-horizontal side drops, the measurement axis was transverse to the cask axis.

Two axial and two transverse mounting positions were provided at each end of the cask. The measurement axes were as close to the cask surface as possible, and the mounting blocks were rigidly welded to the cask. The mounting location and orientation of each accelerometer is shown in Figure 2.12.3-1. The transverse accelerometers at each end were all mounted on the same axial plane with their axes parallel. The two accelerometers located at the azimuth of the seal test port were designated T/U (at test port, upper location) and T/L (at test port, lower location). The two accelerometers located 180° away from the first set were designated OT/U and OT/L, where the 'O' indicates 'opposite', i.e., 180° away from the first set.

The raw data was conditioned and low-pass filtered at a cutoff frequency of 500 Hz. Per the guidance given in TS-G-1.1, *Advisory Material for the IAEA Regulations for the Safe Transport of Radioactive Material*, an appropriate cutoff frequency range is found from:

$$f_c = [100 \text{ to } 200] \times \left(\frac{100}{m}\right)^{\frac{1}{3}} = 280 \text{ to } 560 \text{ Hz}$$

Where m is the mass of the package in metric tonnes (10,100 lb equals 4.59 metric tonnes). From this, a reasonable cutoff frequency of 500 Hz is chosen. Further reduction of accelerometer data is discussed in Section 2.12.3.4, *Free Drop and Puncture Drop Test Results*.

2.12.3.3 Certification Test Unit Configuration

The three CTUs were fabricated in full scale in accordance with the SAR drawings in Appendix 1.3.3, *Packaging General Arrangement Drawings*, except as noted and justified below. CTU #1 used a dummy LTSS payload and lodgment #1. CTU #2 used the same LTSS payload and lodgment #2. The two lodgments were identical and are shown on drawing 1916-01-02-SAR. CTU #3 used an Inner Container (IC), shown on drawing 1916-01-03-SAR, and a dummy shielded device payload. The details of the CTU configurations are given in Table 2.12.3-1 and depicted in Figure 2.12.3.3-1 through Figure 2.12.3.3-5. A number of features are common to all of the CTUs, and these are listed at the beginning of Table 2.12.3-1 and depicted in Figure 2.12.3.3-1. Features specific to each individual CTU are then detailed in the remainder of the table and in Figure 2.12.3.3-2 through Figure 2.12.3.3-5. In each case, the differences between the CTU and the SAR drawings are justified in the numbered paragraphs of this section and indexed in the table and on the figures. The weights of the CTUs are given in Table 2.12.3-2. The dummy LTSS is shown in Figure 2.12.3.3-6 and the dummy shielded device is shown in Figure 2.12.3.3-7. The specific features of the CTUs are identified and justified as follows.

1. CTU #1 and CTU #3 had slightly higher density (nominally 16 lb/ft^3) polyurethane foam installed in the impact limiter compared to the production foam density (nominally 15 lb/ft^3). The higher density foam, when chilled to a temperature of 0 °F as discussed in Section 2.12.2.2, *Initial Test Conditions*, has crush properties essentially equal to those of the production foam at a temperature of -40 °F. The temperature of -40 °F is conservatively below the cold environment temperature of -20 °F found in [1], and corresponds to the minimum environment temperature found in [4]. In this way, the crush strength of the foam in CTUs #1 and #3 at the target test temperature of 0 °F would accurately simulate the higher strength of the production foam at a temperature of -40 °F. The comparison of the stress-

strain curves for the two foam densities at cold temperature is given in Figure 2.12.3-2. The production foam (15 lb/ft^3) is shown for -40 °F and includes a +10% manufacturing strength tolerance and a dynamic adjustment. The test foam (16 lb/ft^3) is shown for the actual manufactured strength, the actual test temperature of -10 °F, and a dynamic adjustment. The properties of the production foam are developed in Appendix 2.12.4, *Finite Element Analysis*.

2. CTU #2 had slightly lower density (nominally 14 lb/ft^3) polyurethane foam installed in the impact limiter compared to the production foam density (nominally 15 lb/ft^3). The lower density foam, when heated to a temperature of 110 °F as discussed in Section 2.12.2.2, *Initial Test Conditions*, has crush properties essentially equal to those of the production foam at a temperature of 150 °F. The temperature of 150 °F is slightly above the foam bulk average temperature under the hot environment conditions presented in Chapter 3, *Thermal Evaluation*. In this way, the crush strength of the foam in CTU #2 at the target test temperature of 110 °F accurately simulated the lower strength of the production foam at a temperature of 150 °F. The comparison of the stress-strain curves for the two foam densities at elevated temperature is given in Figure 2.12.3-2. The production foam (15 lb/ft^3) is shown for 150 °F and includes a -10% manufacturing strength tolerance and a dynamic adjustment. The test foam (14 lb/ft^3) is shown for the actual manufactured strength, the actual test temperature of 117 °F, and a dynamic adjustment. The properties of the production foam are developed in Appendix 2.12.4, *Finite Element Analysis*.

3. CTU #1 and CTU #2 had simulated thermal shields installed on the side of the packages instead of production thermal shields. A production thermal shield on the cylindrical side (shown in Detail R on sheet 5 of drawing 1916-01-01-SAR) was installed on CTU #3, since a puncture test was performed directly on the shield of that unit in order to test its integrity. But since the presence of a thermal shield on the side of CTUs #1 and #2 did not have any significant effect on the tests performed on those units, it was not necessary to include production thermal shields. The simulated thermal shields consisted of a single layer of 0.105-inch thick stainless steel, essentially the full length of the side shield region, without stand-off wires, in order to partially make up the weight of the full shield. It was welded using intermittent welds to the cask shell, and its vertical seam was a lap joint using intermittent welds, as detailed in Figure 2.12.3.3-5. As such, it represented less structural strength than a production shield, which has uninterrupted welds to the body and a full bevel weld vertical seam. Note also that the inner, 0.060" thick thermal shield was conservatively not included with the simulated thermal shields. To account for the effect of the stack-up of steel strips that is used at the top end of the production thermal shield (an area which was deformed in the side drop events), an equivalent strip of 5/16-inch thick stainless steel was welded to the location of the top and lower ends of the production shield. Thus, the simulated thermal shields on CTUs #1 and #2 represented a package having somewhat less structural strength on the side than the production model, while including the hard point that could increase containment boundary strain in a side impact.

4. CTU #1 and CTU #3 did not have a thermal shield on the upper torispherical head. A production head thermal shield (as shown in Detail T on sheet 6 of drawing 1916-01-01-SAR) was installed on CTU #2, since the tests on that unit included the free drop and puncture drop impact on the head. Since the thermal shield provides added structure to the torispherical head of the package, the effect of the absence of the head shield on CTUs #1

and #3 is conservative. Since the weight of the head thermal shield is relatively small (~ 67 lb), it was not necessary to make up the weight of the missing shield.

5. Because the testing performed on the CTUs was structural and not thermal, it was not necessary to provide a production finish to the internal surfaces of the production thermal shields used on CTU #2 (top head shield) and #3 (side shield). The finishes specified for the production package (see flag note 42 on sheet 2 of drawing 1916-01-01-SAR) are provided only to reduce heat transfer by radiation. The surface finish used on the CTUs was as-received.
6. To facilitate leak testing during the certification test series, an auxiliary vent port was placed in each CTU on the side near the top head joint, in an azimuth location that prevented significant damage to the 1-inch NPT hole. The presence of the hole did not have a significant effect on any of the tests.
7. In order to facilitate rigging and lifting the CTUs, the threaded hole on the top of the upper head was increased to 1-8 UNC thread and a correspondingly large swivel hoist ring was used. The production hole is ¾-10 UNC, and is used only to lift the top assembly (the bell). The larger hole and hoist ring allowed for safe lifting of the entire package. This difference had no effect on any tests. To further facilitate rigging, carbon steel plates having a threaded hole were attached by welding to the lower sides of the impact limiter. The plates are depicted in Figure 2.12.3.3-1 and are shown in numerous photographs, such as in the lower right-hand corner of Figure 2.12.3-17. These plates were distant from the deformation of the impact limiter in each case, and had no effect on any tests.
8. To record impact accelerations of the free drops, four accelerometers were used with each drop. To mount the accelerometers, Type 304 stainless steel blocks, 1-inch cubic in size, were mounted to the package as shown in Figure 2.12.3-1. The mounting locations required small cutouts to be made in the production (CTU #3) and simulated (CTU #1 and #2) side thermal shields. The blocks and cutouts had no effect on any of the tests.
9. To record the temperature of the polyurethane foam, three thermocouple wires were used in holes that were placed in the three plastic melt-out plugs on the side of the impact limiter. The holes were 9 inches deep and 1/4 inches in diameter. This depth placed the thermocouples at essentially the volumetric center of the foam body. Two additional holes were placed through the impact limiter steel shell, at the same height, on CTU #2. These holes did not have a significant effect on the crush behavior of the impact limiters in any drop or puncture event.
10. Due to flange distortion during fabrication, the vent and test ports became misaligned to the package axis. They were repaired by placing new ports in a block welded to the flange. The production design uses the same welded block, except the block is configured such that no flange counter bore is necessary. In addition, the production design has a 50% larger vent hole diameter, a different configuration in the flange, and an additional weld. Because both designs depend for strength on the same 3/16-inch all-around fillet weld between the block and the flange, they have the same resistance to damage. The as-tested and production designs are compared in Figure 2.12.3-3. The production designs are formally detailed in Section M-M and Section N-N of sheet 6 of drawing 1916-01-01-SAR. Furthermore, during testing, no significant loadings were transmitted to the vent or test port regions, as

demonstrated by the relatively large distance between the port areas and external damage areas. Therefore the difference in the port designs had no effect on the test results.

11. To ensure that the lodgment was azimuthally oriented properly for the worst-case damage to occur, two aluminum tabs were welded to the lower internal impact limiter assemblies at a distance of 14 inches from the center of the plate. The tabs are shown in Figure 2.12.3-8 in the 6 o'clock position. The tabs are not used on the production package. Since their purpose was to ensure the test damage was maximized, their presence in the test units was conservative.
12. The lid of the IC features three radial ribs. In the production design, the ribs are welded to the inner sheet of the lid using intermittent fillet welds as shown in Section B-B on sheet 2 of drawing 1916-01-03-SAR. Instead, a continuous fillet weld was used on the test articles. The performance of the 435-B does not depend on the IC lid. The IC lid is a relatively thin structure that simply transmits any impact loading from inside the IC to the upper internal impact limiter. The IC lid is not designed to resist loads using the rib-to-inner sheet welds. Therefore, the performance of the 435-B would be the same whether the welds were intermittent or continuous.
13. The CTUs did not have any caps over the guide pin holes in the upper flange. The caps in the production design keep the region surrounding the bolt access tubes closed to the environment, and are shown in Section F-F on sheet 4 of drawing 1916-01-01-SAR. The lack of these caps (two) had no effect on the test results.
14. The CTUs did not have a lead-in chamfer on the bell opening, which is depicted in Detail AA on sheet 6 of drawing 1916-01-01-SAR. This had no effect on the test results.
15. The CTU used three melt-out plugs on the outer circumference of the external impact limiter. The production quantity is six melt-out plugs. This difference had no effect on the test results.
16. The diameter of the containment and test O-rings was 44.6 inches for CTU #1 and #3, and 44.1 inches for CTU #2. The production diameter is 44.1 inches. The small difference in diameter (0.5 inches for CTU #1 and #3) had no effect on the test results.
17. The outer diameter of the lodgment and IC used in the CTUs was nominally 43.0 inches. The production nominal diameter is 42.75 inches, or a difference of 0.25 inches. In addition, the height of the lower corner of the lodgment was nominally 8.0 inches from the base. The production nominal dimension is 10.0 inches, as shown in View B-B on sheet 2 of drawing 1916-01-02-SAR. These small differences did not have a significant effect on the test results.

The dummy LTSS was used for tests in CTU #1 and CTU #2, and is shown in Figure 2.12.3.3-6 and Figure 2.12.3-21. It was constructed using the same bounding outer dimensions as the production LTSS. It included all of the same external steel shells, protrusions, welds, and lead fill. The dummy LTSS used a solid steel central barrel, without any longitudinal holes or drawers. The dummy LTSS did not have operating hinges for the end doors, having instead welded steel blocks that simulated the size, shape, attachment, and location of the production hinges. The internal security plates were installed loose instead of bolted in place. The dummy LTSS weighed 4,460 lb from Table 2.12.3-2, which is within 4.3% of the weight of the production LTSS which weighs nominally 4,660 lb from Table 2.1-2. These differences were not material to the test.

The dummy shielded device was used for tests in CTU #3 and is shown in Figure 2.12.3.3-7 and Figure 2.12.3-39. It was designed to simulate the weight of a generic shielded device. The body is a pipe, 20 inches in diameter, filled with lead, and closed with rigid steel ends. The overall length is 34 inches. It had a weight of 3,570 lb, essentially equal to the maximum device weight limit of 3,500 lb. It was held in place within the IC using wood dunnage. The dunnage was of two kinds: pallets and end caps. The pallets were made from 4×4 lumber attached to a disc of ½-inch thick plywood. The end caps were made of 1-1/8-inch thick plywood sheets. One end cap (with test damage) is shown in Figure 2.12.3-38.

2.12.3.4 Free Drop and Puncture Drop Test Results

Results of the free drop and puncture drop tests are given below. Tests on the three CTUs were arranged in six series of two on each CTU, consisting of one, 4-ft NCT free drop followed by one, 30-ft HAC free drop, and concluded by at least one, 40-inch puncture drop test. Thus there were a total of six, 4-ft NCT free drop tests, six, 30-ft HAC free drop tests and seven 40-inch puncture drop tests. The test series were performed in the order D1 (D1N, D1H, & P1), D5 (D5N, D5H, & P6), D2 (D2N, D2H, & P2), D3 (D3N, D3H, & P3), D6 (D6N, D6H, P5 & P7), and D4 (D4N, D4H, & P4). The tests are depicted in Figure 2.12.2-1 and Figure 2.12.2-2 and summarized in Table 2.12.2-1 from Appendix 2.12.2, *Certification Test Plan.* Photographs of each test, including post-test examinations, are given in Figure 2.12.3-4 through Figure 2.12.3-49. Low pass filtered accelerometer time histories are given below in Section 2.12.3.6, *Filtered Accelerometer Time Histories.* The acceleration peak values are then resolved to a value that is perpendicular to the ground. Due to the necessity of mounting some accelerometers with their mounting threads facing upwards and others with the threads facing downwards, both positive and negative signals were recorded. However, all results shown in the following summaries are given as positive. Since the data was collected orthogonal to the cask axes, the resultant of the average of the peak acceleration data in the oblique impact cases is as follows.

For free drop tests D1 and D5, which were vertical bottom-down drops, the accelerometers were mounted with their measurement axes parallel to the impact direction. Therefore, the accelerometer readings require no adjustment.

For tests D2, D4, and D6, which were identical side drops in which the upper knuckle and impact limiter corner contacted the pad simultaneously, the cask axis was inclined at an angle of 13° to the ground. The accelerometers were mounted with their measuring axes transverse to the cask axis. The accelerometer reading is divided by the cosine of 13° to obtain the impact which occurred perpendicular to the ground.

For test D3, which was the c.g.-over-knuckle free drop, the accelerometers were mounted with their measurement axes parallel to the cask axis. The accelerometer reading is divided by the cosine of 27°, which corresponds to the recorded angle between the cask axis and the vertical, to obtain the impact perpendicular to the ground.

All puncture drop tests were performed from a height of 40 inches above the top of the 24-inch long puncture bar. The bar remained securely attached to the drop pad during the test, and was not observed to experience permanent deformation. The radius became damaged from contact with the CTUs and was re-dressed prior to further use.

For each test, the temperature of the polyurethane foam (for test D3, the exposed steel surface on the top) was recorded, depending on which was relevant to the test impact. As discussed in Section 2.12.3.3, *Certification Test Unit Configuration*, the cold temperature target for the bulk of the polyurethane foam was 0 °F, and the warm temperature target was 110 °F. The temperature of the steel and of the foam for puncture drops was accepted at the prevailing temperature and recorded at the time of the test.

After the completion of each series of 4-ft, 30-ft, and puncture drop tests (with the single exception of the D3 series), the CTUs were opened for internal inspection. Each time this was done, a helium leakage rate test with a criteria of leak tight per [3] was performed to test the integrity of the main containment O-ring seal and vent port containment sealing washer. (All leakage rate tests mentioned in this SAR used the same leak tight criteria from [3].) This was followed by a measurement of the removal torque of the closure bolts and inspections of the internal components. Removal torque was measured using a dial-type torque wrench loaded in the counter-clockwise direction. Loading was manually increased until the reversal torque reached a maximum, which was recorded. The torque was not removed from any bolt until all of the bolts had been checked. Note that, due to the inclined angle of the threads, the removal torque is somewhat less than the application torque. Trials have shown that bolt removal torque will be between 2/3 and 3/4 of the application torque for joints that have not undergone drop testing. Thus an even lower value would be expected from impact tested joints. It was noted during removal that some of the bolt washers were scored. Subsequently, care was taken to lubricate not only the threads but also the washers during reassembly. Prior to resuming tests (if any), the components of the CTU were cleaned, reassembled according to drawing requirements, and leakage rate tested.

At the conclusion of all free drop and puncture testing, each CTU was subjected to a helium leakage rate test of the containment boundary. All surface obstructions, such as, for example, the head thermal shield, or the sheet enclosing the bolt tube region, were removed or cut open to ensure free access of helium to the entire bell and upper heavy flange surface. On the base, the impact limiter foam was not removed before leakage rate testing. Since the base containment boundary (consisting of the lower torispherical head and lower heavy flange) did not experience any recorded deformations, and in light of the fact that the material (ASTM Type 304 stainless steel) is capable of very large strains before fracture and is not subject to low-strain cracking, the presence of a crack or fissure resulting from any of the tests is not credible. Therefore testing with the polyurethane foam in place was acceptable. The integrated leak rates for each containment boundary are summarized in Table 2.12.3-3.

2.12.3.4.1 Test Series D1

Test series D1 was performed on CTU #1 and consisted of a 4-ft NCT and a 30-ft HAC free drop in the bottom-down orientation, with the axis vertical, followed by a puncture drop test on the flat bottom of the impact limiter, with the cask axis inclined at 30° from the vertical. The tests were designated D1N, D1H, and P1 for the 4-ft, 30-ft, and puncture drops, respectively. The free drop orientation (identical for D1N and D1H) is shown in Figure 2.12.3-4. The polyurethane foam temperature readings for test D1N were -10.0 °F, -11.3 °F, and -11.2 °F, and for test D1H, -9.0 °F, -9.5 °F, and -10.4 °F. Accelerometer results are shown in the table below.

Accelerations, Free Drop Test D1					
Location	**T/U**	**T/L**	**OT/U**	**OT/L**	**Avg. ⊥**
Test D1N	316g	315g	353g	330g	**329g**
Test D1H	856g	815g	696g	705g	**768g**

Both of these impacts imparted no visible damage to the CTU. The only external measurement taken at the time of the drops was the overall height. The height after D1N was 83-7/16 inches, compared to an as-fabricated height of 83-3/4 inches, for an apparent decrease of 5/16 inches. The same measurement taken after the D1H drop was the same as for the D1N drop, seeming to indicate no further compression of the impact limiter. It appears anomalous that a small drop height would produce more deformation than a larger one. In fact, the actual changes in overall height of the package were probably too small to be accurately measured using the techniques used. In any case, the external deformation was negligible. As discussed below, energy was absorbed internally.

After the D1H free drop, a ¼-inch diameter hole was drilled at the center of the bottom sheet of the impact limiter and through the foam to the lowest point on the lower torispherical head. After subtracting a total of 0.66 inches for the steel shell, the insulating paper, and an observed gap, the thickness of the foam was measured to be 3.9 inches. Since a pre-test measurement of this dimension was not made, the post-test result must be compared to the fabricated nominal dimension, which was 3.4 inches. Since this value is less than the post-test result, it is postulated that an unobserved gap was created between the torispherical head lower surface and the inner surface of foam by the impact. In any case, it appears that the crush of foam in the free drop events was very small. The package after the D1H drop is shown in Figure 2.12.3-5.

The puncture drop P1 orientation is shown in Figure 2.12.3-6. The axis of the puncture bar was directed through the c.g. at an oblique angle of 29.5° to the bottom surface. The temperatures of the foam were 12.1 °F, 12.7 °F, and 15.2 °F. The bar made a dent 3-1/8 inches deep and cut a small, approximately 1.5-inch wide perforation in the bottom sheet. (This was, incidentally, the only exposure of polyurethane foam from any of the drops or puncture tests.) The puncture damage is shown in Figure 2.12.3-7.

After Test Series D1 was complete, CTU #1 was disassembled for inspection. Prior to disassembly, a leak test was performed on the containment closure and vent port seals as discussed above. The results showed no detectable leak. The average removal torque of the closure bolts was 150 ft-lb, with a low value of 60 ft-lb and a high of 230 ft-lb. Initial installation torque was 300 ft-lb.

There was no sign of any weld failure or distress of the welds connecting the impact limiter to the lower flange. The only deformation of the lodgment was a slight bowing of the angle segments connecting the bottom ribs, caused by contact with the deformed plate of the lower internal impact limiter. The lodgment was still flat on the bottom. The total deformation of the lower internal impact limiter tubes, based on measurements of the lodgment relative to the lower brackets, was 1.43 inches downward, achieved by buckling of the tubes. The lower internal impact limiter top view is shown in Figure 2.12.3-8 and the underside view, showing the buckling of the tubes, in Figure 2.12.3-9. The upper internal impact limiter was not significantly damaged. Two of the lodgment toggle clamps became unclamped, and one was damaged. The LTSS was not damaged or deformed.

After Test Series D1 inspection was complete, CTU #1 was reassembled using all the same components. The closure bolts were tightened to drawing requirements and leakage rate tested.

2.12.3.4.2 Test Series D5

Test series D5 was performed on CTU #3 and consisted of a 4-ft NCT and a 30-ft HAC free drop in the bottom-down orientation, with the axis vertical, followed by a puncture drop test on the flat bottom of the impact limiter, with the cask axis inclined at 30° from the vertical. (Note: the D5 series was identical to the D1 series.) The tests were designated D5N, D5H, and P6 for the 4-ft, 30-ft, and puncture drops, respectively. The free drop orientation (identical for D5N and D5H) is shown in Figure 2.12.3-10. The polyurethane foam temperature readings for test D5N were -5.3 °F, -4.5 °F, and -6.5 °F, and for test D5H, -2.9 °F, -2.1 °F, and -3.0 °F. Accelerometer results are shown in the table below.

Accelerations, Free Drop Test D5					
Location	**T/U**	**T/L**	**OT/U**	**OT/L**	**Avg. ⊥**
Test D5N	256g	256g	206g	203g	**230g**
Test D5H	797g	794g	855g	802g	**812g**

Like the D1 series, neither of these impacts imparted any visible damage to the CTU. The only external measurement taken at the time of the drops was the overall height. The height after D5N was 83-15/32 inches, compared to an as-fabricated height of 83-1/2 inches, for an apparent decrease of 1/32 inches. The same measurement taken after the D5H drop was 83-5/16 inches, for a further apparent decrease of 5/32 inches. The actual changes in overall height of the package were probably too small to be accurately measured using the techniques used. In any case, the external deformation was negligible. As discussed below, energy was absorbed internally.

After the D5H free drop, a ¼-inch diameter hole was drilled at the center of the bottom sheet of the impact limiter and through the foam to the lowest point on the lower torispherical head. After subtracting a total of 0.54 inches for the steel shell, the insulating paper, and an observed gap, the thickness of the foam was measured to be 4.0 inches. Since a pre-test measurement of this dimension was not made, the post-test result must be compared to the fabricated nominal dimension, which was 3.4 inches. Since this value is less than the post-test result, it is postulated that an unobserved gap was created by the impact between the torispherical head lower surface and the inner surface of foam. In any case, it appears that the crush of foam in the free drop events was very small. The package after the D5H drop is shown in Figure 2.12.3-11.

The puncture drop P6 orientation is shown in Figure 2.12.3-12. The axis of the puncture bar was directed through the c.g. at an oblique angle of 30.0° to the bottom surface. The temperatures of the foam were +1 °F and -1 °F, with one thermocouple not reading. The bar made a dent 1-9/16 inches deep without perforating the impact limiter shell or exposing any foam. The puncture damage is shown in Figure 2.12.3-13.

After Test Series D5 was complete, CTU #3 was disassembled for inspection. Prior to disassembly, a leak test was performed on the containment closure and vent port seals as discussed above. The results showed no detectable leak. The average removal torque of the closure bolts was 138 ft-lb, with a low value of 80 ft-lb and a high of 190 ft-lb.

There was no sign of any weld failure or distress of the welds connecting the impact limiter to the lower flange. The IC showed a downward deformation of the bottom structure by approximately 0.9 inches, along with some dents in the IC sidewall from impact with the dummy payload. Inside the IC, the lower wood dunnage was significantly crushed. The upper dunnage was not crushed, but the 'donut' section of the dunnage became unattached from the 'disk' portion. Two views of the damaged lower dunnage are given in Figure 2.12.3-14 and Figure 2.12.3-15. The dummy payload was not damaged. The IC rested firmly on the bottom internal impact limiter. The deformation of the lower internal impact limiter tubes was considerably less than in the D1 (lodgment) case, since there was significant energy absorption in the wood dunnage and some further deformation in the bottom structure of the IC. The upper internal impact limiter was not significantly damaged.

After Test Series D1 inspection was complete, CTU #3 was reassembled using a new IC, dunnage, and dummy payload, but using the same internal impact limiters. The closure bolts were tightened to drawing requirements and leakage rate tested.

2.12.3.4.3 Test Series D2

Test Series D2 was performed on CTU #1 and consisted of a 4-ft NCT and a 30-ft HAC free drop in the side orientation (where the impact limiter corner and the knuckle contacted simultaneously), followed by a puncture drop test on the knuckle in the region damaged by the free drop tests. The tests were designated D2N, D2H, and P2 for the 4-ft, 30-ft, and puncture drops, respectively. The free drop orientation (approximately 13° from horizontal, and identical for D2N and D2H) is shown in Figure 2.12.3-16. The free drop impact occurred on the opposite side of the package from the vent port. The polyurethane foam temperature readings for test D2N were -9.0 °F, -9.4 °F, and -9.5 °F. Due to the short time interval between tests D2N and D2H, and to the cold ambient temperature, the foam temperatures for test D2H were negligibly different from those recorded for test D2N, and well below the target value of 0 °F. Accelerometer results are shown in the table below.

Accelerations, Free Drop Test D2								
Location	**T/U**	**T/L**	**OT/U**	**OT/L**	**Avg. Upper**	**Avg. Lower**	**Resolved ⊥ Upper**	**Resolved ⊥ Lower**
Test D2N	154g	84g	154g	110g	154g	97g	**158g**	**100g**
Test D2H	449g	225g	459g	260g	454g	243g	**466g**	**249g**

The damage consisted of flat spots on the impact limiter and knuckle. After the D2H drop, the combined damage from both the NCT and HAC drops were as follows: the impact limiter flat was 25-1/4 inches long (along cask axis) and 33-1/4 inches wide (orthogonal). The knuckle flat was 12 inches long and 18 inches wide. At the height of the weld seam at the top of the cylindrical side of the impact limiter (essentially the lower impact point), the radial crush distance was 4-3/8 inches, using measurements based on the cask body O.D. Since the crush occurred with the cask axis at an angle of 13° to the ground, the crush in the direction of impact was 4-3/8 × cos(13) = 4.27 inches. (The crush at the knuckle was significantly less). An approximation of the amount of foam remaining was obtained by drilling a hole perpendicular to the flat damage surface, 17.5 inches from the bottom of the limiter. The bottom of the hole was approximately at the nearest point of hard flange material to the impact. The distance of foam, less the ¼-inch thick shell, was 5.94 – 0.25 = 5.69 inches. It was noted that all of the rain shield bolts were snug. The package after the D2H drop is shown in Figure 2.12.3-17.

Puncture drop P2 orientation is shown in Figure 2.12.3-18. The package was suspended essentially upside down over the puncture bar. The axis of the puncture bar was aimed at the knuckle at the location of the free drop damage and directed at the c.g. of the package. The temperature of the steel surface near the impact point was 31.4 °F. The puncture bar left a six-inch diameter impression at impact, the center of which was approximately 16 inches radially from the package centerline. The dent was ¾-inches deep. There was no evidence of cracking in the containment boundary material. Note that this test was conservative since the 0.105-inch thick head thermal shield was not present. The puncture damage is shown in Figure 2.12.3-19.

After Test Series D2 was complete, CTU #1 was disassembled for inspection. Prior to disassembly, a leak test was performed on the containment closure and vent port seals as discussed above. The results showed no detectable leak. The average removal torque of the closure bolts was 154 ft-lb, with a low value of 50 ft-lb and a high of 250 ft-lb.

The upper internal impact limiter was not crushed significantly, but the aluminum plate was somewhat buckled in the region of impact. The lower internal impact limiter, somewhat crushed in test series D1, did not experience significant additional damage. One guide pin in the base, located at the impact point, was slightly bent. Since the flange was not deformed, this likely occurred due to a misalignment between the bell and base during final disassembly. The side impact caused some minor radial deformations of the bell side wall of 1/8 inches maximum at locations which corresponded to the main structural members of the lodgment.

The lodgment was not significantly damaged, and the LTSS was essentially still in the original location. One toggle clamp was broken. The eight clevises connecting the two halves of the lodgment were intact. All eight bolts were slightly bent, occurring most likely during the D1 end impact. The LTSS was essentially undamaged, showing some surface waviness of approximately 1/8 inches on the impact side, corresponding to the main structural members of the lodgment. Internal damage from the D2 series is shown in Figure 2.12.3-20 and Figure 2.12.3-21. After all testing and disassembly, the containment boundary of CTU #1 was helium leakage rate tested. The maximum leakage rate was $2.9(10^{-8})$ He-cc/sec against a criteria of $2.2(10^{-7})$ He-cc/sec. Thus the package, after two complete series of free drop and puncture tests, was leaktight.

2.12.3.4.4 Test Series D3

Test series D3 was performed on CTU #2 and consisted of a 4-ft NCT and a 30-ft HAC free drop in the c.g.-over-top knuckle orientation, followed by a puncture drop through the c.g., directly on the free drop damage. The tests were designated D3N, D3H, and P3 for the 4-ft, 30-ft, and puncture drops, respectively. The free drop orientation (identical for both D3N and D3H) is shown in Figure 2.12.3-22. The package was oriented 27° from the vertical as shown. CTU #2 had the thermal shield installed on the upper torispherical head. The temperature of the outer shield shell was approximately 50 °F, based on the overnight environment temperature, the relatively short exposure to the cold ambient, and the thermal delay caused by the head shield. Accelerometer results are shown in the table below.

Accelerations, Free Drop Test D3						
Location	**T/U**	**T/L**	**OT/U**	**OT/L**	**Avg.**	**Resolved ⊥**
Test D3N	108g	No signal	106g	113g	109g	**122g**
Test D3H	162g	No signal	164g	152g	159g	**178g**

The damage consisted of a flat spot on the torispherical head, offset towards one side. After the D3H drop, the combined damage from both the NCT and HAC drops was a flat spot 21 inches long in the radial direction and 33-1/2 inches long in the circumferential direction. Another characterization showed the change in vertical location of the surface, illustrated in the figure below. Results are provided in the table below.

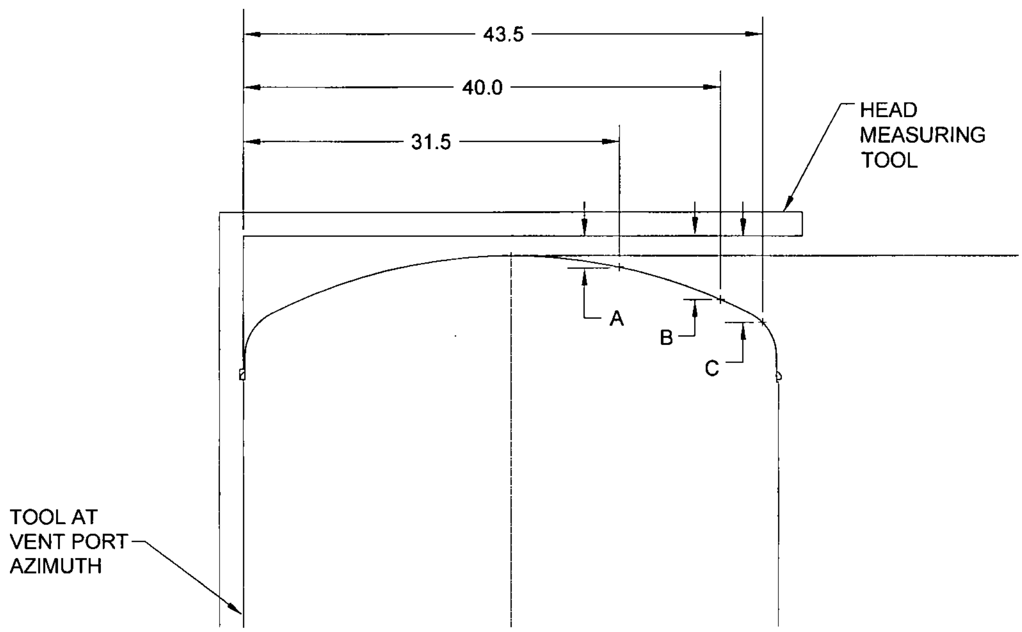

	Axial measurement, inches (after D3H)		
Location	**Pre-test**	**Post-test**	**Change (deformation)**
A	2-7/8	4.0	1-1/8
B	5-3/8	9-13/16	4-7/16
C	6-15/16	11-1/4	4-5/16

The package after the D3H drop is shown in Figure 2.12.3-23.

The puncture drop P3 orientation is shown in Figure 2.12.3-24. The axis of the puncture bar was directed through the c.g. of the package with the impact point (outermost edge) of the bar located at 3 inches from the outer edge of the buckle as shown in Figure 2.12.3-25. The package was oriented at the same angle as for the free drops. The internal lodgment ribs were placed to straddle the puncture impact, thus minimum support to puncture was afforded by internal structures. The bar made a dent approximately 1-3/8 inches deep, based on a straight edge laid across the entire damaged surface. The thermal shield shell did not tear or perforate, and there were no weld failures of the shield. The nominally 0.102-inch diameter wires in the puncture damage were somewhat flattened by the impact. Some of the intermittent welds attaching the simulated side thermal shield cracked, but the simulated shield was not displaced. The puncture damage is shown in Figure 2.12.3-25 and Figure 2.12.3-26. After the D3 test series, a vacuum was placed on the containment seal in the test annulus in lieu of a full helium leakage rate test, according to the test procedure. A vacuum of $7.5(10^{-4})$ Torr was sustained, indicating a leaktight containment seal. A full helium leakage rate test of the containment and vent port seals was performed following Test Series D4. The closure bolts were not retightened or nor was the vent port disturbed between the D3 and D4 series of tests.

2.12.3.4.5 Test Series D6

Test Series D6 was performed on CTU #3 and consisted of a 4-ft NCT and a 30-ft HAC free drop in the side orientation (identical to the free drop orientation of Series D2), followed by two puncture drop tests: one on the side on the production side thermal shield, and one on the side on the bolt tube/rain shield region. The tests were designated D6N, D6H, P7 and P5 for the 4-ft, 30-ft, thermal shield puncture drop, and bolt tube puncture drops, respectively. The free drop orientation (approximately 13° from horizontal, and identical for D6N and D6H) is shown in Figure 2.12.3-27. The free drop impact occurred on the opposite side of the package from the vent port. The polyurethane foam temperature readings for test D6N were -3.5 °F, -4.0 °F, and -3.0 °F. Due to the short time interval between tests D6N and D6H, and to the cold ambient temperature, the foam temperatures for test D6H were negligibly different from those recorded for test D6N, and were thus below the target temperature of 0 °F. Accelerometer results are shown in the table below.

Accelerations, Free Drop Test D6								
Location	**T/U**	**T/L**	**OT/U**	**OT/L**	**Avg. Upper**	**Avg. Lower**	**Resolved ⊥ Upper**	**Resolved ⊥ Lower**
Test D6N	158g	75g	166g	78g	162g	77g	**166g**	**79g**
Test D6H	395g	159g	404g	178g	400g	169g	**411g**	**173g**

Like Test Series D2, the damage consisted of flat spots on the impact limiter and knuckle. After the D6H drop, the combined damage from both the NCT and HAC drops were as follows: the impact limiter flat was 21-3/4 inches long (along cask axis) and 30 inches wide (orthogonal). The knuckle flat was 11-1/4 inches long and 14-1/2 inches wide. At the height of the weld seam at the top of the cylindrical side of the impact limiter (essentially the lower impact point), the radial crush distance was 3-1/8 inches, using measurements based on the cask body O.D. Since the crush occurred with the cask axis at an angle of 13° to the ground, the crush in the direction of impact was 3-1/8 × cos(13) = 3.04 inches. (The crush at the knuckle was significantly less). An approximation of the amount of foam remaining was obtained by drilling a hole perpendicular to the flat damage surface, 17.5 inches from the bottom of the limiter. The bottom of the hole was approximately at the nearest point of hard flange material to the impact. The distance of foam, less the ¼-inch thick shell, was 7.0 – 0.25 = 6.75 inches. (This measurement was essentially confirmed after dissecting the impact limiter). It was noted that all of the rain shield bolts were snug. The package after the D6H drop is shown in Figure 2.12.3-28.

Puncture drop P7 orientation is shown in Figure 2.12.3-29. It occurred at the same azimuth as the free drops, i.e., opposite the vent port. The package was suspended over the puncture bar with the axis inclined at 30°, impact limiter up, and the axis of the puncture bar was aimed through the c.g. of the package. The temperature of the outermost thermal shield steel surface was 21.5 °F. The puncture bar struck the package approximately halfway up the cylindrical side and left an oblique dent 1-7/8 inches deep (measured on the outside). The 0.105-inch thick, outermost thermal shield was not ripped by the puncture bar, and there was no exposure of the inner thermal shield. The P7 puncture damage is shown in Figure 2.12.3-30.

Puncture drop P5 orientation is shown in Figure 2.12.3-31. It occurred at the azimuth of the vent port. The package was suspended essentially horizontally, with the puncture bar axis aiming perpendicularly to the package axis, slightly towards the bottom end from the c.g. This orientation was chosen to ensure that the puncture bar impact would occur on the tube sheet/rain shield region. Due to the difficulty in achieving a perfect impact location, trying to aim at the c.g. would present too large a risk of missing the desired impact point, given that the angle between the puncture bar and impact limiter slanted top surface was a very small acute angle. It was therefore judged that a horizontal package orientation represented the best choice for maximum damage. The puncture bar hit the slanted top of the impact limiter, and skidded up until it struck the tube sheet, which it deformed radially by ½-inches. The buckling of the ¼-inch thick tube sheet essentially stopped the impact progress, until the package bounced off of the bar and a secondary impact with the side thermal shield occurred. The rain shield was locally very slightly bent. The deformation of the top of the limiter caused the vent port tube opening to collapse onto the vent port insulation cylinder, which needed to be pried out. The P5 puncture damage is shown in Figure 2.12.3-32 and Figure 2.12.3-33. The dent in the vent port tube that trapped the vent port cylinder is shown in Figure 2.12.3-34. The vent port insulation cylinder was held securely in position by both the fully intact rain shield as well as the collapsed tube.

After Test Series D6 was complete, CTU #3 was disassembled for inspection. Prior to disassembly, a leak test was performed on the containment closure and vent port seals as discussed above. The results showed no detectable leak. The average removal torque of the closure bolts was 157 ft-lb, with a low value of 40 ft-lb and a high of 290 ft-lb.

The upper internal impact limiter was not crushed significantly, but the aluminum plate was somewhat buckled in the region of impact. The lower internal impact limiter was not significantly damaged. The P7 puncture dent, measured radially from the inside, was 1-1/2 inches high. An internal view of the dent is shown in Figure 2.12.3-35. A slightly different view is given in Figure 2.12.3-36, which shows the impression made on the inner surface of the containment boundary by the IC ribs, demonstrating that the puncture bar struck just adjacent to the ribs. Thus the bar was not supported by the IC ribs. The damage caused by the secondary bounce onto the bar in test P5, measured radially from the inside, was 9/16 inches high.

Since the IC was locked into the CTU #3 bell by the puncture sidewall damage, it was necessary to cut the bottom out and remove the IC wall by piecemeal cutting. The dummy payload cut through the IC wall somewhat in one location in the side drop (see Figure 2.12.3-37), but any buckling of the egg-crate reinforcements of the outside of the IC were minimal. The dummy payload did not engage more than one or two of the plywood sheets in the dunnage (top and bottom), and these sheets were significantly damaged in the side drop (see Figure 2.12.3-38). The balance of the dunnage was undamaged. The dummy payload was undamaged as shown in Figure 2.12.3-39. Two of the six bolts holding on the IC lid sheared off.

After all testing and disassembly, the containment boundary of CTU #3 was helium leakage rate tested. The maximum leakage rate was $1.9(10^{-7})$ He-cc/sec against a criteria of $2.2(10^{-7})$ He-cc/sec. Thus the package, after two complete series of free drop and puncture tests, was leaktight.

2.12.3.4.6 Test Series D4

Test Series D4 was performed on CTU #2 and consisted of a 4-ft NCT and a 30-ft HAC free drop in the side orientation (identical to the free drop orientations of Series D2 and D6), followed by a puncture drop test on the cylindrical side of the impact limiter through the c.g. The tests were designated D4N, D4H, and P4 for the 4-ft, 30-ft, and puncture drop, respectively. The free drop orientation (approximately 13° from horizontal, and identical for D4N and D4H) is shown in Figure 2.12.3-40. The free drop impact occurred at the vent port. The polyurethane foam temperature readings for test D4N were 118 °F and 120 °F. In contrast to the cold test cases, these readings were taken approximately 12 inches on either side of the impact point, at the regular depth of 9 inches. At a depth of 4.5 inches, the D4N temperatures were 112 and 120 °F. For test D4H, the corresponding temperatures at 9 inches were 116 and 119 °F, and at 4.5 inches, 90 and 116 °F. (The 90 °F temperature reading is doubtful.) Accelerometer results are shown in the table below.

Accelerations, Free Drop Test D4								
Location	**T/U**	**T/L**	**OT/U**	**OT/L**	**Avg. Upper**	**Avg. Lower**	**Resolved ⊥ Upper**	**Resolved ⊥ Lower**
Test D4N	144g	74g	130g	82g	137g	78g	**141g**	**80g**
Test D4H	356g	168g	372g	187g	364g	178g	**374g**	**183g**

Like Test Series D2 and D6, the damage consisted of flat spots on the impact limiter and knuckle. After the D4H drop, the combined damage from both the NCT and HAC drops were as follows: the impact limiter flat was 25-1/2 inches long (along cask axis) and 33 inches wide (orthogonal). The knuckle flat was 11-1/2 inches long and 18-1/2 inches wide. At the height of the weld seam at the top of the cylindrical side of the impact limiter (essentially the lower impact point), the radial crush distance was 4-13/16 inches, using measurements based on the cask body O.D. Since the crush occurred with the cask axis at an angle of 13° to the ground, the crush in the direction of impact was 4-13/16 × cos(13) = 4.68 inches. (The crush at the knuckle was significantly less). A measure of the amount of foam remaining was not obtained until after the puncture drop was complete. It was noted that all of the rain shield bolts were snug. The package after the D4H drop is shown in Figure 2.12.3-41.

Puncture drop P4 orientation is shown in Figure 2.12.3-42. It occurred on the free drop damage on the impact limiter (thus, at the vent port azimuth) with the bar aimed through the c.g. of the package. The measured angle of the package axis was 36° to the horizontal. The polyurethane foam temperature was 114 °F at 9 inches deep, and 99 °F at 4.5 inches deep. The puncture bar struck the package approximately 7-1/2 inches up the side from the flat bottom and skidded approximately 3-1/2 inches before stopping. There was no fissure or perforation of the impact limiter shell and no exposure of foam. The maximum depth of the puncture dent was 1-1/2 inches. The P4 puncture damage is shown in Figure 2.12.3-43.

After Test Series D4 was complete, CTU #2 was disassembled for inspection. Prior to disassembly, a leak test was performed on the containment closure and vent port seals as discussed above. The results showed no detectable leak. The average removal torque of the closure bolts was 101 ft-lb, with a low value of 0 ft-lb (found on two adjacent bolts) and a high of 270 ft-lb. Note that the closure bolts were not re-tightened between Test Series D3 and D4, and therefore these residual torques resulted from two complete test series.

Upon disassembly, the test O-ring seal was observed to be cut over an approximately 3-inch length. Since the leakage rate test was successful, it is presumed that this cut occurred during removal of the bell from the base. Since the bell and base were difficult to separate, the bell was not drawn off slowly but fell, with a sudden misalignment of the base to the bell, at which time the seal likely became cut by the sharp edge of the bell.

As expected, the tubes located at the impact of test D3 were crushed flat, and the plate of the upper internal impact limiter was buckled from both the D3 and D4 impacts. The pattern of tube crushing is shown in Figure 2.12.3-44. The deformation of the package due to Test Series D3 is shown in Figure 2.12.3-45 and Figure 2.12.3-46, where the head thermal shield has been locally cut away to expose the containment boundary. The lower internal impact limiter had little damage. The lodgment showed some buckling of the radial plate adjacent to the impact of the D3 test, but little other damage (see Figure 2.12.3-47). The LTSS was supported in essentially its original position. Note that the LTSS was thoroughly tested in Test Series D1 and D2. The only additional damage to the LTSS from Test Series D3 and D4 was some shallow deformations (approximately 1/8 inches or less) due to support from the lodgment's circular plates in the side (D4) free drops.

In the region of the D4 and P4 damage, the impact limiter was cut away on the plane of the free drop and puncture drop and measurements of the foam thickness made. The minimum depth of foam (not including the shell and gap), measured perpendicular to the outer surface of the foam to the hard flange upper corner, was 5-1/8 inches, and is shown in Figure 2.12.3-48. The distance from the bottom of the P4 puncture damage to the hard flange lower corner was 6-1/4 inches, and is shown in Figure 2.12.3-49.

After all testing and disassembly, the containment boundary of CTU #2 was helium leakage rate tested. The maximum leakage rate was $1.1(10^{-7})$ He-cc/sec against a criteria of $2.2(10^{-7})$ He-cc/sec. Thus the package, after two complete series of free drop and puncture tests, was leaktight.

2.12.3.5 Summary of Test Results

Certification testing was performed on the 435-B packaging design using three full scale CTUs. A total of six, 4-ft NCT free drops, six, 30-ft HAC free drops, and seven puncture drops were performed on the test units. After all tests, the CTUs were helium leaktight. Free drop accelerations were recorded for use in finite element model benchmarking and other structural analyses. The deformations of the packaging that could have an effect on performance in the HAC fire event were recorded. The deformations of the LTSS or the dummy shielded device were negligible, such that no change in the shielding performance is expected.

Table 2.12.3-1 – Certification Test Unit Configuration

CTU Configuration	SAR Production Unit Configuration	Justified in Section 2.12.3.3 paragraph number
Configuration Common to All CTUs (1, 2, and 3)		
Auxiliary vent port in sidewall	No vent port in sidewall	6
Threaded hole top of bell 1-8 UNC	Threaded hole top of bell ¾-10 UNC	7
Lifting plates on impact limiter	No plates	7
Accelerometer mounting blocks	No blocks	8
Thermocouple wire holes in melt-out plugs and foam	No holes	9
Vent and test port repair configuration shown in Figure 2.12.3-3	Configuration shown on 1916-01-01-SAR, sheet 6, Section M-M and Section N-N	10
Payload orienting tabs	No tabs	11
No caps over guide pin holes	Caps as shown on 1916-01-01-SAR sheet 4, Section F-F	13
No lead-in chamfer on bell opening	Lead-in chamfer as shown on 1916-01-01-SAR sheet 6, Detail AA	14
Three melt-out plugs equally spaced on impact limiter OD	Six plugs equally spaced	15
Additional Configuration Information for CTU #1		
Payload: Dummy LTSS in lodgment #1		
Impact limiter foam was 16 lb/ft^3	15 lb/ft^3 per 1916-01-01-SAR list of materials, I/N 19	1
Simulated thermal shield on side as shown in Figure 2.12.3.3-5	Full side thermal shield shown on 1916-01-01-SAR sheet 5, Detail R	3
No thermal shield on upper torispherical head	Full head thermal shield shown on 1916-01-01-SAR sheet 6, Detail T	4
Containment and Test O-ring diameter 44.6 inches	Diameter 44.1 inches	16
Lodgment OD 43 inches and lower corner 8 inches from base	Lodgment OD 42.75 inches and lower corner 10 inches from base	17

Table 2.12.3-1, continued

CTU Configuration	SAR Production Unit Configuration	Justified in Section 2.12.3.3 paragraph number
Additional Configuration Information for CTU #2		
Payload: Dummy LTSS in lodgment #2		
Impact limiter foam was 14 lb/ft^3	15 lb/ft^3 per 1916-01-01-SAR list of materials, I/N 19	2
Simulated thermal shield on side as shown in Figure 2.12.3.3-5	Full side thermal shield shown on 1916-01-01-SAR sheet 5, Detail R	3
Full head thermal shield shown on 1916-01-01-SAR sheet 6, Detail T	Full head thermal shield shown on 1916-01-01-SAR sheet 6, Detail T	4
Thermal shield interior surface finish not maintained	Interior surfaces of thermal shield finished per 1916-01-01-SAR, flag note 42	5
Containment and Test O-ring diameter 44.1 inches	Diameter 44.1 inches (i.e., same)	16
Lodgment OD 43 inches and lower corner 8 inches from base	Lodgment OD 42.75 inches and lower corner 10 inches from base	17
Additional Configuration Information for CTU #3		
Payload: IC with dummy device and dunnage		
Impact limiter foam was 16 lb/ft^3	15 lb/ft^3 per 1916-01-01-SAR list of materials, I/N 19	1
Full side thermal shield shown on 1916-01-01-SAR sheet 5, Detail R	Full side thermal shield shown on 1916-01-01-SAR sheet 5, Detail R	3
No thermal shield on upper head	Full head thermal shield shown on 1916-01-01-SAR sheet 6, Detail T	4
Thermal shield interior surface finish not maintained	Interior surfaces of thermal shield finished per 1916-01-01-SAR, flag note 42	5
IC lid rib continuous weld	Intermittent weld per 1916-01-03-SAR, sheet 2	12
Containment and Test O-ring diameter 44.6 inches	Diameter 44.1 inches	16
IC OD 43 inches	IC OD 42.75 inches	17

Table 2.12.3-2 – Certification Test Unit Weight, lb

	CTU #1	CTU #2	CTU #3
Base	2,280	2,216	2,285
Bell	2,315	2,394	2,435
Lodgment	512	508	1,110②
LTSS	4,460	4,460	3,870③
Total①	**9,642**	**9,653**	**9,775**

Notes:

1. Total weight includes 75 lb for closure bolts, washers, and rain shields.
2. Weight of inner container (IC).
3. CTU #3 used a dummy device weighing 3,570 lb and wood blocking weighing 300 lb. Tests D5N, D5H, and P6 used IC #1, and tests D6N, D6H, P5, and P7 used IC #2. Both ICs, when fully assembled, weighed the same.

Table 2.12.3-3 – Summary of Containment Boundary Integrated Leakage Rate Tests②

Test Unit	Leakage Rate, He-cc/sec①	Pass/Fail
CTU #1	$2.9(10^{-8})$	Pass
CTU #2	$1.1(10^{-7})$	Pass
CTU #3	$1.9(10^{-7})$	Pass

Notes:

1. Leak tight criteria is $2.2(10^{-7})$ He-cc/sec, which is equivalent to $1.0(10^{-7})$ std-cc/sec, air.
2. Containment seal and vent port seals were leak tight whenever checked (prior to each test series, and after test series D1, D2, D4, D5, and D6). After test series D3, a hard vacuum was sustained in lieu of a helium leakage rate test. The containment and vent port seals were not disturbed until after the next drop test series (D4) and subsequent helium leakage rate test had been successfully performed, thus assuring helium leaktightness after test series D3.

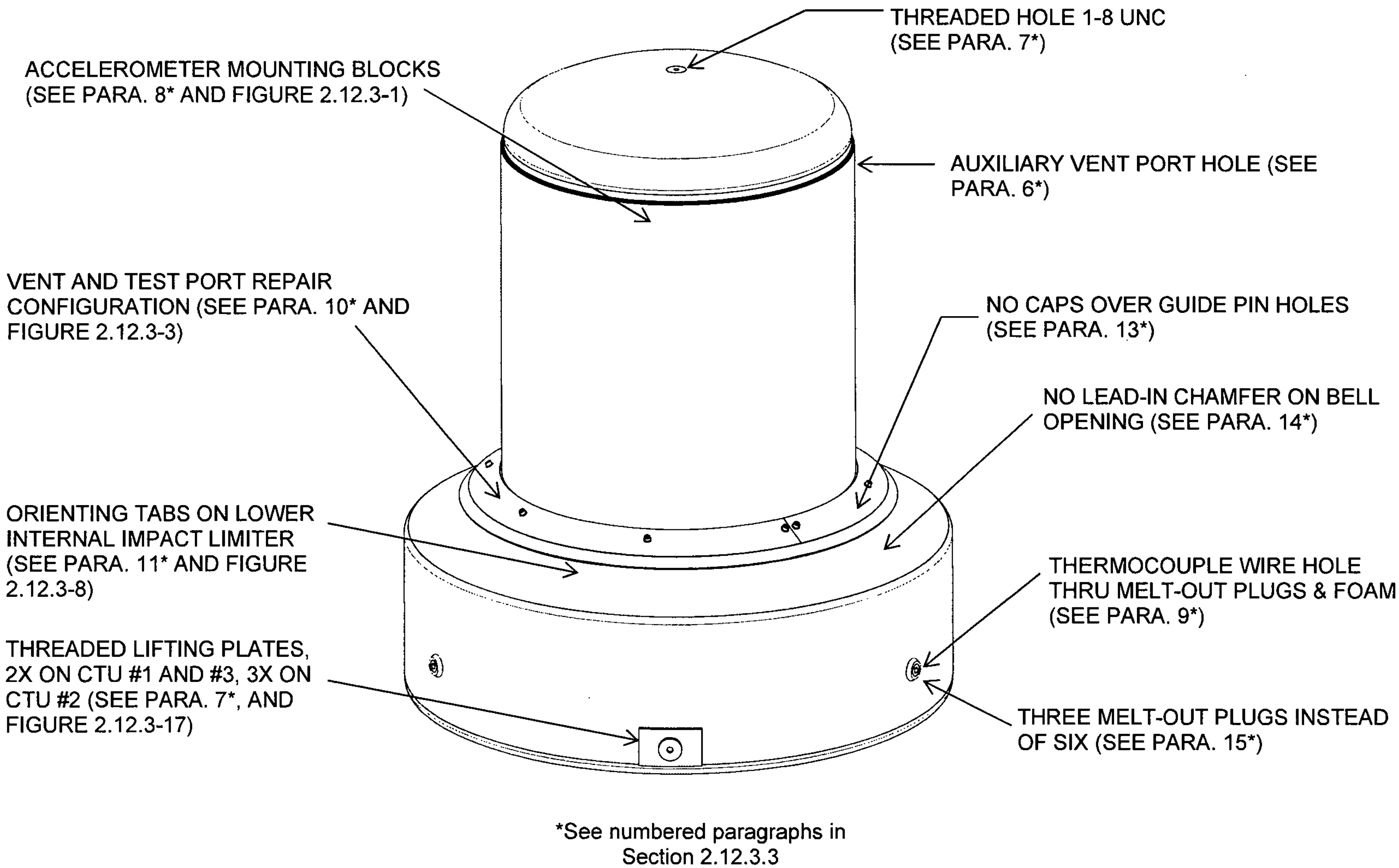

Figure 2.12.3.3-1 – CTU Common Configuration (Applies to CTU 1, 2, and 3)

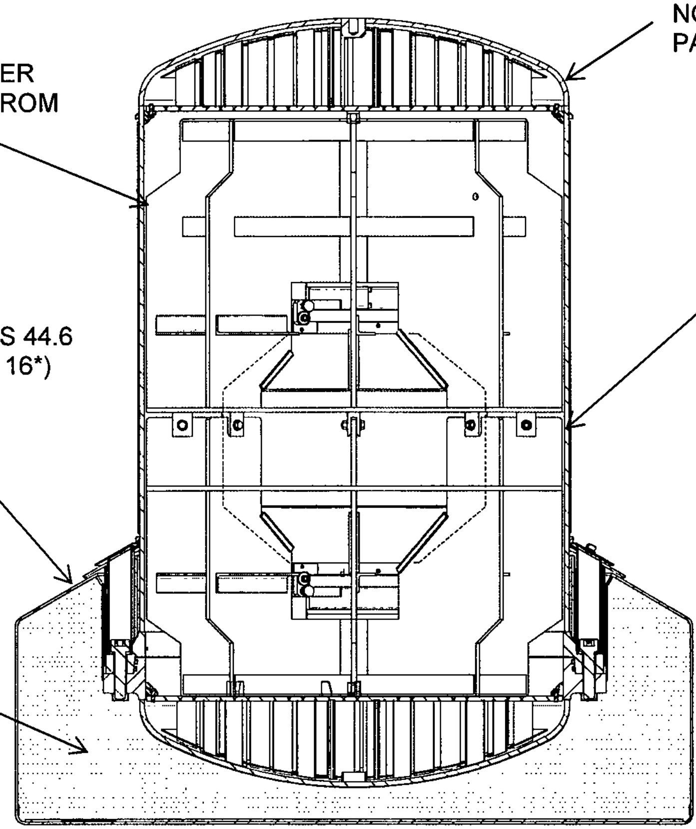

Payload: Lodgment and Dummy LTSS

*See numbered paragraphs in Section 2.12.3.3

Figure 2.12.3.3-2 – Additional Configuration Information for CTU #1 (All 'Common Configuration' Notations in Figure 2.12.3.3-1 Apply)

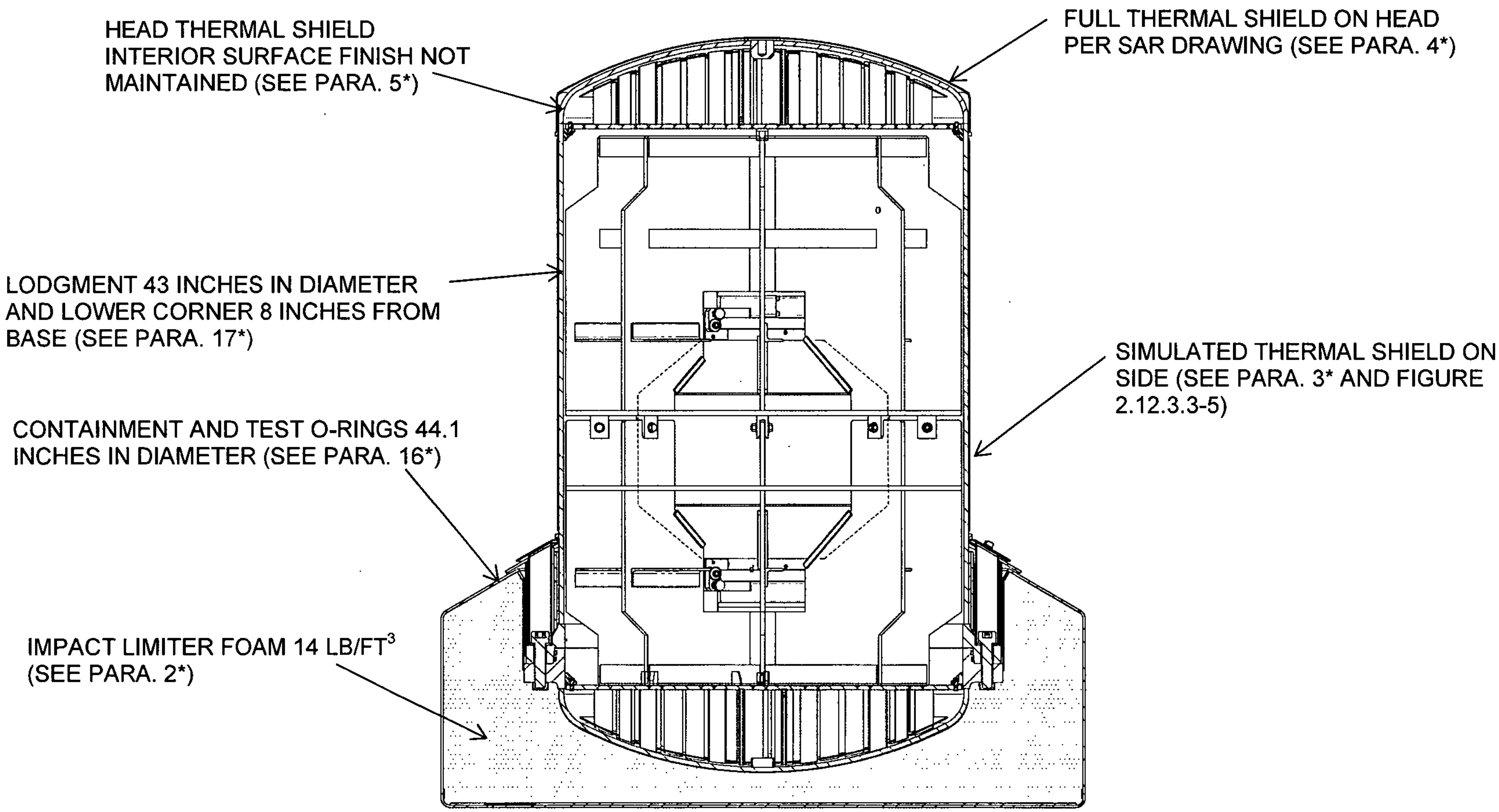

Payload: Lodgment and Dummy LTSS

Figure 2.12.3.3-3 – Additional Configuration Information for CTU #2 (All 'Common Configuration' Notations in Figure 2.12.3.3-1 Apply)

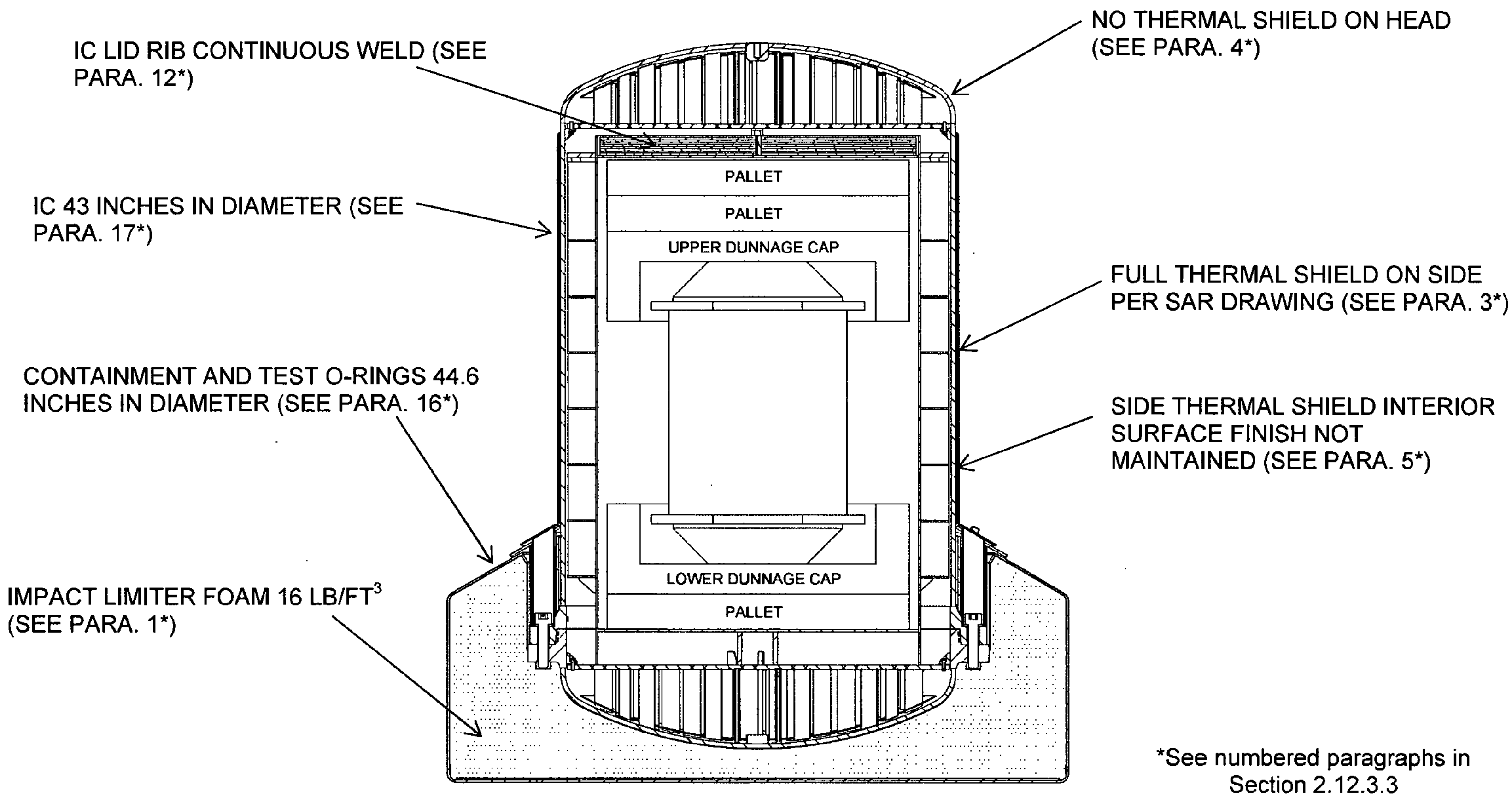

Payload: Inner Container (IC) with Dummy Device and Dunnage

Figure 2.12.3.3-4 – Additional Configuration Information for CTU #3 (All 'Common Configuration' Notations in Figure 2.12.3.3-1 Apply)

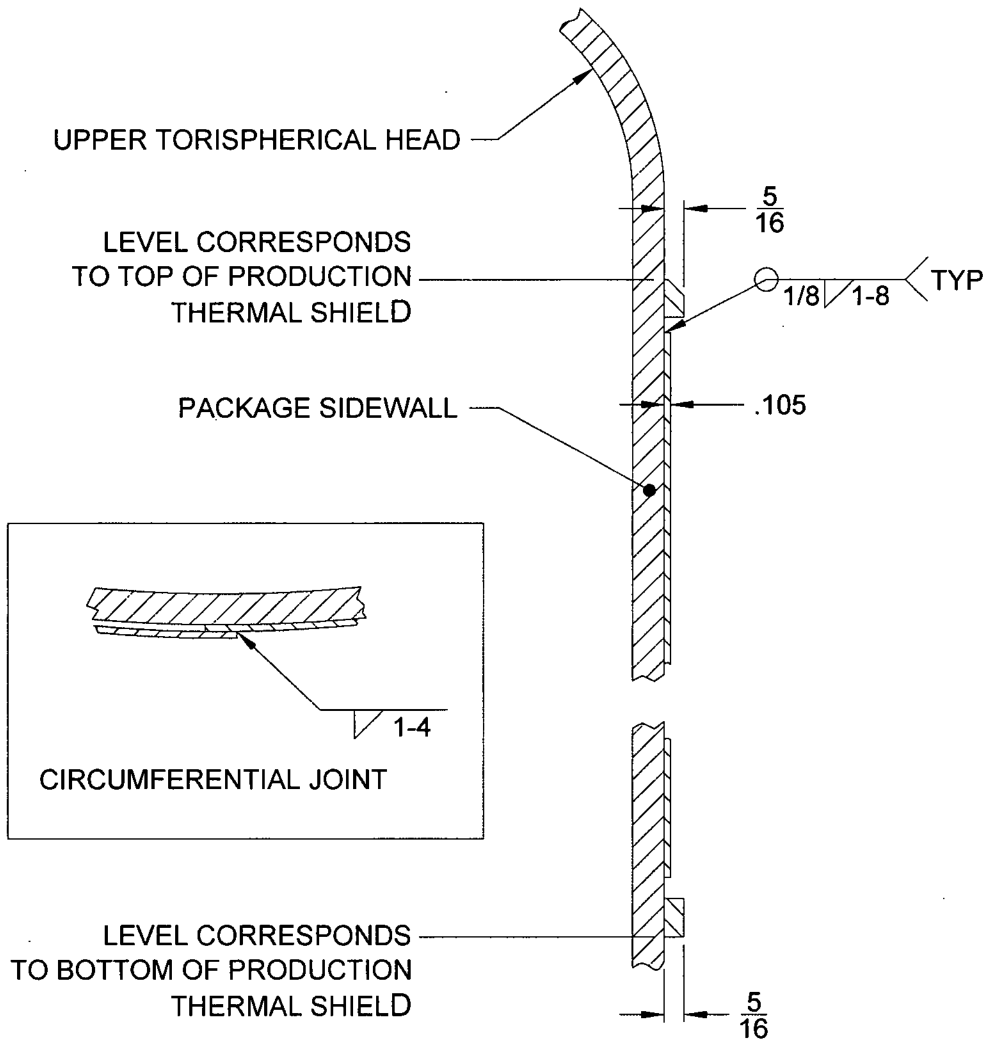

Figure 2.12.3.3-5 – Simulated Side Thermal Shield Detail (CTU #1 and CTU #2)

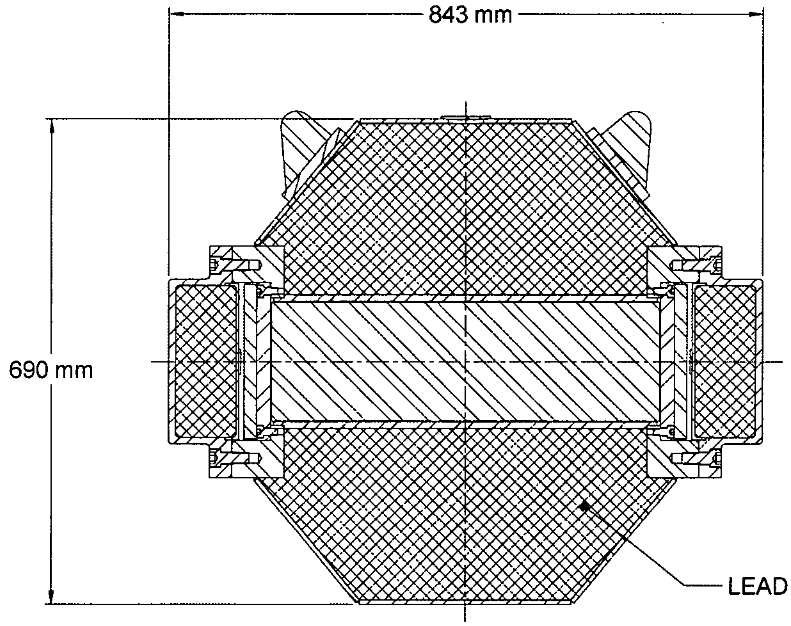

Figure 2.12.3.3-6 – Dummy LTSS

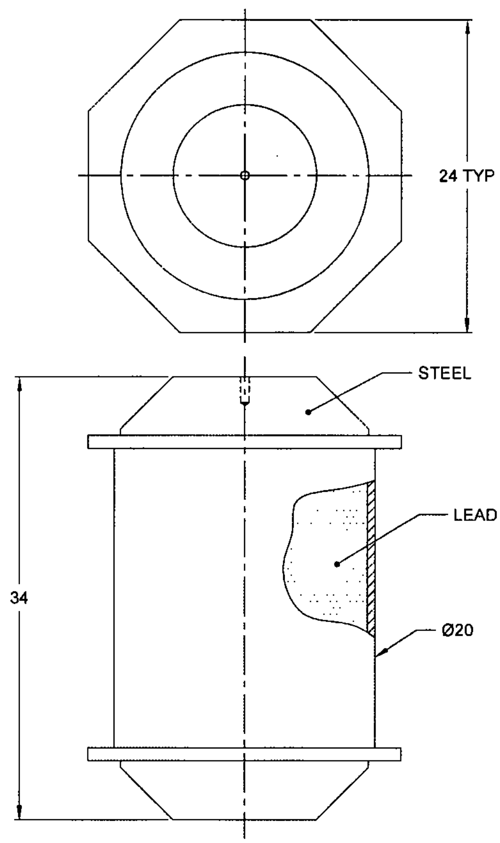

Figure 2.12.3.3-7 – Dummy Shielded Device

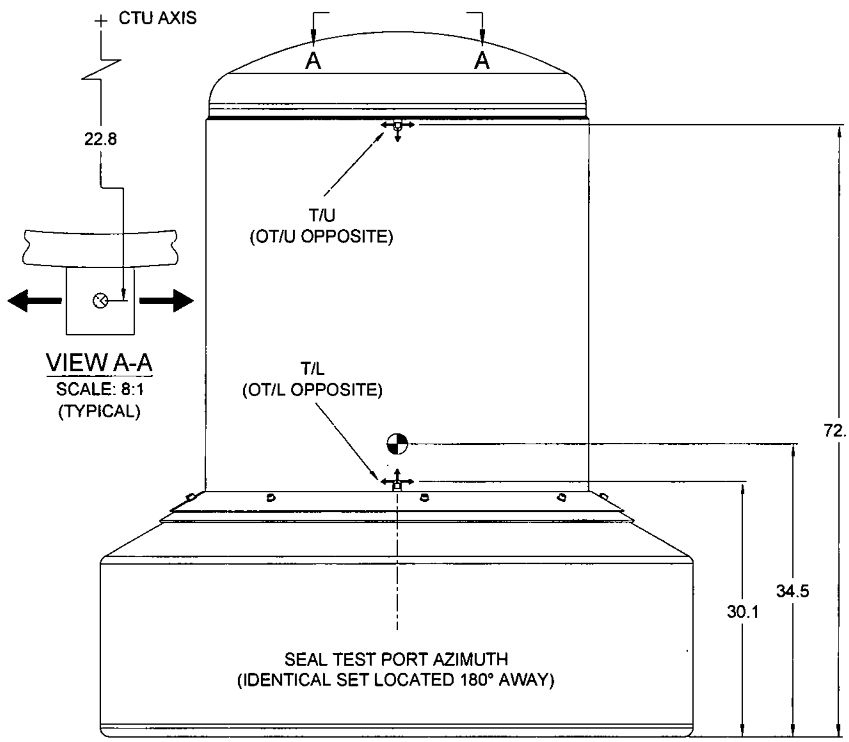

Figure 2.12.3-1 – Accelerometer Mounting

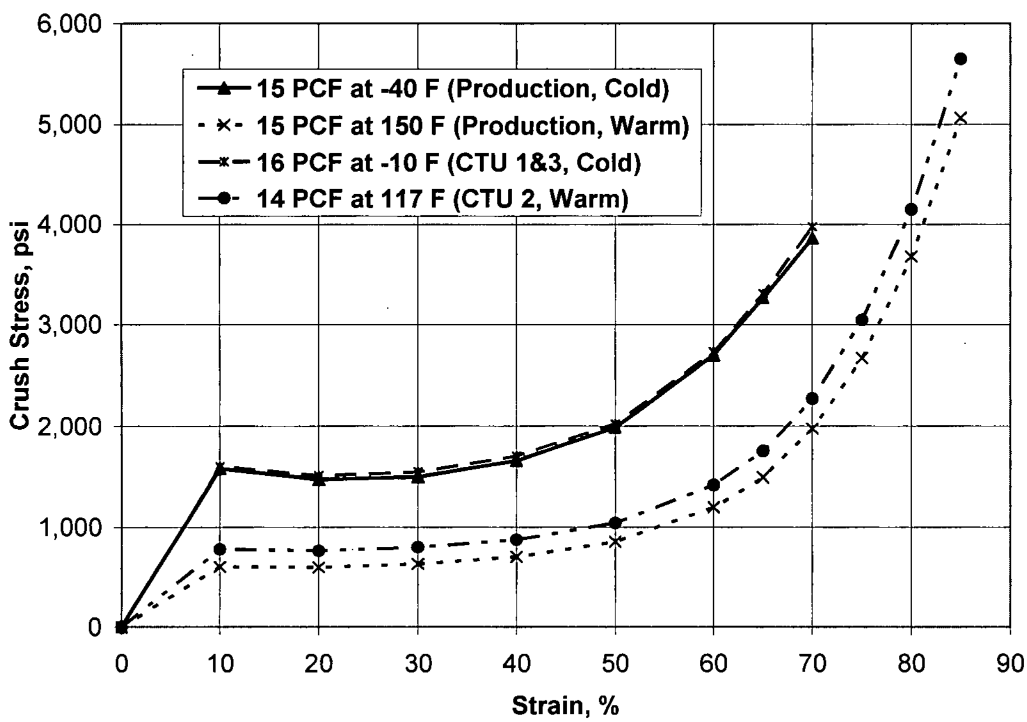

Figure 2.12.3-2 – Comparison of Foam Stress-Strain at Cold and Warm Conditions

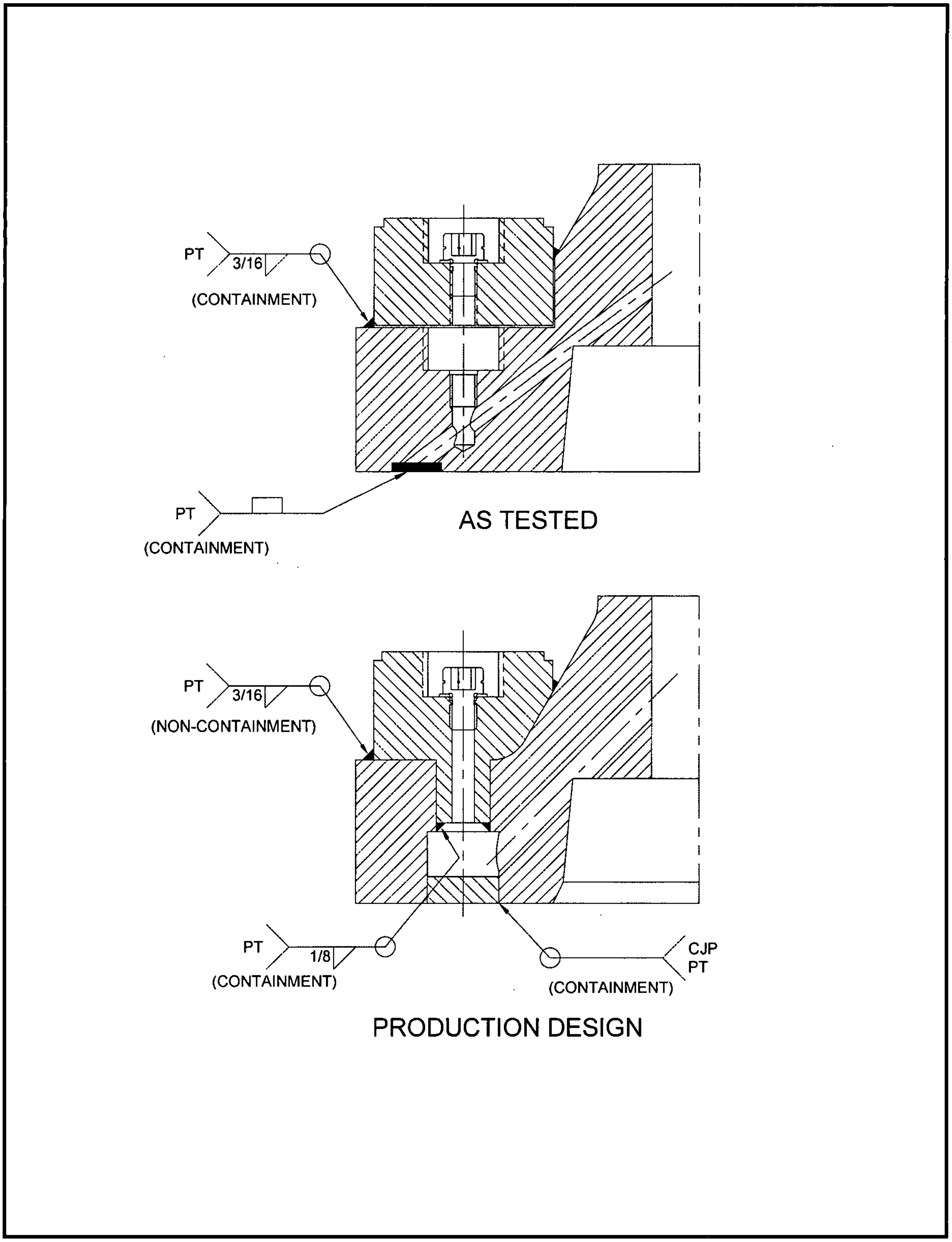

Figure 2.12.3-3 – Vent/Test Port Configuration Differences (Vent Port Shown)

Figure 2.12.3-4 – Free Drop Test D1N/D1H Orientation

Figure 2.12.3-5 – CTU #1 Condition After Free Drop Test D1H

Figure 2.12.3-6 – Puncture Drop Test P1 Orientation

Figure 2.12.3-7 – Damage to Impact Limiter Bottom Due to Puncture Drop Test P1

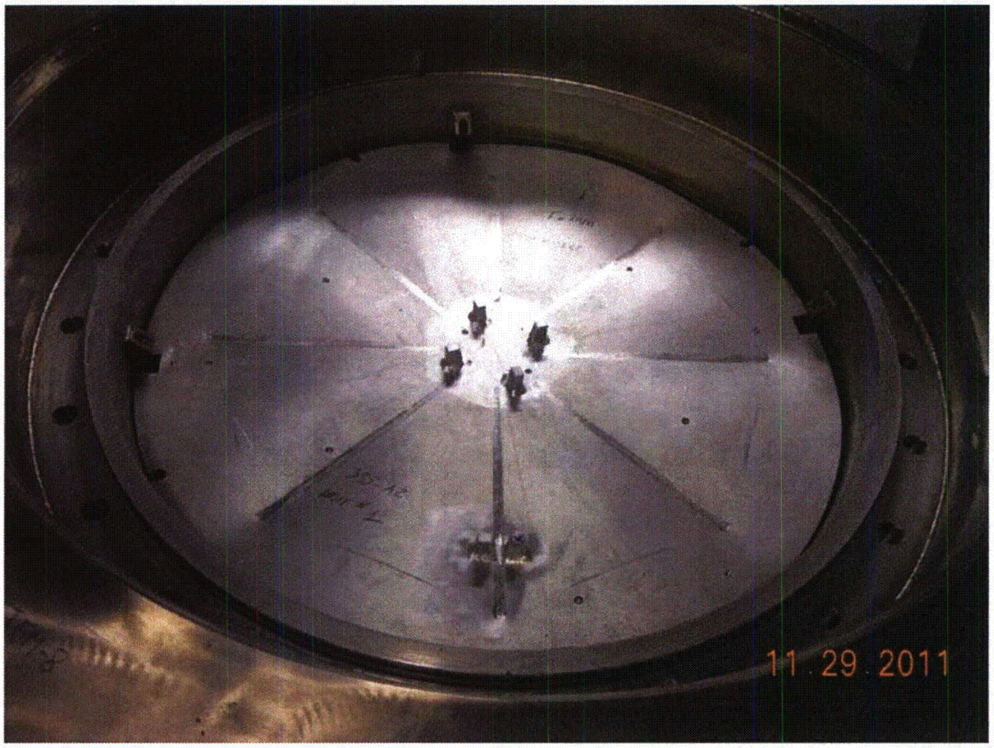

Figure 2.12.3-8 – Lower internal impact limiter, After D1 Series

Figure 2.12.3-9 – Lower internal impact limiter, View From Beneath, After D1 Test Series

Figure 2.12.3-10 – Free Drop Test D5N/D5H Orientation

Figure 2.12.3-11 – CTU #3 Condition After Free Drop Test D5H

Figure 2.12.3-12 – Puncture Drop Test P6 Orientation

Figure 2.12.3-13 – Damage to Impact Limiter Bottom Due to Puncture Drop Test P6

Figure 2.12.3-14 – Inner Container Lower Dunnage After D5 Test Series

Figure 2.12.3-15 – Detail of Lower Dunnage Damage After D5 Test Series

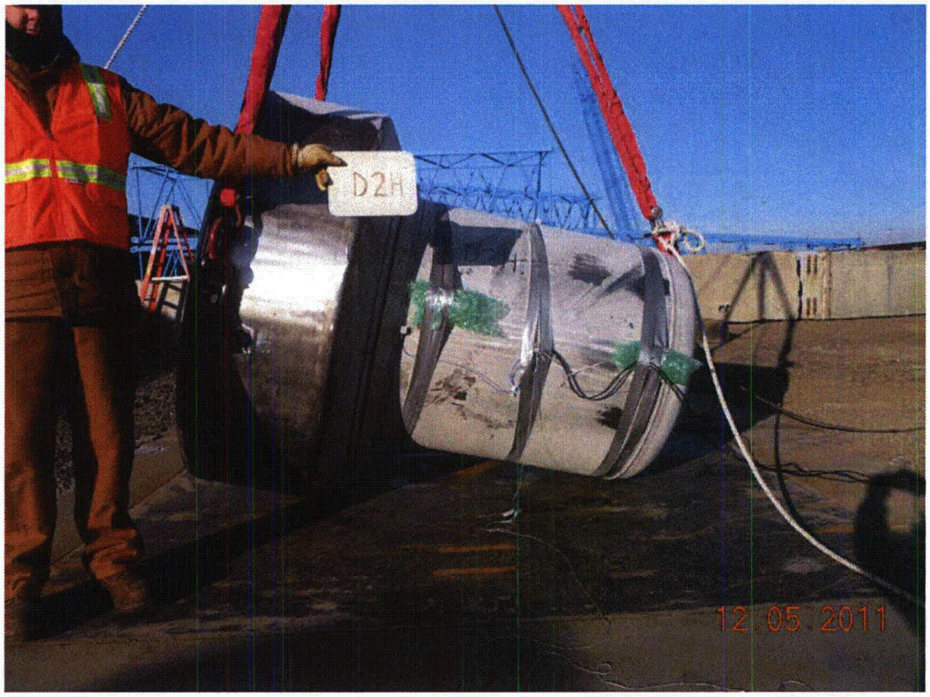

Figure 2.12.3-16 – Free Drop Test D2N/D2H Orientation

Figure 2.12.3-17 – CTU #1 Condition After Free Drop Test D2H

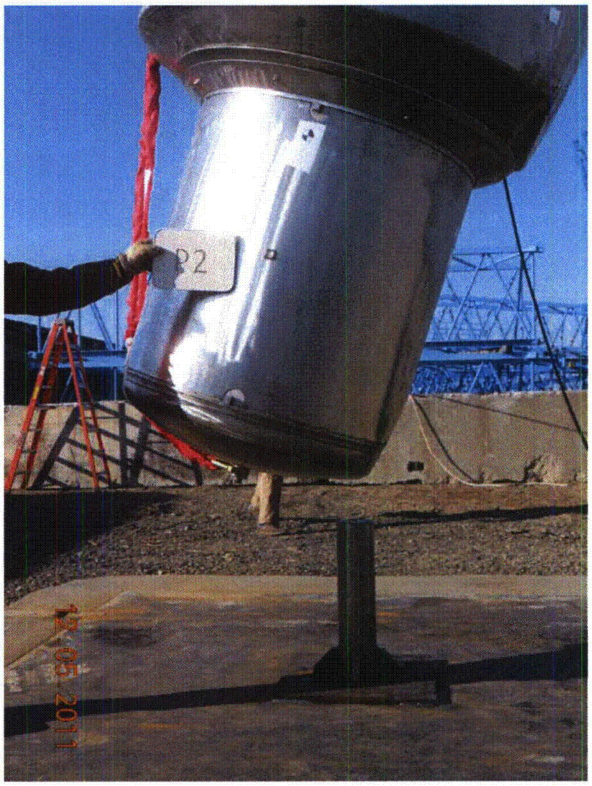

Figure 2.12.3-18 – Puncture Drop Test P2 Orientation

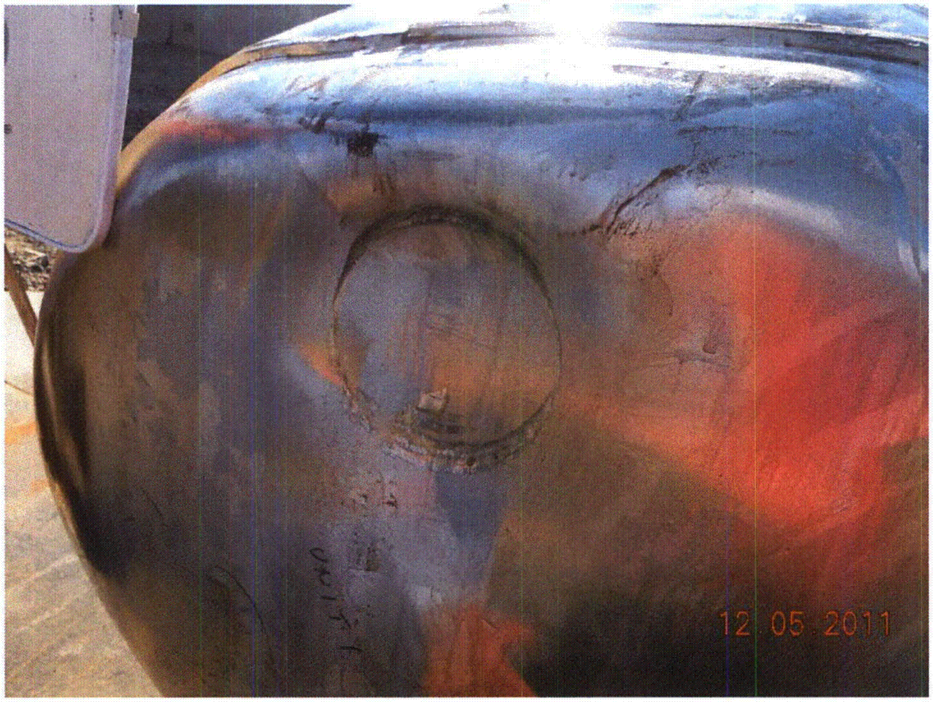

Figure 2.12.3-19 – Damage to Package Top Due to Puncture Drop Test P2

Figure 2.12.3-20 – General Condition of Lodgment & LTSS After D1 and D2 Test Series

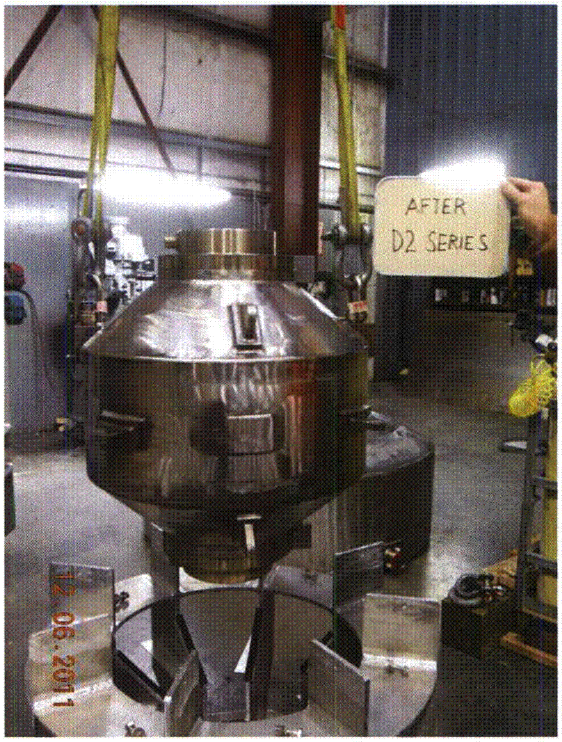

Figure 2.12.3-21 – Condition of LTSS After D1 and D2 Test Series

Figure 2.12.3-22 – Free Drop Test D3N/D3H Orientation

Figure 2.12.3-23 – CTU #2 Condition After Free Drop Test D3H

Figure 2.12.3-24 – Puncture Drop Test P3 Orientation

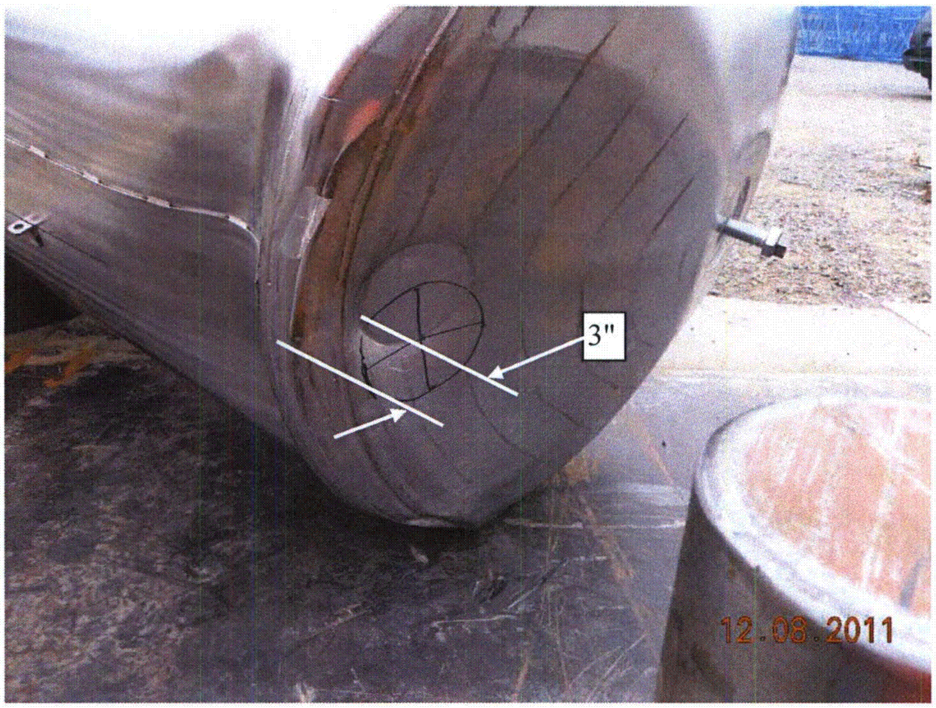

Figure 2.12.3-25 – Damage to Package Top Due to Puncture Drop Test P3

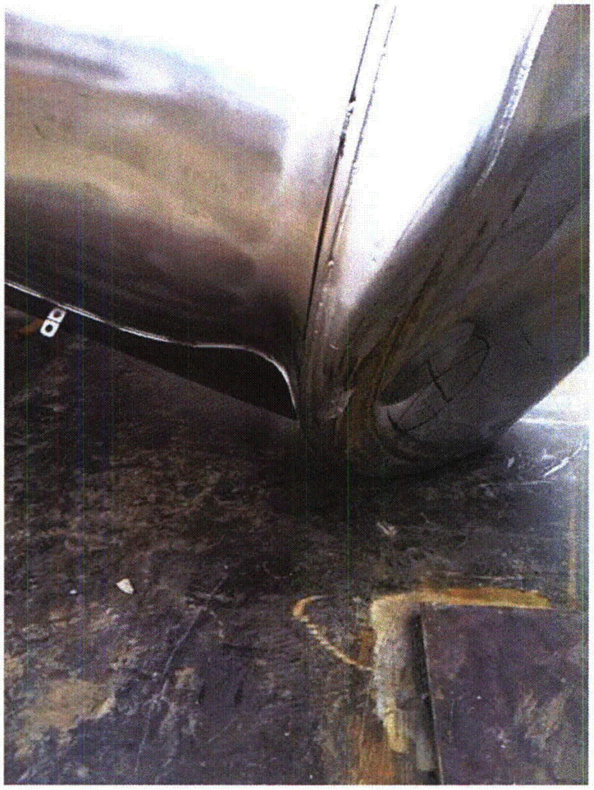

Figure 2.12.3-26 – Detail of Puncture Test P3 Damage

Figure 2.12.3-27 – Free Drop Test D6N/D6H Orientation

Figure 2.12.3-28 – CTU #3 Condition After Free Drop Test D6H (Also Showing P7)

Figure 2.12.3-29 – Puncture Drop Test P7 Orientation

Figure 2.12.3-30 – Damage to Package Side Due to Puncture Drop Test P7

Figure 2.12.3-31 – Puncture Drop Test P5 Orientation

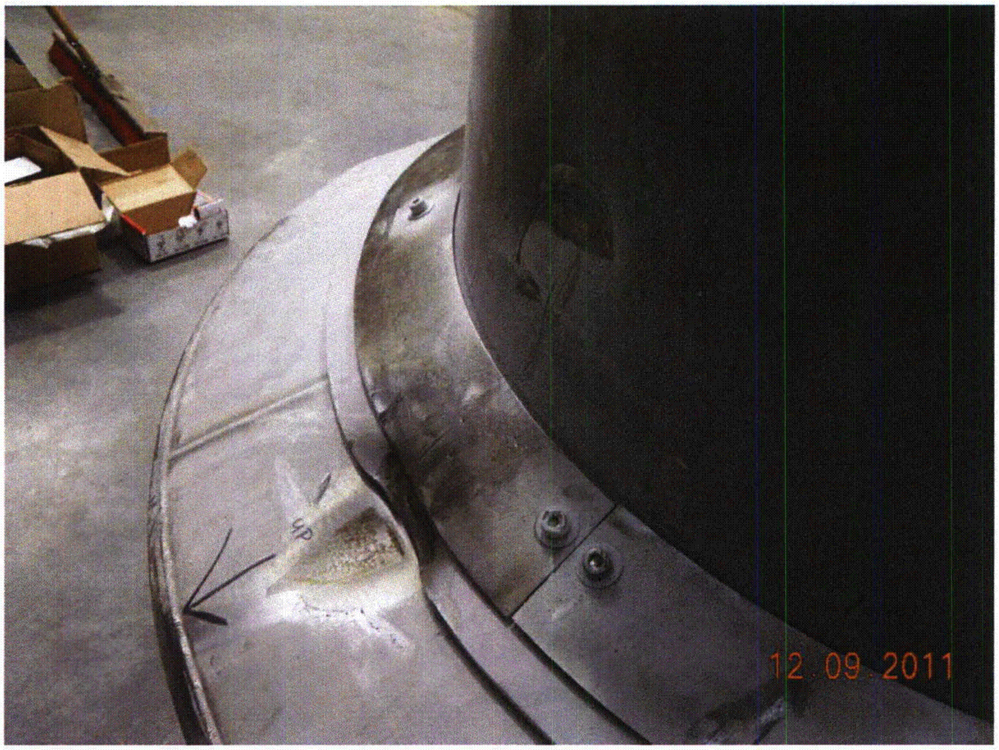

Figure 2.12.3-32 – Damage to Package Side Due to Puncture Drop Test P5

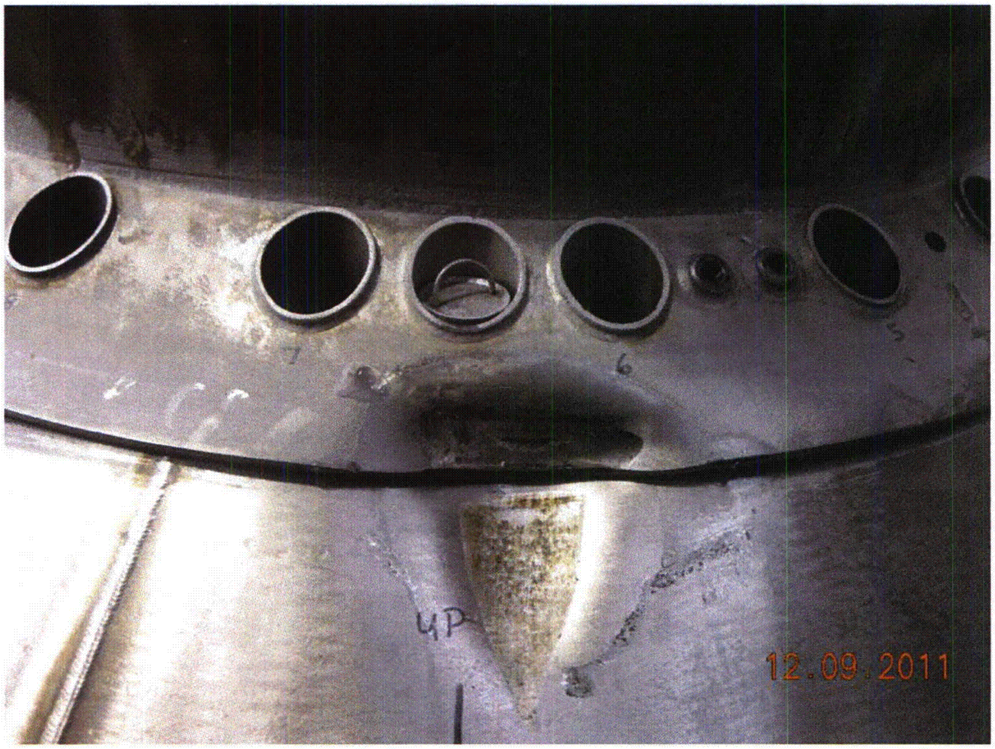

Figure 2.12.3-33 – Detail of Puncture Test P5 Damage (Rain Shield Removed)

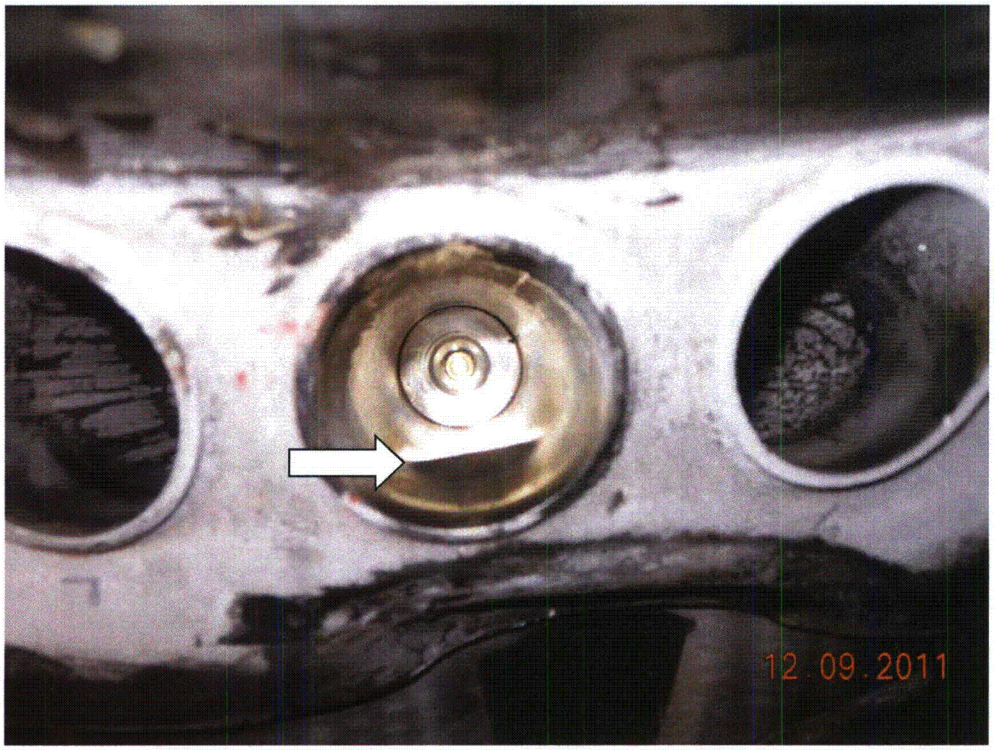

Figure 2.12.3-34 – Puncture Test P5 Damage Showing Internal Dent in Vent Port Tube

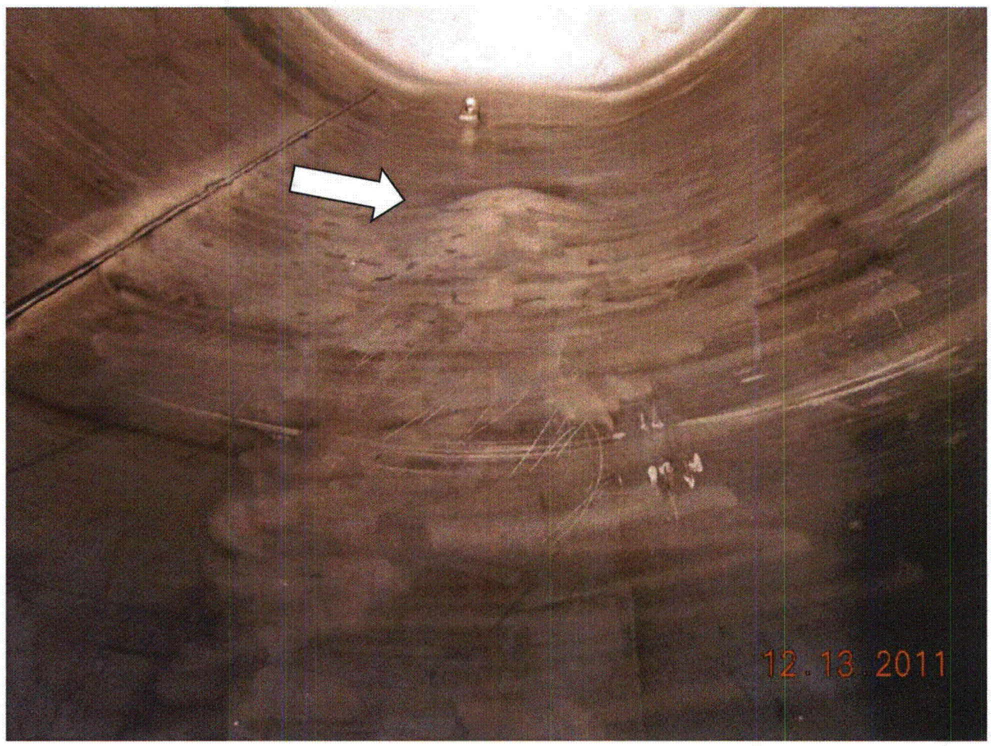

Figure 2.12.3-35 – Internal View of Damage from Puncture Test P7

Figure 2.12.3-36 – Internal View of Damage from Puncture Test P7, Detail

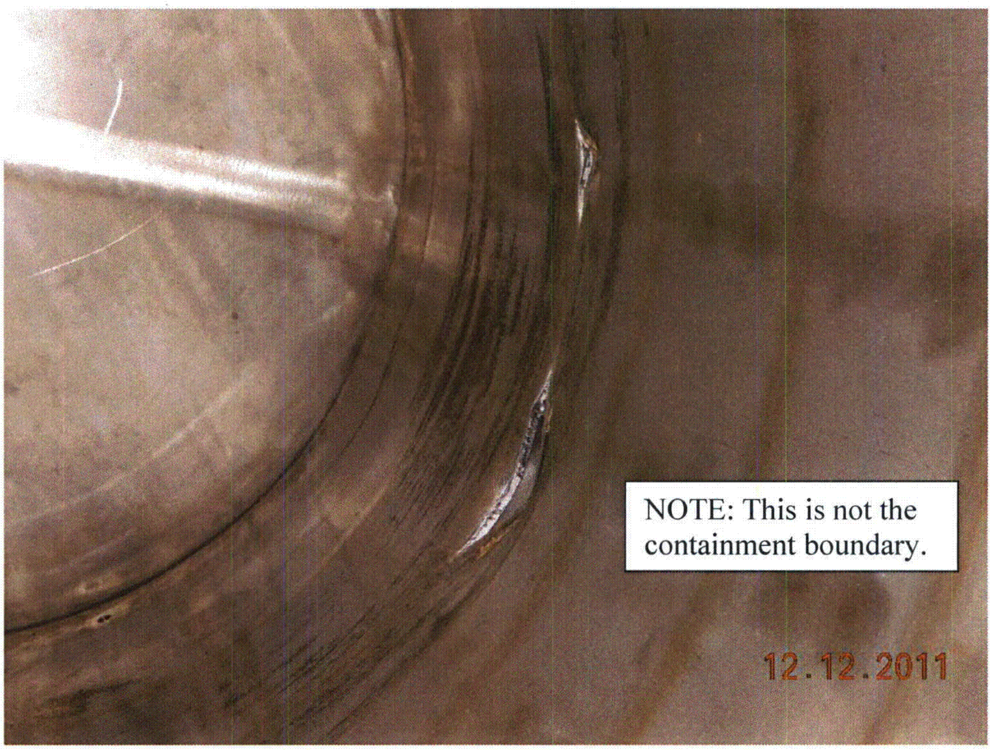

Figure 2.12.3-37 – Cut in Inner Container (IC) Wall Due to Dummy Payload Side Impact

Figure 2.12.3-38 – Dunnage After D6 Test Series

Figure 2.12.3-39 – Dummy Payload After D6 Test Series

Figure 2.12.3-40 – Free Drop Test D4N/D4H Orientation

Figure 2.12.3-41 – CTU #2 Condition After Free Drop Test D4H (Also Showing P4)

Figure 2.12.3-42 – Puncture Drop Test P4 Orientation

Figure 2.12.3-43 – Damage to Impact Limiter Side Due to Puncture Drop Test P4

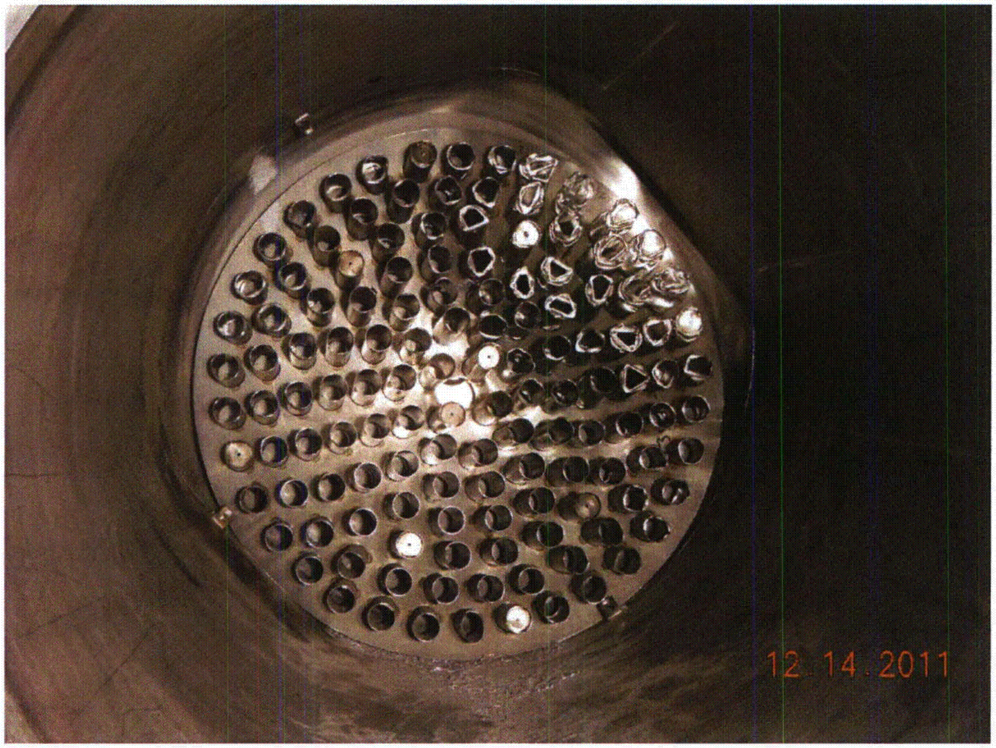

Figure 2.12.3-44 – Crushed Internal impact limiter Tubes (Upper) Due to Free Drop D3

Figure 2.12.3-45 – View of Damage Due to Test Series D3, Head Shield Cut Away (arrow indicates puncture bar impact location)

Figure 2.12.3-46 – View of Damage Due to Test Series D3

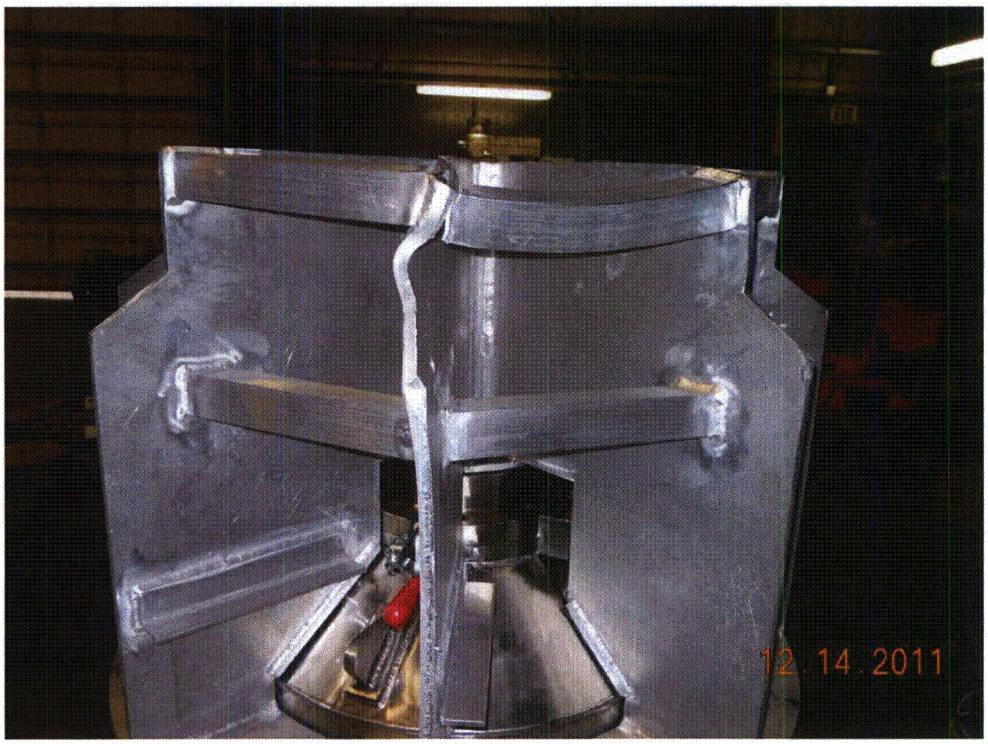

Figure 2.12.3-47 – Damage to Lodgment After Test Series D3 and D4

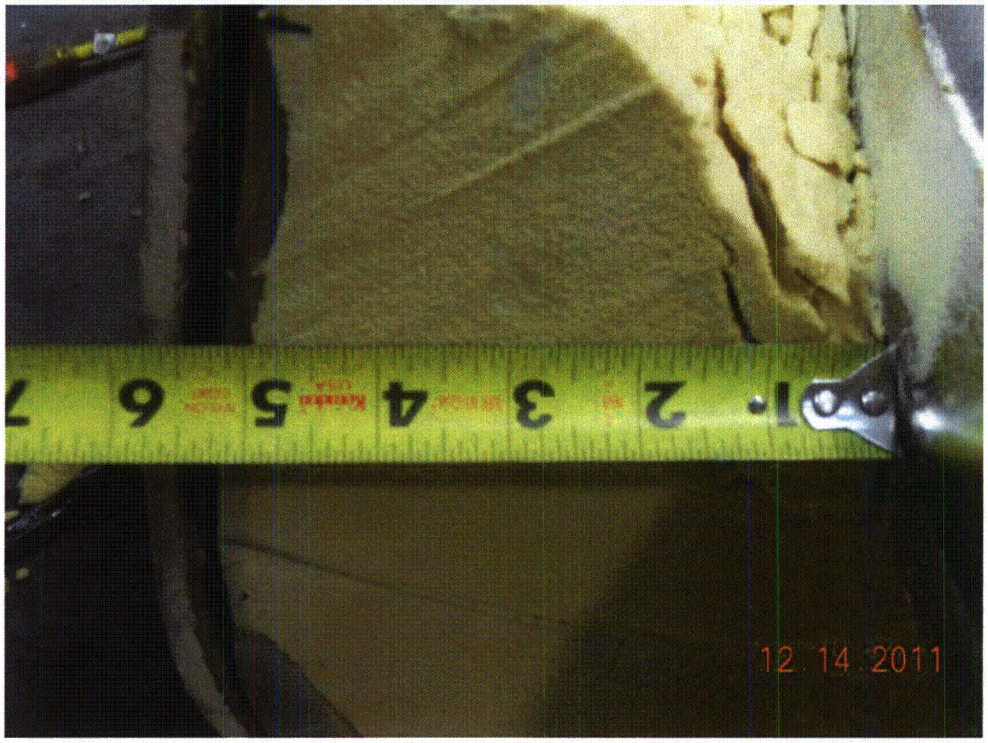

Figure 2.12.3-48 – Minimum Foam Remaining After Free Drop D4H

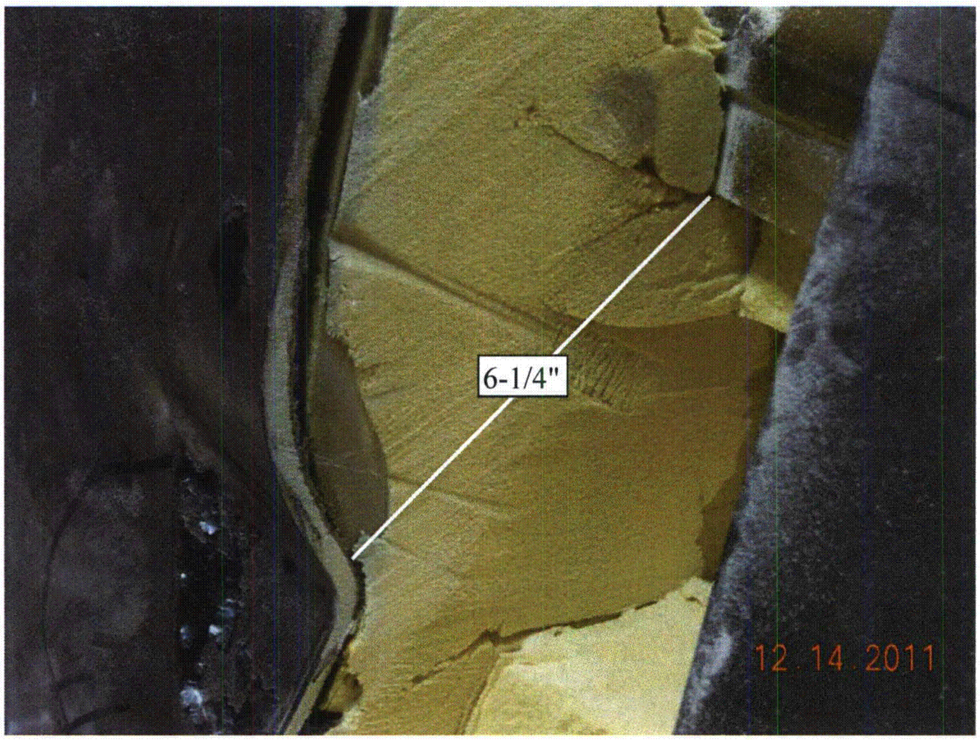

Figure 2.12.3-49 – Minimum Foam Remaining After Puncture P4

2.12.3.6 Filtered Accelerometer Time Histories

Accelerometer time history plots are provided below. Information identifying each plot is given above the figure as: drop test I.D.; drop height in ft; channel no.; location on CTU (see Section 2.12.3.2.2, *Instrumentation*, for description); filter cutoff frequency (500 Hz in all cases); and peak value, g.

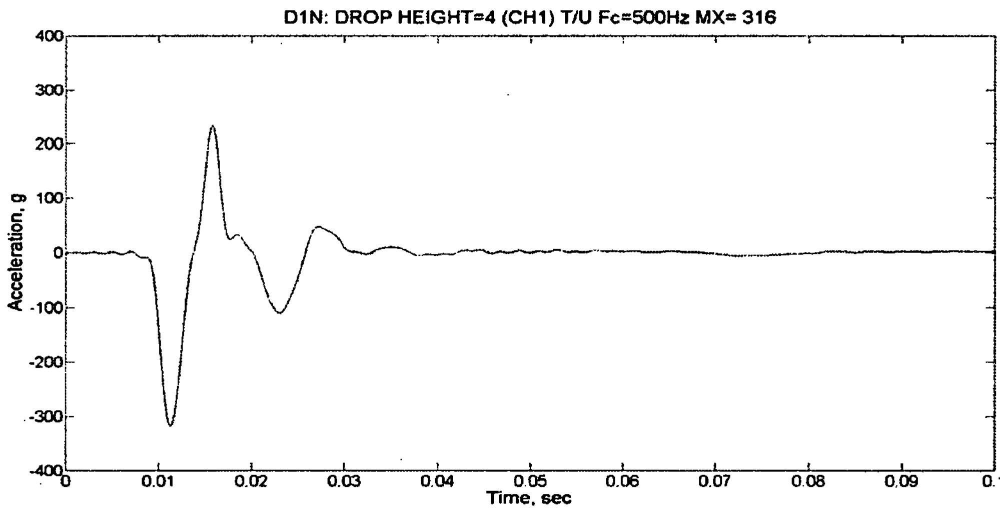

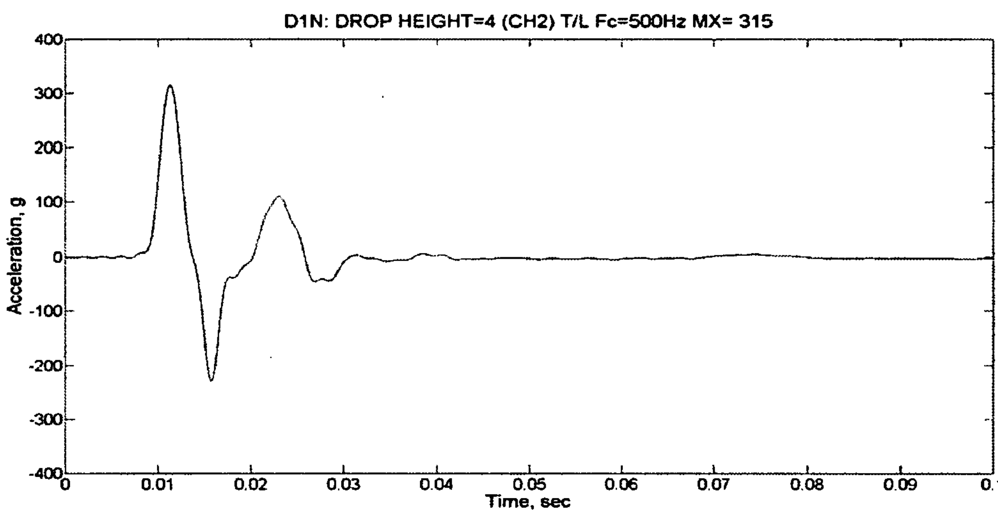

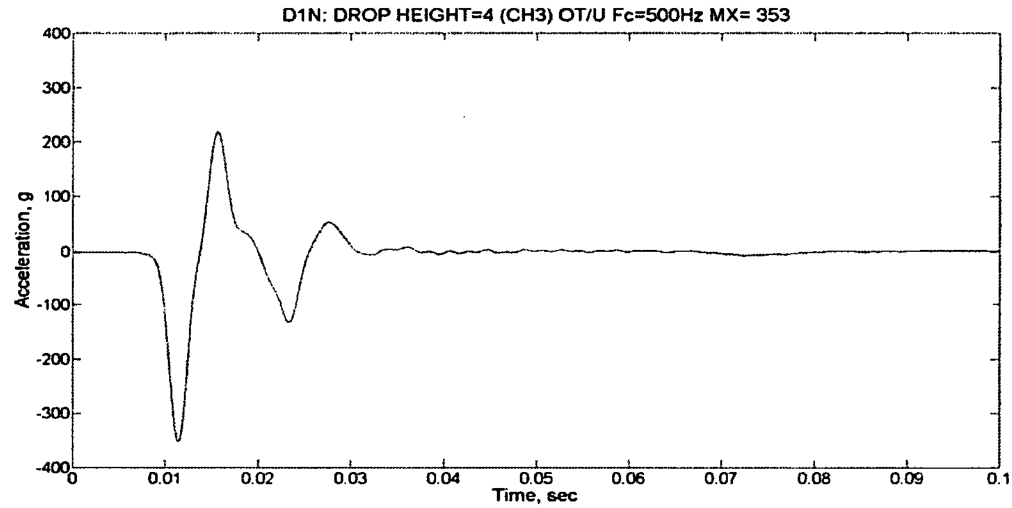
D1N: DROP HEIGHT=4 (CH3) OT/U Fc=500Hz MX= 353
Acceleration, g
Time, sec

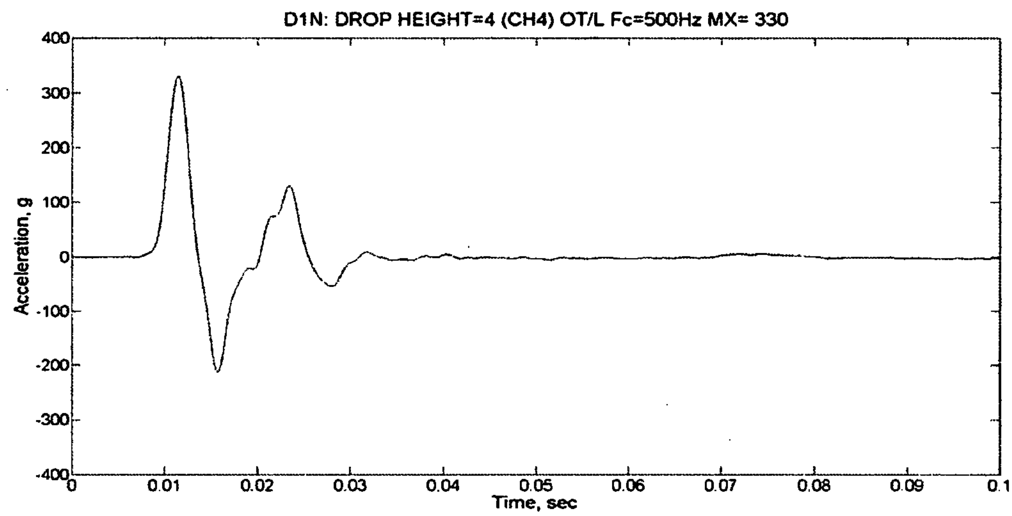
D1N: DROP HEIGHT=4 (CH4) OT/L Fc=500Hz MX= 330
Acceleration, g
Time, sec

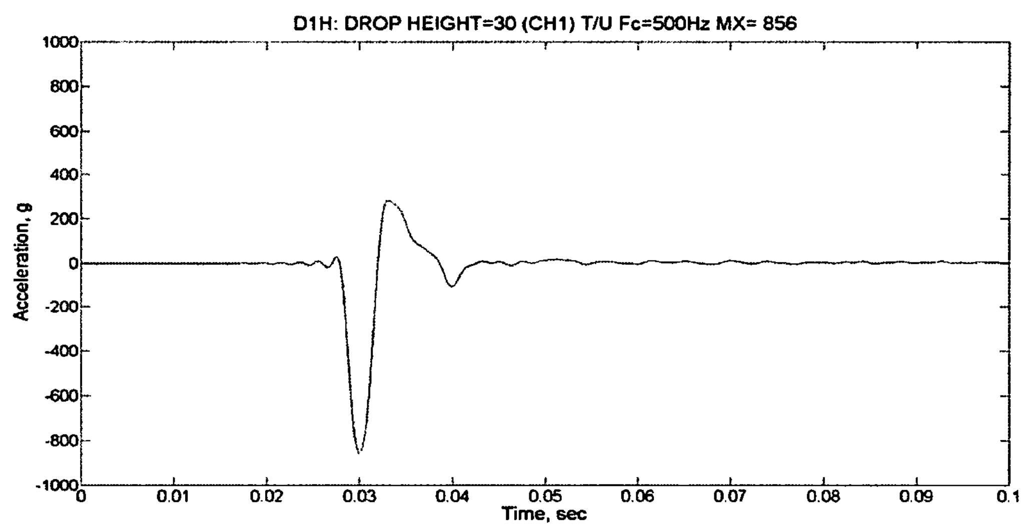
D1H: DROP HEIGHT=30 (CH1) T/U Fc=500Hz MX= 856
Acceleration, g
Time, sec

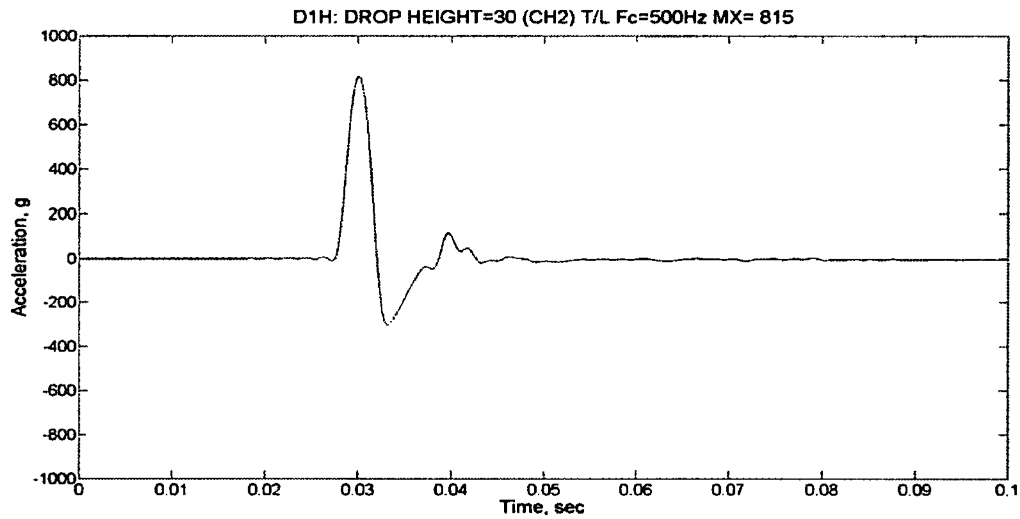
D1H: DROP HEIGHT=30 (CH2) T/L Fc=500Hz MX= 815
Acceleration, g
Time, sec
1000
800
600
400
200
0
-200
-400
-600
-800
-1000
0
0.01
0.02
0.03
0.04
0.05
0.06
0.07
0.08
0.09
0.1

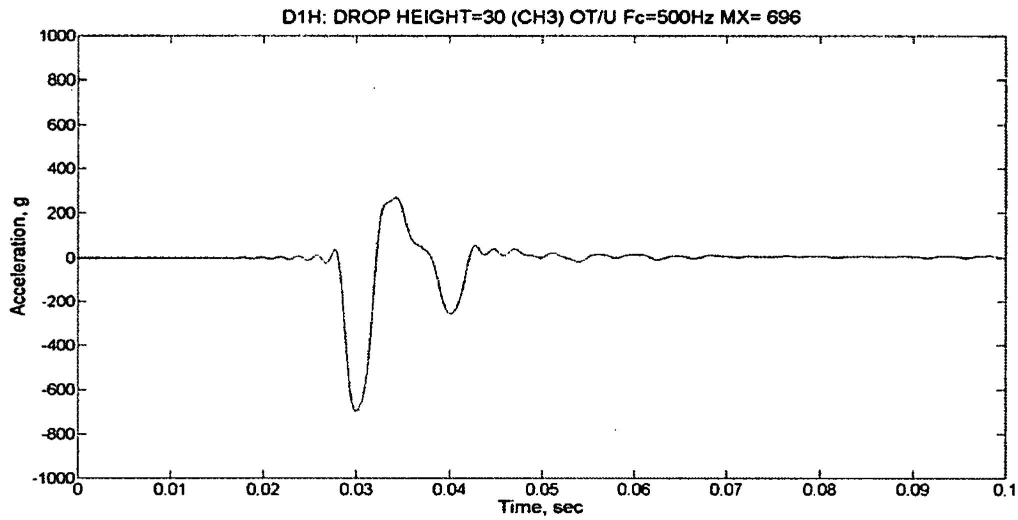
D1H: DROP HEIGHT=30 (CH3) OT/U Fc=500Hz MX= 696
Acceleration, g
Time, sec
1000
800
600
400
200
0
-200
-400
-600
-800
-1000
0
0.01
0.02
0.03
0.04
0.05
0.06
0.07
0.08
0.09
0.1

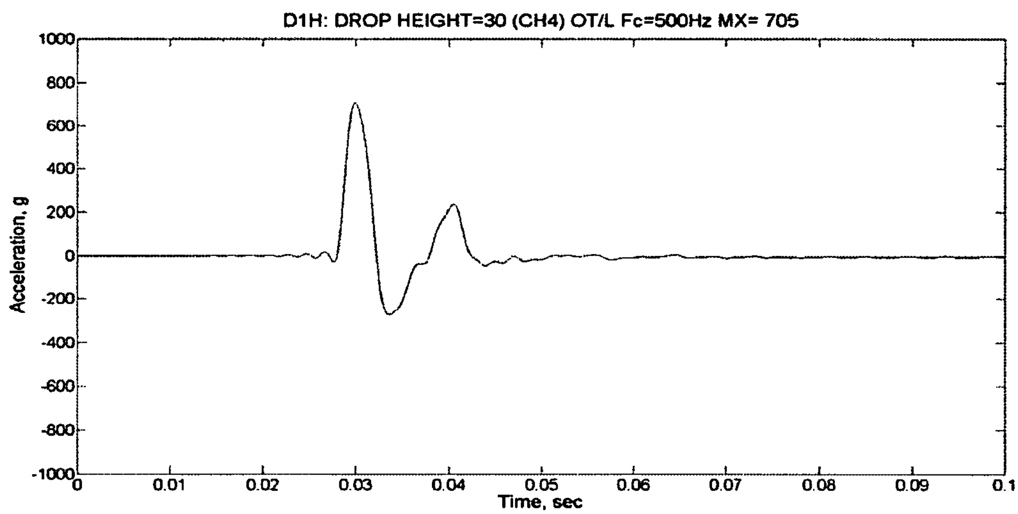
D1H: DROP HEIGHT=30 (CH4) OT/L Fc=500Hz MX= 705
Acceleration, g
Time, sec
1000
800
600
400
200
0
-200
-400
-600
-800
-1000
0
0.01
0.02
0.03
0.04
0.05
0.06
0.07
0.08
0.09
0.1

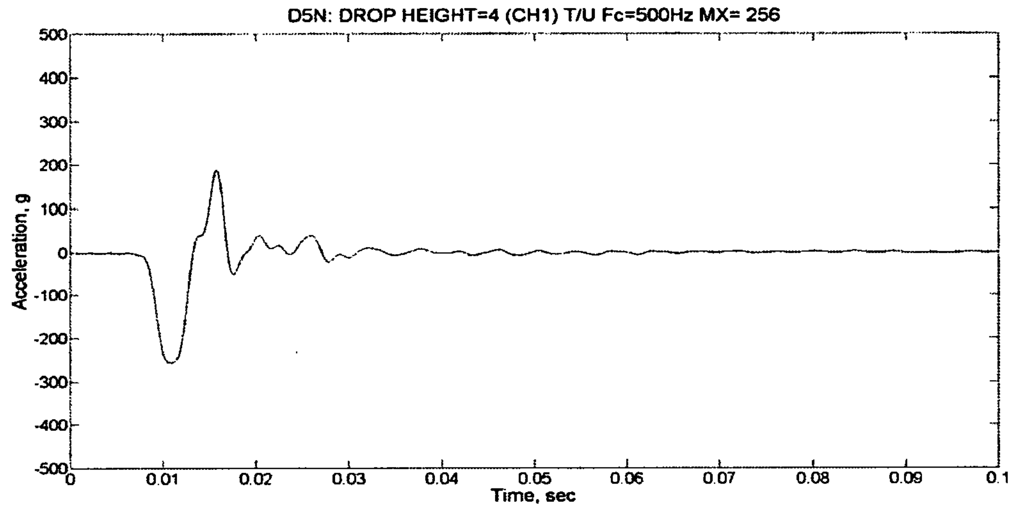
D5N: DROP HEIGHT=4 (CH1) T/U Fc=500Hz MX= 256
Acceleration, g
500
400
300
200
100
0
-100
-200
-300
-400
-500
0
0.01
0.02
0.03
0.04
0.05
0.06
0.07
0.08
0.09
0.1
Time, sec

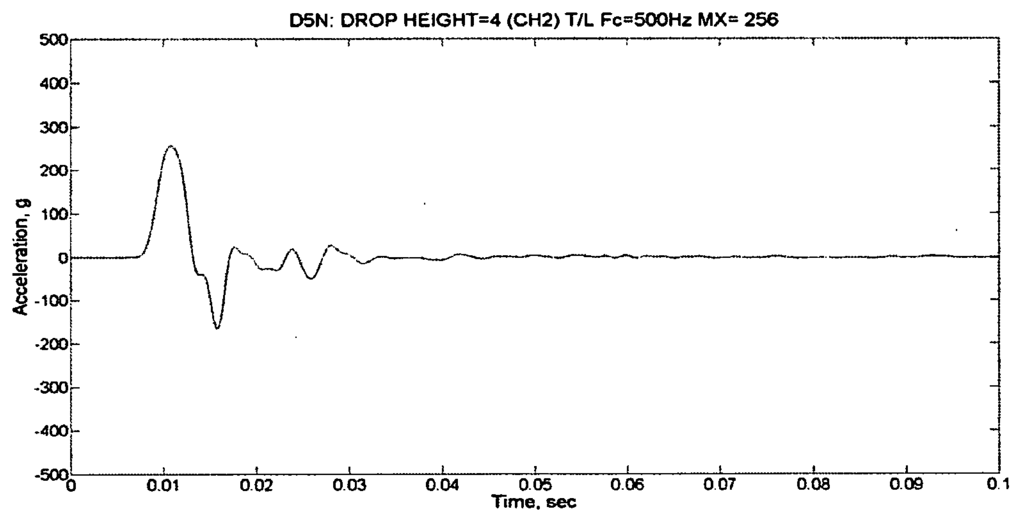
D5N: DROP HEIGHT=4 (CH2) T/L Fc=500Hz MX= 256
Acceleration, g
500
400
300
200
100
0
-100
-200
-300
-400
-500
0
0.01
0.02
0.03
0.04
0.05
0.06
0.07
0.08
0.09
0.1
Time, sec

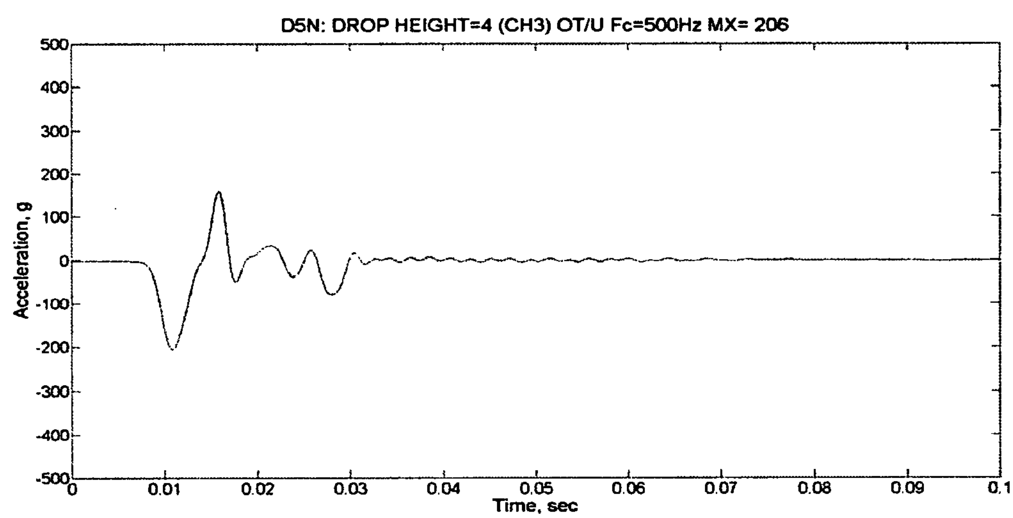
D5N: DROP HEIGHT=4 (CH3) OT/U Fc=500Hz MX= 206
Acceleration, g
500
400
300
200
100
0
-100
-200
-300
-400
-500
0
0.01
0.02
0.03
0.04
0.05
0.06
0.07
0.08
0.09
0.1
Time, sec

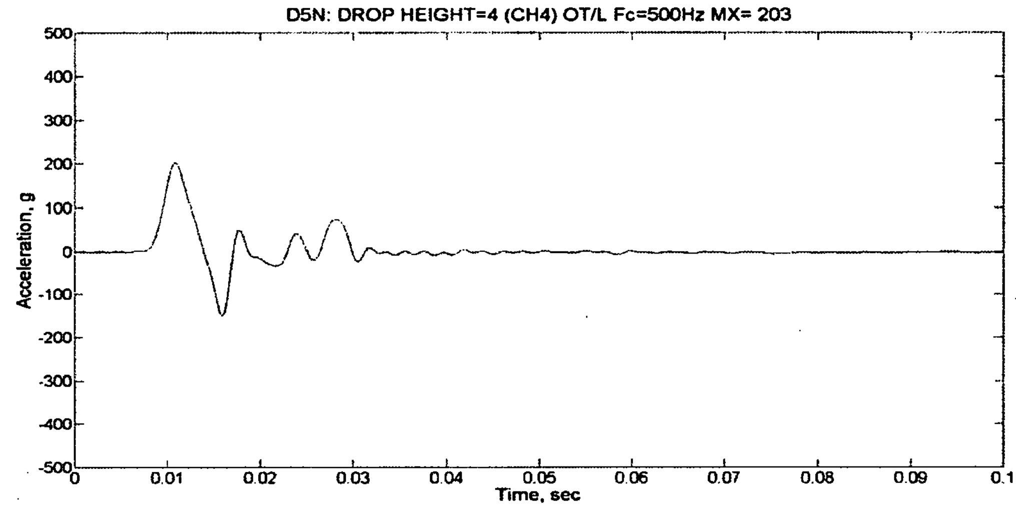
D5N: DROP HEIGHT=4 (CH4) OT/L Fc=500Hz MX= 203
Acceleration, g
Time, sec

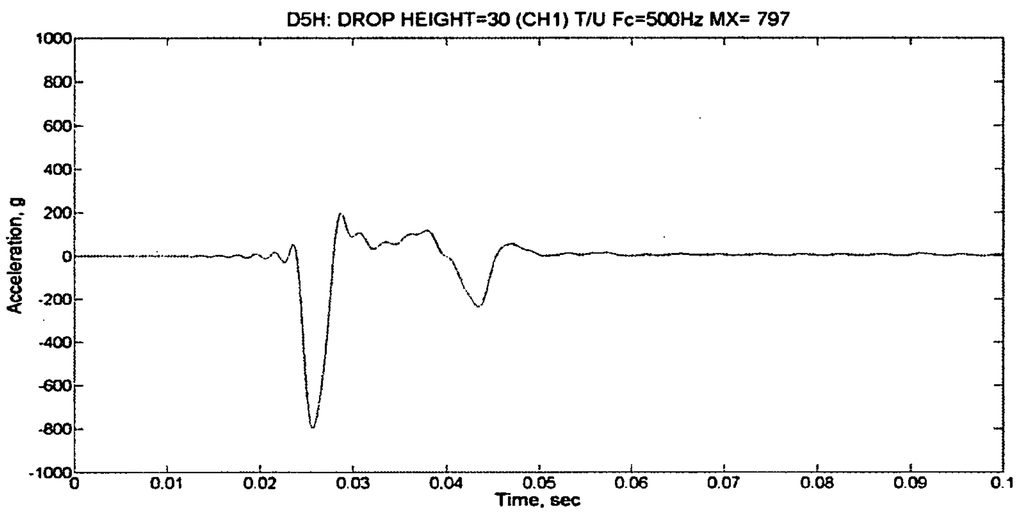
D5H: DROP HEIGHT=30 (CH1) T/U Fc=500Hz MX= 797
Acceleration, g
Time, sec

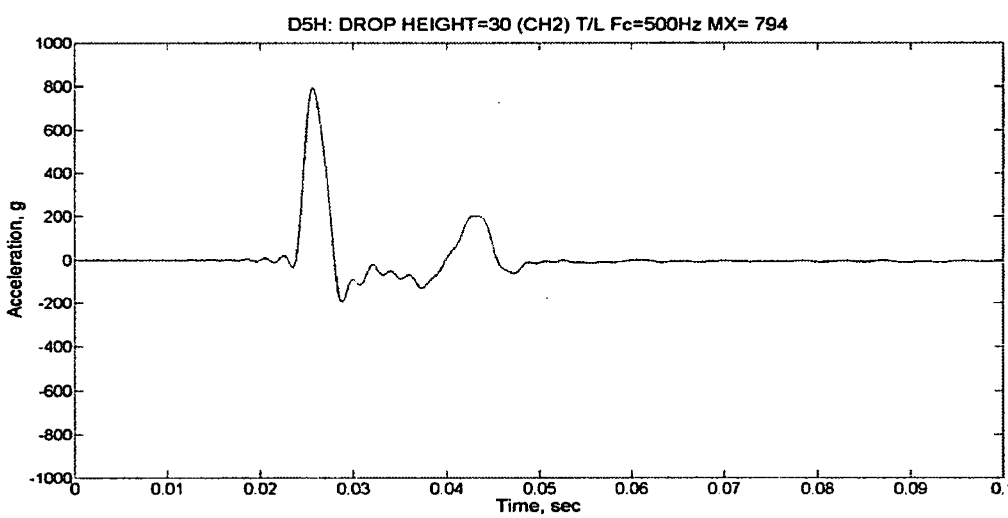
D5H: DROP HEIGHT=30 (CH2) T/L Fc=500Hz MX= 794
Acceleration, g
Time, sec

D5H: DROP HEIGHT=30 (CH3) OT/U Fc=500Hz MX= 855

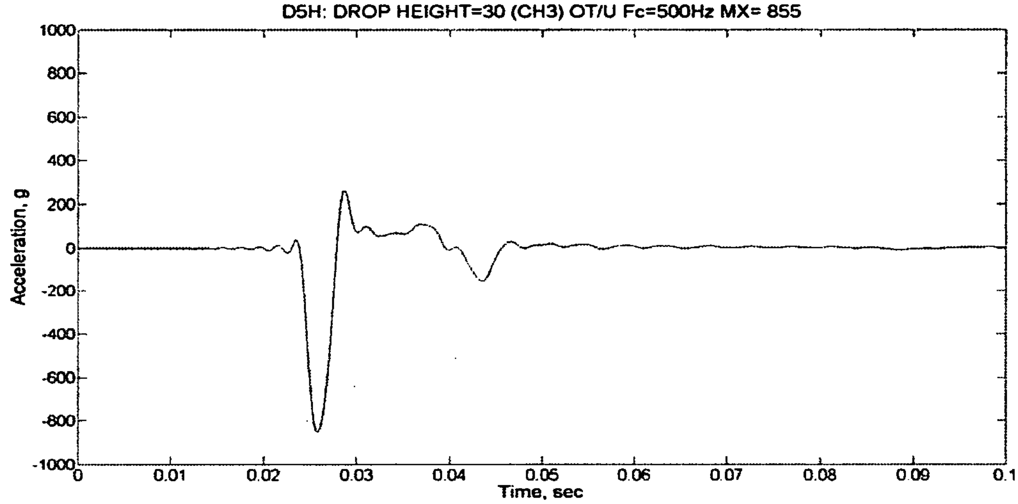

D5H: DROP HEIGHT=30 (CH4) OT/L Fc=500Hz MX= 802

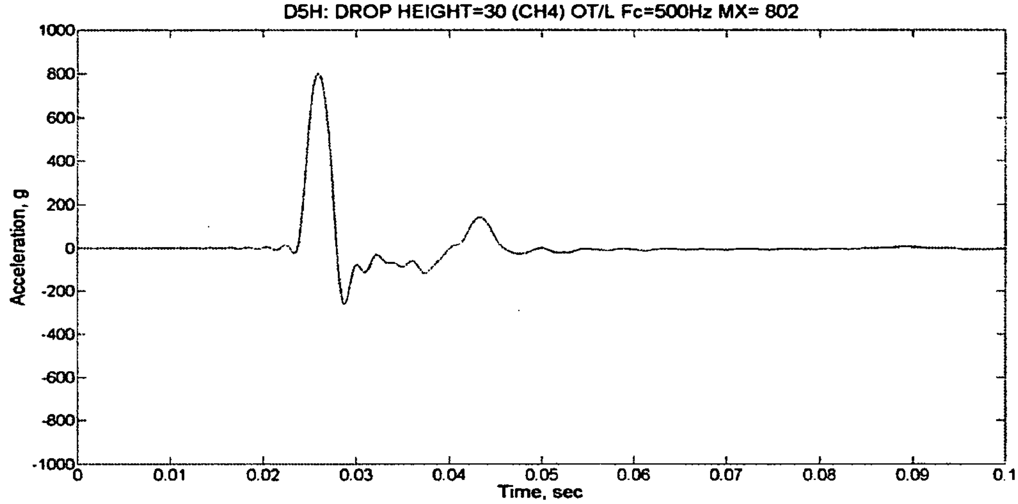

D2N: DROP HEIGHT=4 (CH1) T/U Fc=500Hz MX= 154

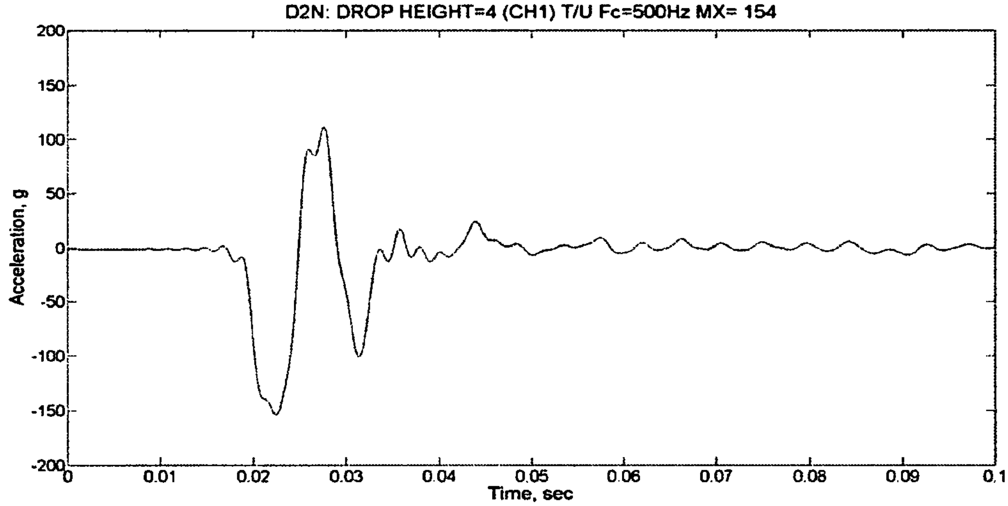

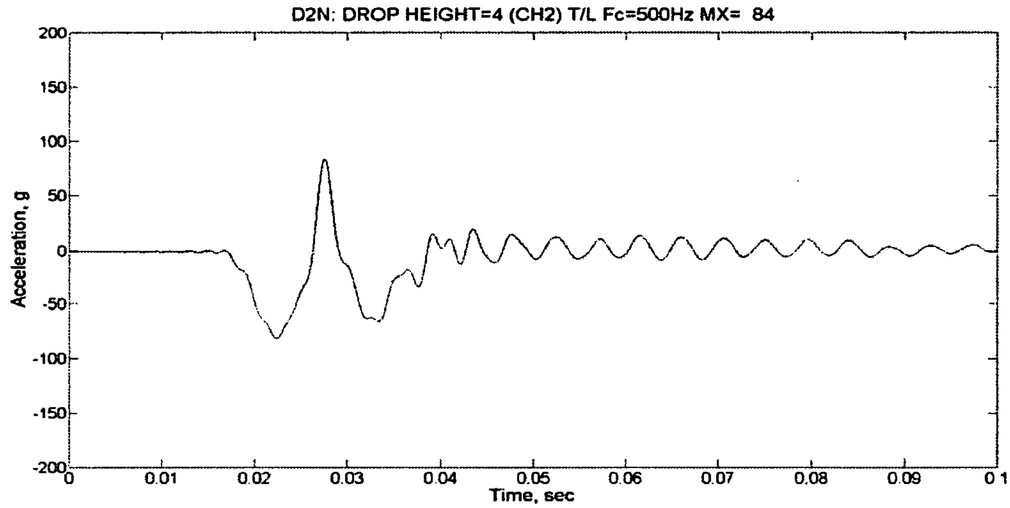
D2N: DROP HEIGHT=4 (CH2) T/L Fc=500Hz MX= 84
Acceleration, g
Time, sec
200
150
100
50
0
-50
-100
-150
-200
0
0.01
0.02
0.03
0.04
0.05
0.06
0.07
0.08
0.09
0.1

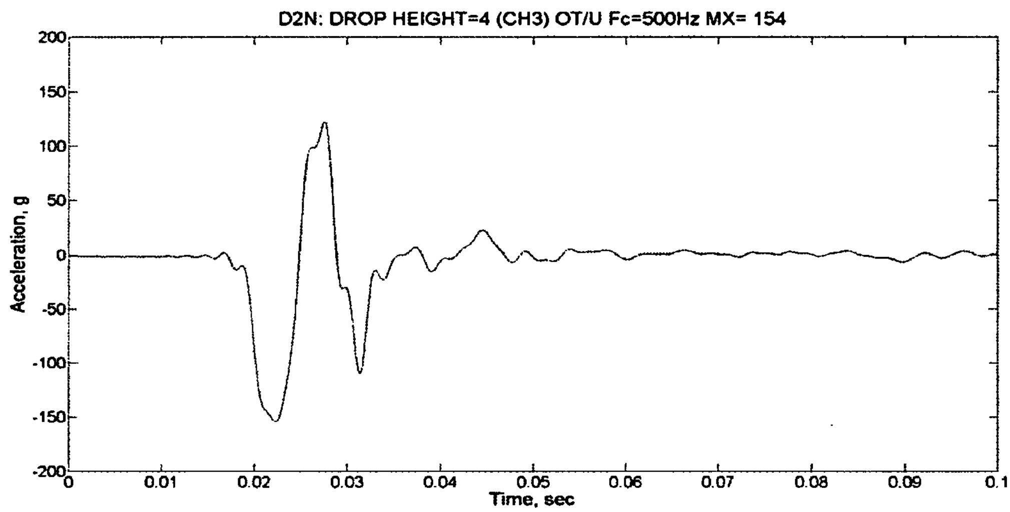
D2N: DROP HEIGHT=4 (CH3) OT/U Fc=500Hz MX= 154
Acceleration, g
Time, sec
200
150
100
50
0
-50
-100
-150
-200
0
0.01
0.02
0.03
0.04
0.05
0.06
0.07
0.08
0.09
0.1

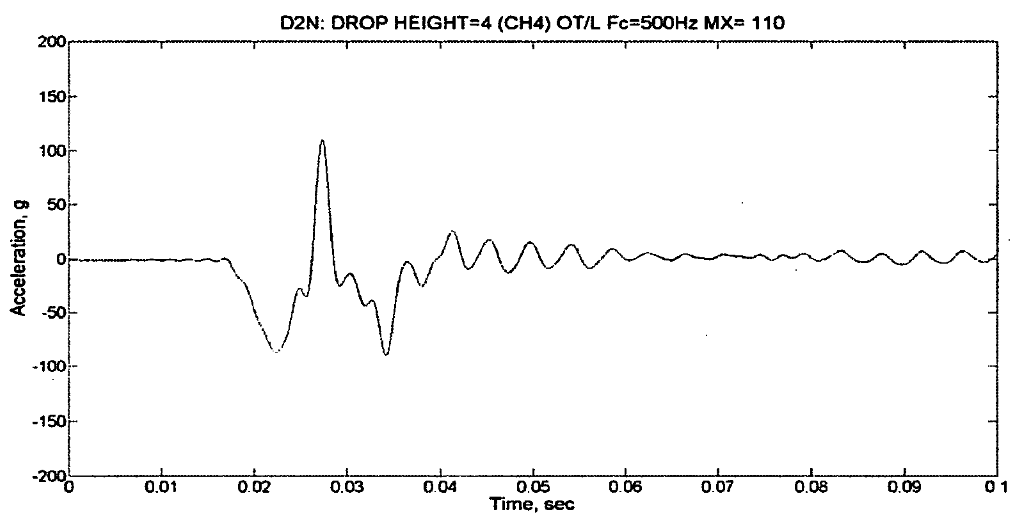
D2N: DROP HEIGHT=4 (CH4) OT/L Fc=500Hz MX= 110
Acceleration, g
Time, sec
200
150
100
50
0
-50
-100
-150
-200
0
0.01
0.02
0.03
0.04
0.05
0.06
0.07
0.08
0.09
0.1

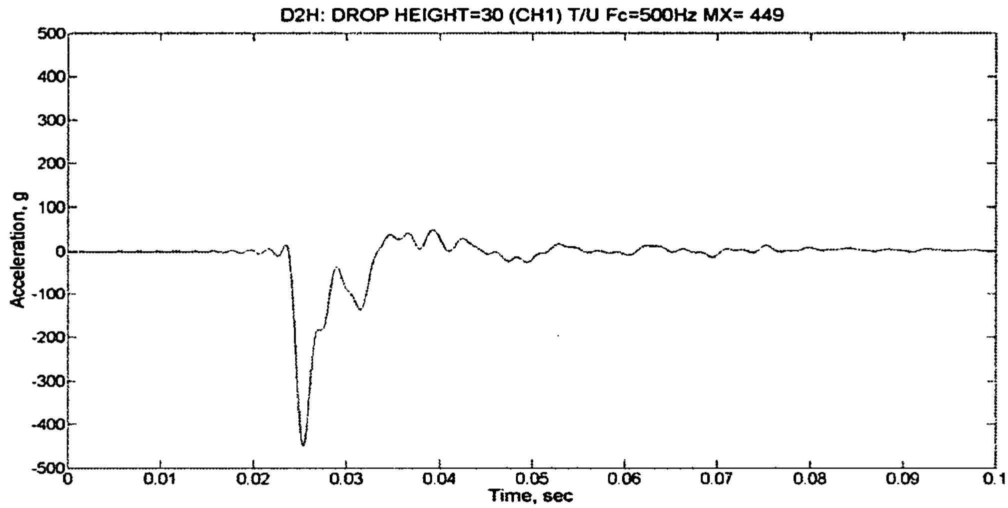
D2H: DROP HEIGHT=30 (CH1) T/U Fc=500Hz MX= 449
Acceleration, g
Time, sec

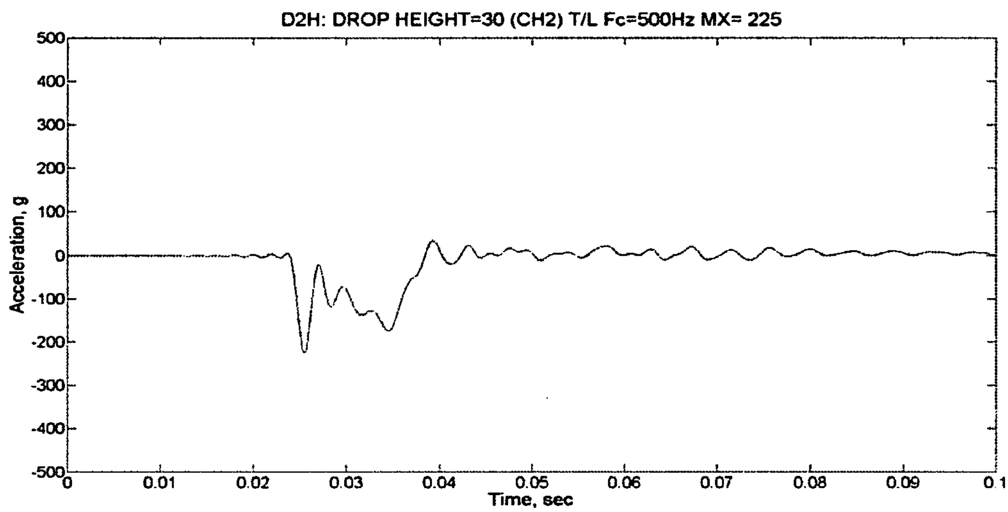
D2H: DROP HEIGHT=30 (CH2) T/L Fc=500Hz MX= 225
Acceleration, g
Time, sec

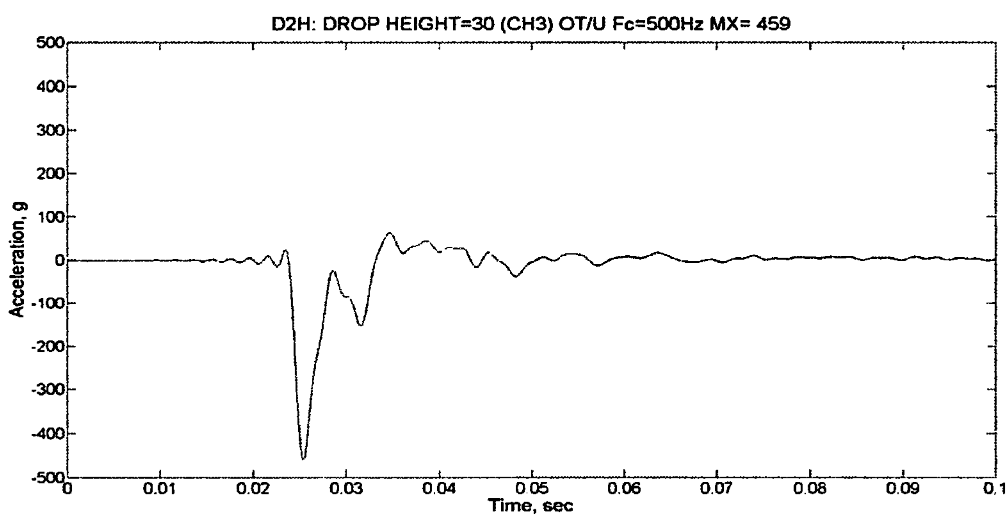
D2H: DROP HEIGHT=30 (CH3) OT/U Fc=500Hz MX= 459
Acceleration, g
Time, sec

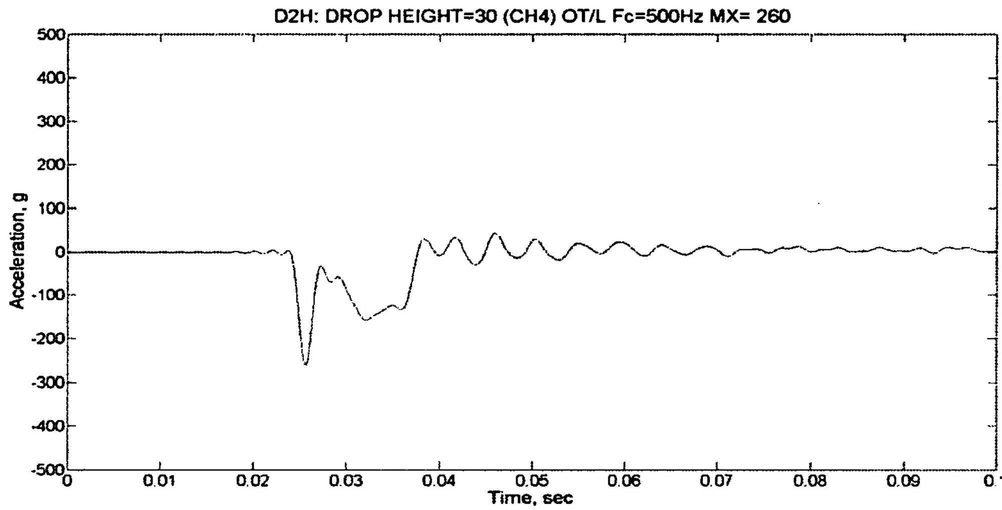
D2H: DROP HEIGHT=30 (CH4) OT/L Fc=500Hz MX= 260
Acceleration, g
Time, sec

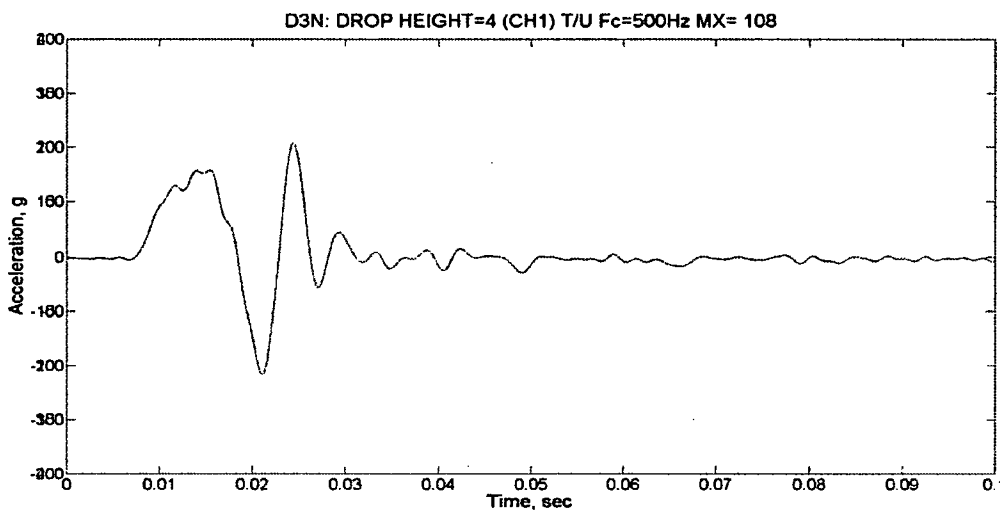
D3N: DROP HEIGHT=4 (CH1) T/U Fc=500Hz MX= 108
Acceleration, g
Time, sec

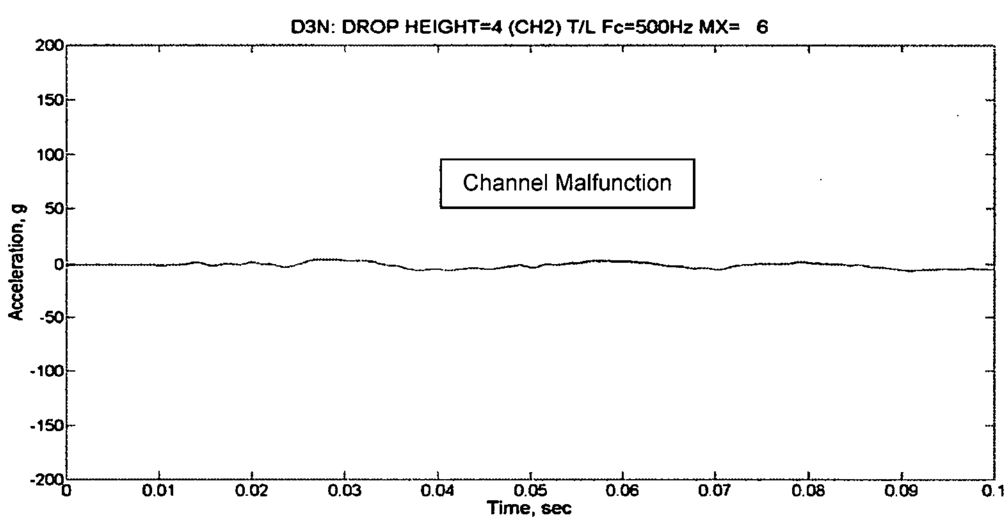
D3N: DROP HEIGHT=4 (CH2) T/L Fc=500Hz MX= 6
Channel Malfunction
Acceleration, g
Time, sec

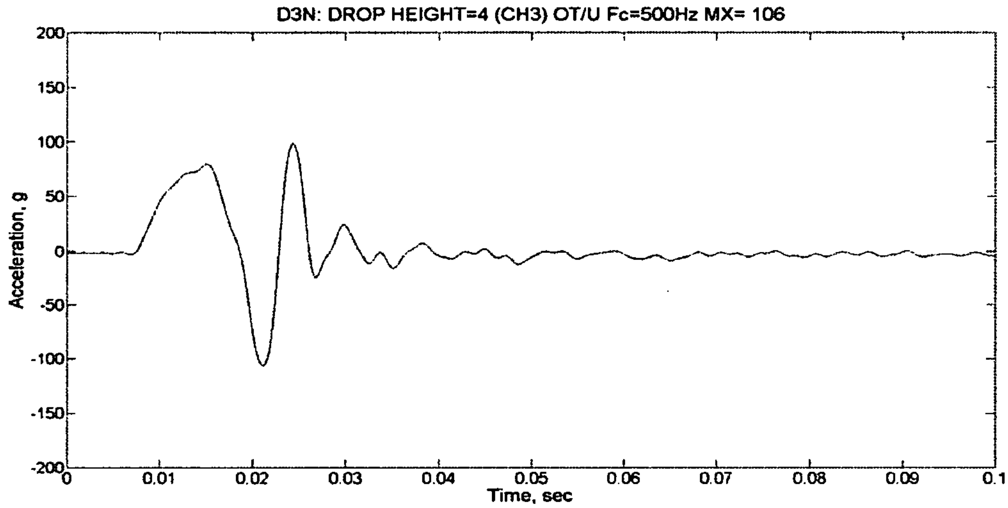
D3N: DROP HEIGHT=4 (CH3) OT/U Fc=500Hz MX= 106
Acceleration, g
Time, sec
200
150
100
50
0
-50
-100
-150
-200
0
0.01
0.02
0.03
0.04
0.05
0.06
0.07
0.08
0.09
0.1

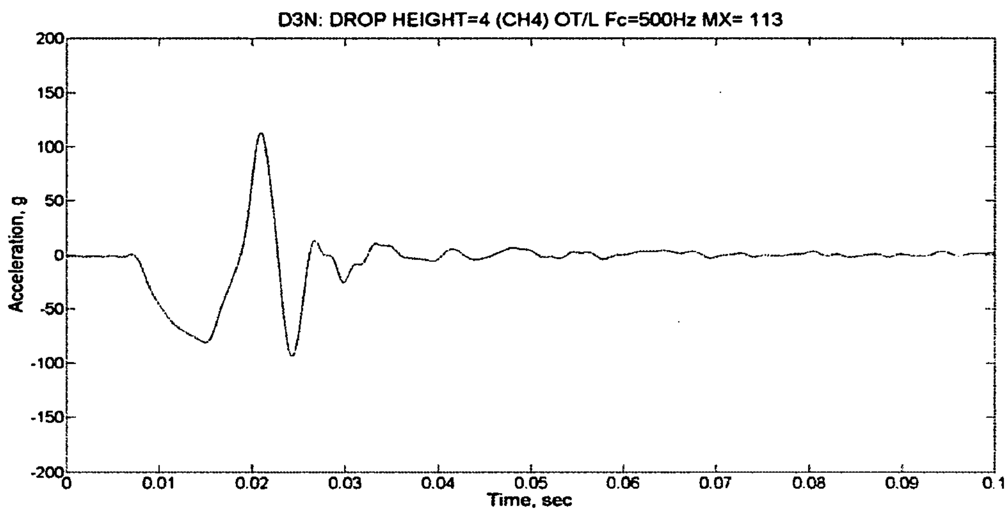
D3N: DROP HEIGHT=4 (CH4) OT/L Fc=500Hz MX= 113
Acceleration, g
Time, sec
200
150
100
50
0
-50
-100
-150
-200
0
0.01
0.02
0.03
0.04
0.05
0.06
0.07
0.08
0.09
0.1

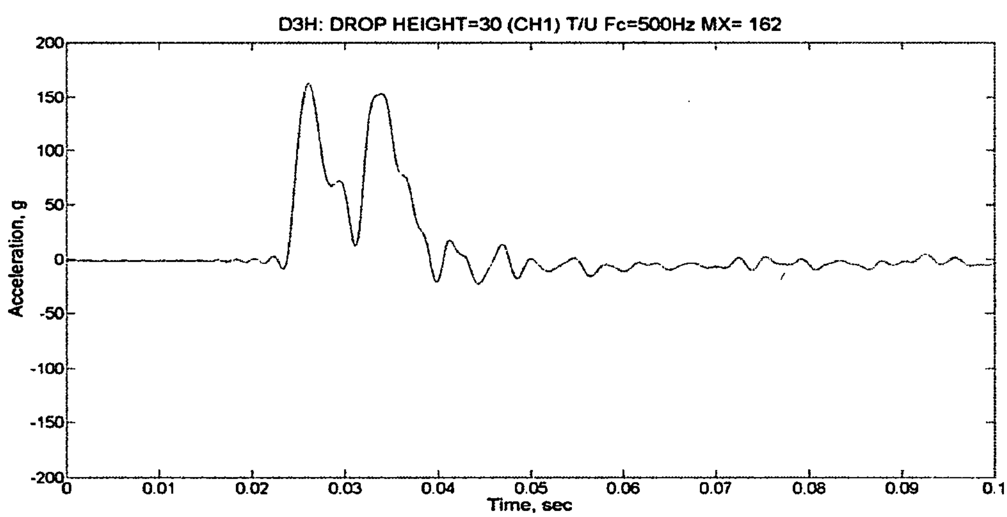
D3H: DROP HEIGHT=30 (CH1) T/U Fc=500Hz MX= 162
Acceleration, g
Time, sec
200
150
100
50
0
-50
-100
-150
-200
0
0.01
0.02
0.03
0.04
0.05
0.06
0.07
0.08
0.09
0.1

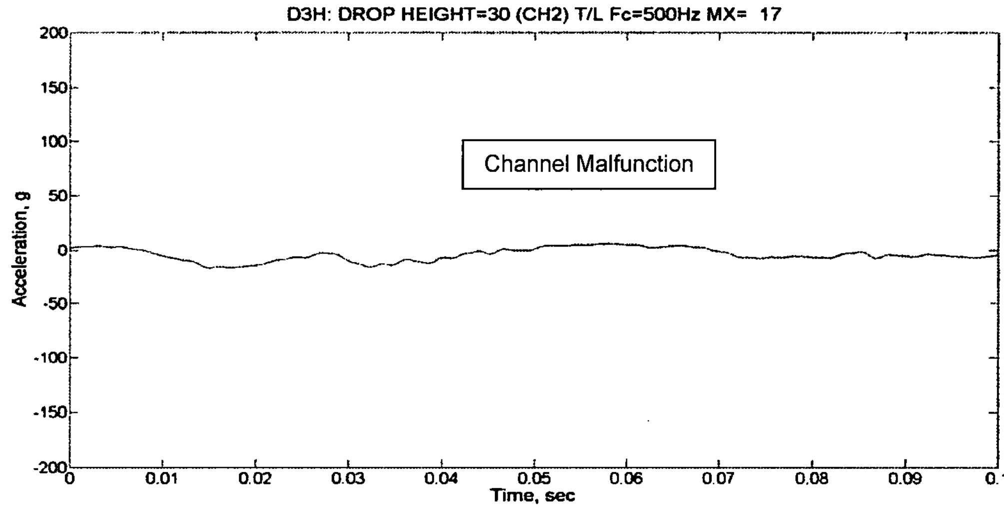
D3H: DROP HEIGHT=30 (CH2) T/L Fc=500Hz MX= 17
Channel Malfunction
Acceleration, g
Time, sec

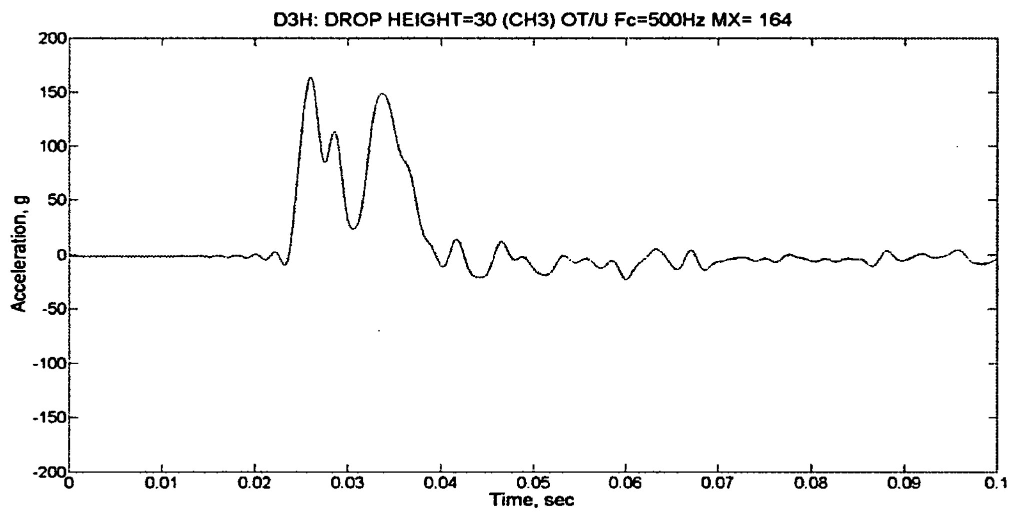
D3H: DROP HEIGHT=30 (CH3) OT/U Fc=500Hz MX= 164
Acceleration, g
Time, sec

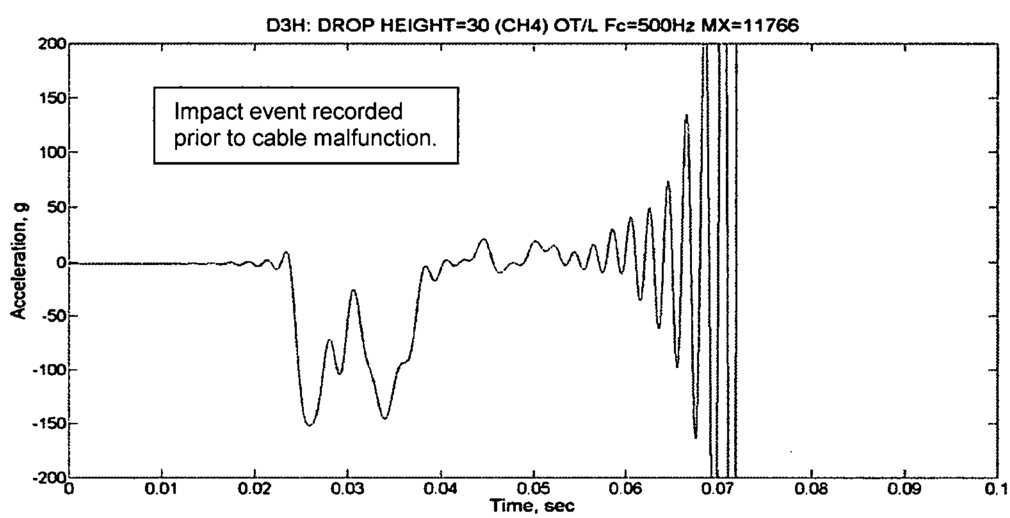
D3H: DROP HEIGHT=30 (CH4) OT/L Fc=500Hz MX=11766
Impact event recorded
prior to cable malfunction.
Acceleration, g
Time, sec

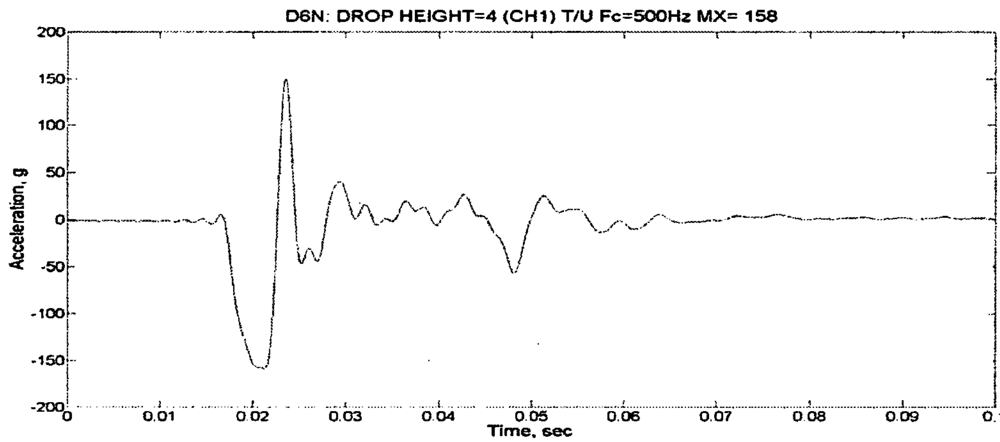
D6N: DROP HEIGHT=4 (CH1) T/U Fc=500Hz MX= 158
Acceleration, g
Time, sec

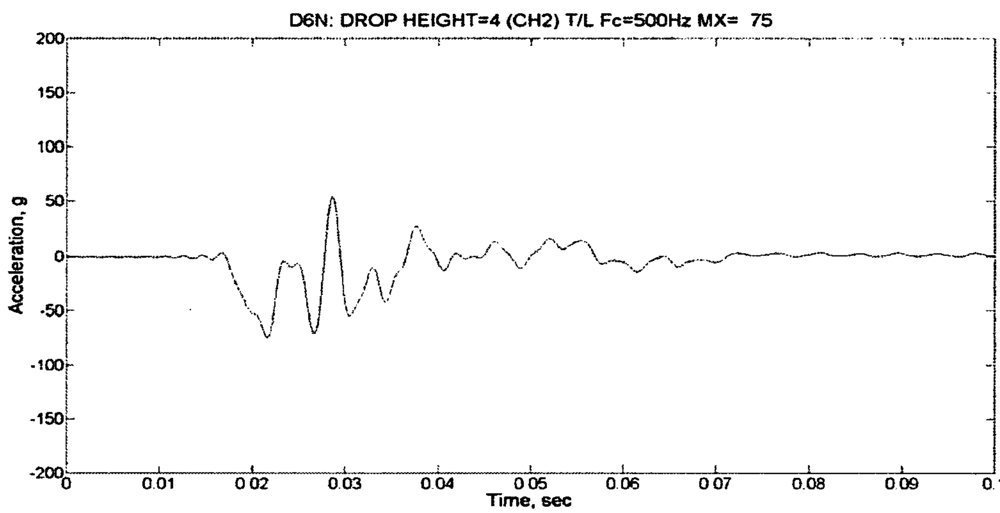
D6N: DROP HEIGHT=4 (CH2) T/L Fc=500Hz MX= 75
Acceleration, g
Time, sec

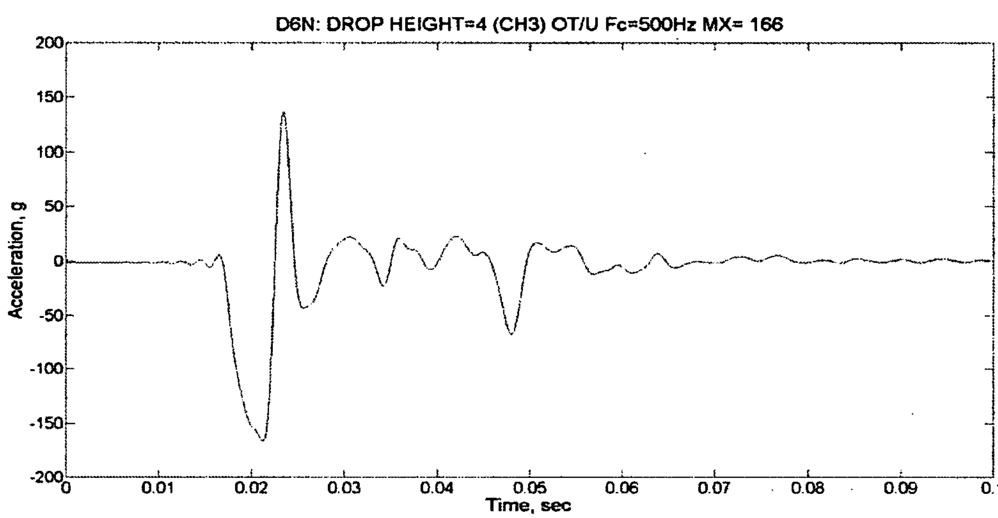
D6N: DROP HEIGHT=4 (CH3) OT/U Fc=500Hz MX= 166
Acceleration, g
Time, sec

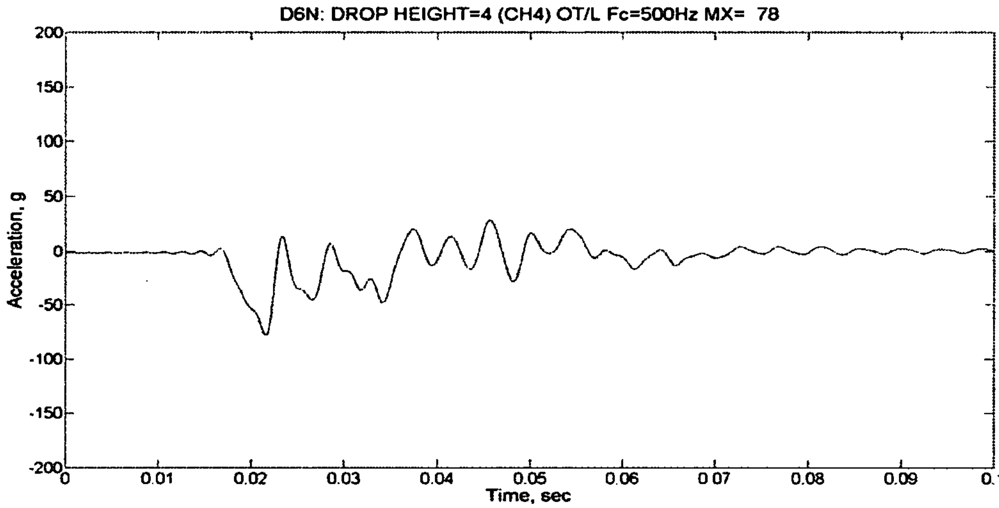
D6N: DROP HEIGHT=4 (CH4) OT/L Fc=500Hz MX= 78
Acceleration, g
Time, sec

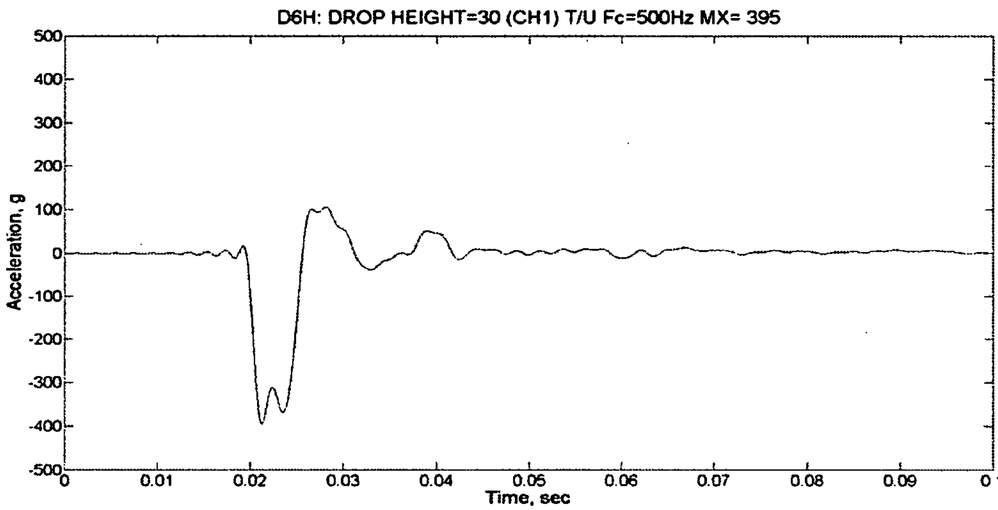
D6H: DROP HEIGHT=30 (CH1) T/U Fc=500Hz MX= 395
Acceleration, g
Time, sec

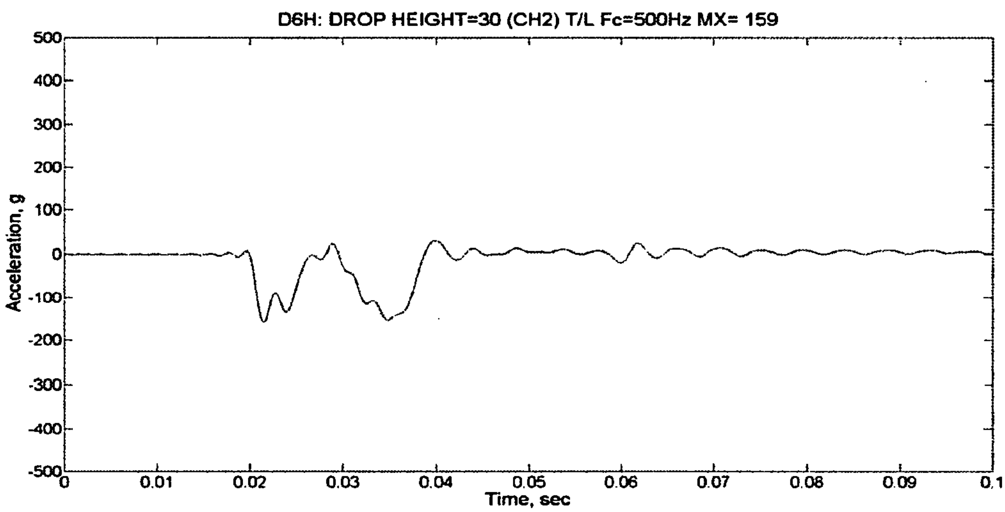
D6H: DROP HEIGHT=30 (CH2) T/L Fc=500Hz MX= 159
Acceleration, g
Time, sec

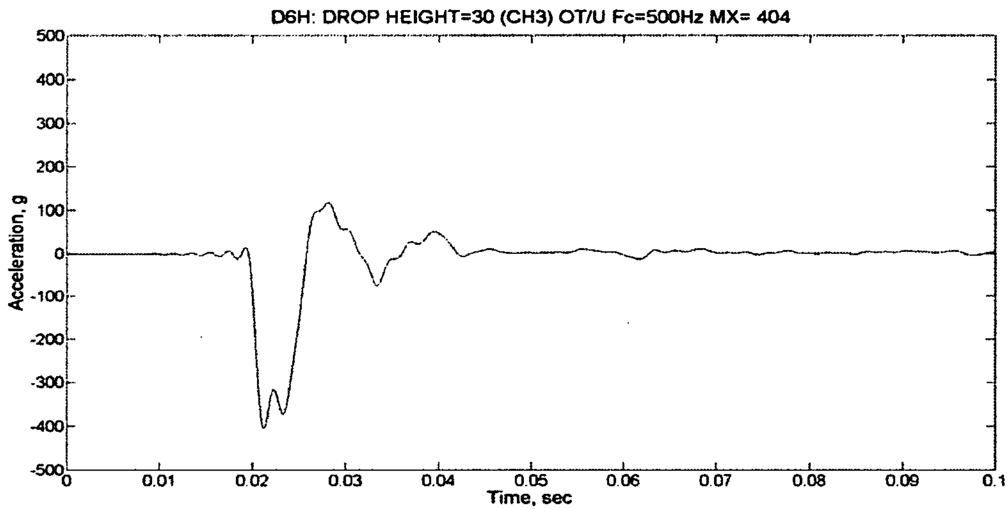
D6H: DROP HEIGHT=30 (CH3) OT/U Fc=500Hz MX= 404
Acceleration, g
Time, sec

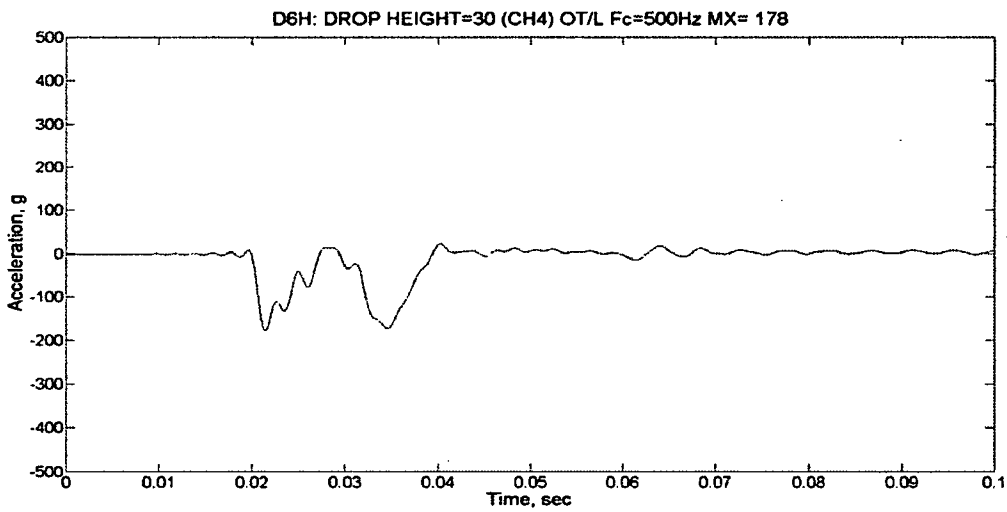
D6H: DROP HEIGHT=30 (CH4) OT/L Fc=500Hz MX= 178
Acceleration, g
Time, sec

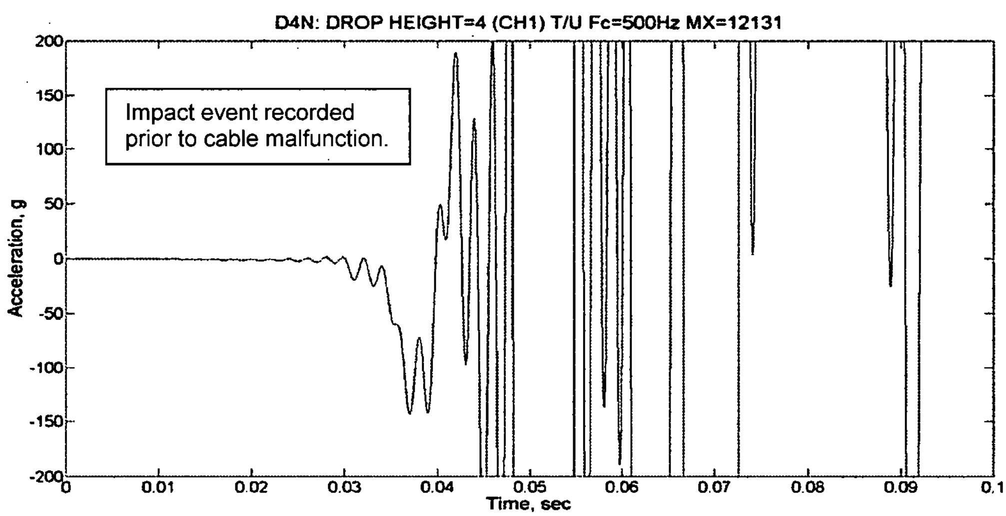
D4N: DROP HEIGHT=4 (CH1) T/U Fc=500Hz MX=12131
Impact event recorded
prior to cable malfunction.
Acceleration, g
Time, sec

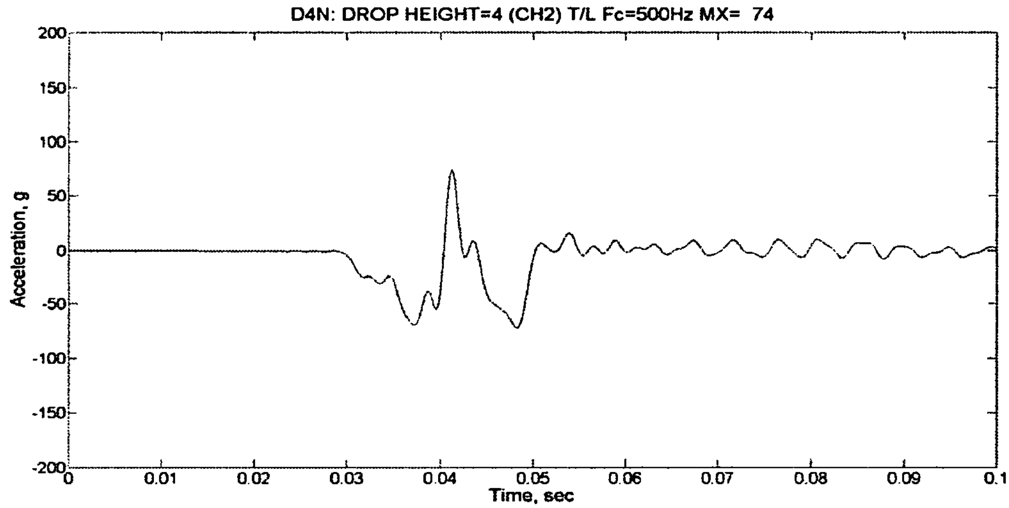
D4N: DROP HEIGHT=4 (CH2) T/L Fc=500Hz MX= 74
Acceleration, g
Time, sec
200
150
100
50
0
-50
-100
-150
-200
0
0.01
0.02
0.03
0.04
0.05
0.06
0.07
0.08
0.09
0.1

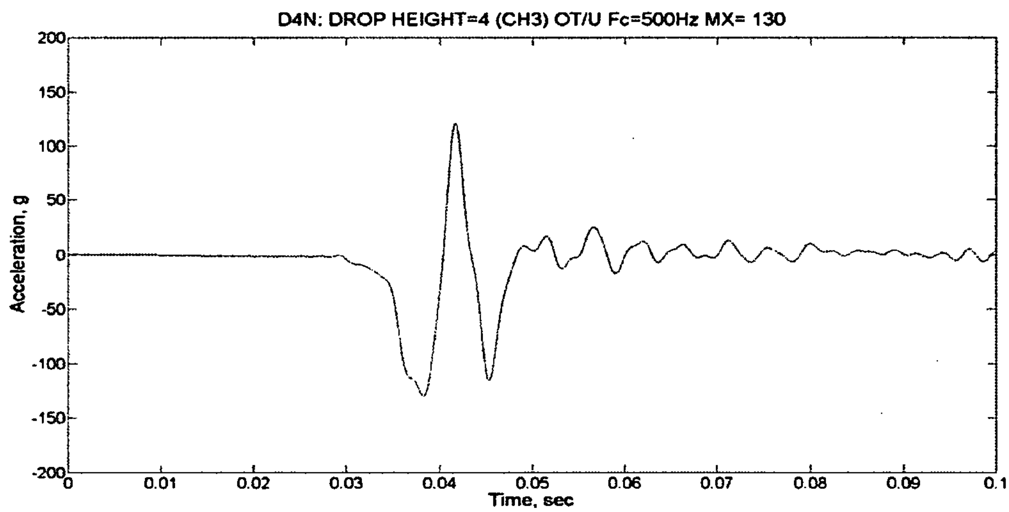
D4N: DROP HEIGHT=4 (CH3) OT/U Fc=500Hz MX= 130
Acceleration, g
Time, sec
200
150
100
50
0
-50
-100
-150
-200
0
0.01
0.02
0.03
0.04
0.05
0.06
0.07
0.08
0.09
0.1

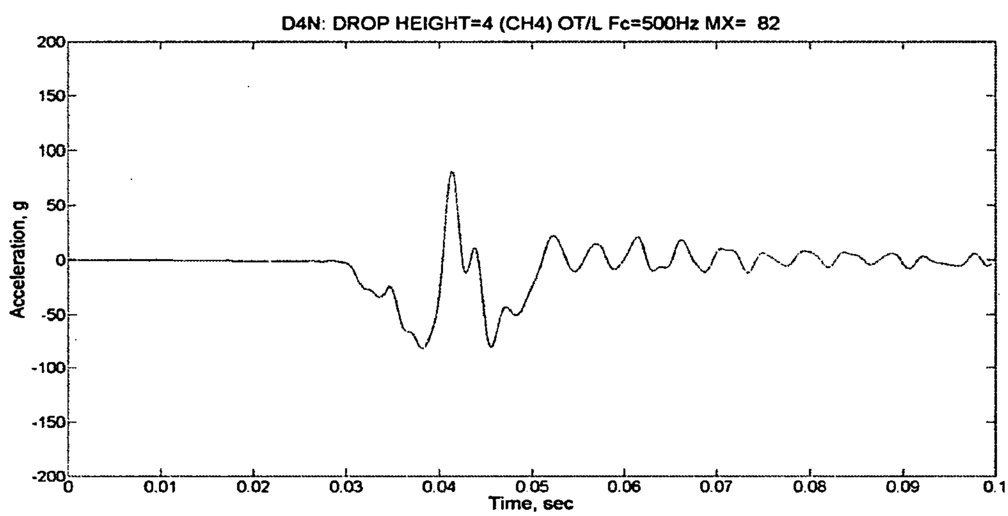
D4N: DROP HEIGHT=4 (CH4) OT/L Fc=500Hz MX= 82
Acceleration, g
Time, sec
200
150
100
50
0
-50
-100
-150
-200
0
0.01
0.02
0.03
0.04
0.05
0.06
0.07
0.08
0.09
0.1

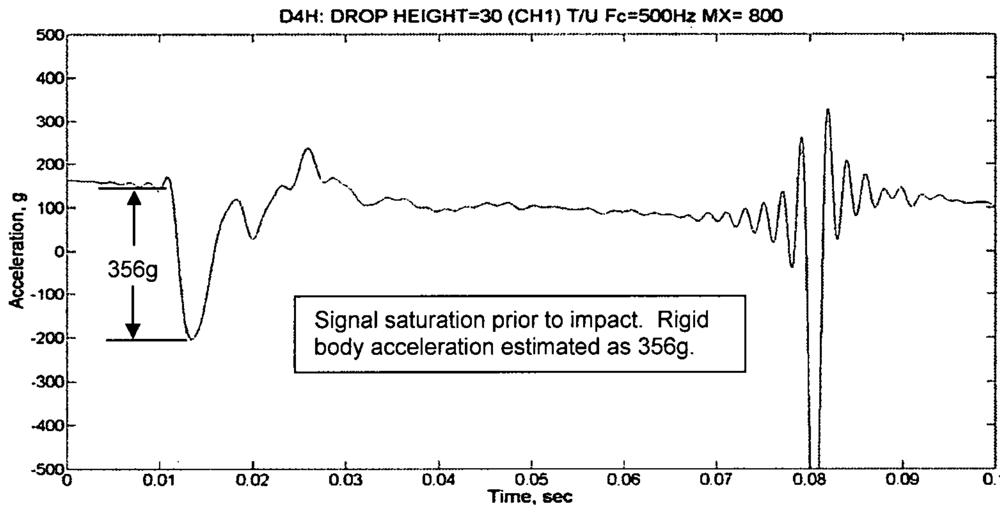
D4H: DROP HEIGHT=30 (CH1) T/U Fc=500Hz MX= 800
Acceleration, g
Time, sec
356g
Signal saturation prior to impact. Rigid body acceleration estimated as 356g.

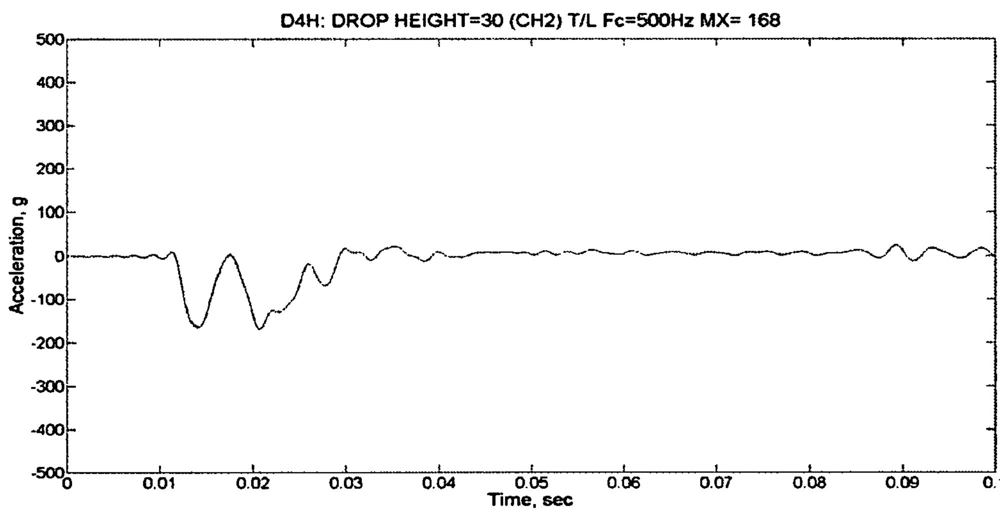
D4H: DROP HEIGHT=30 (CH2) T/L Fc=500Hz MX= 168
Acceleration, g
Time, sec

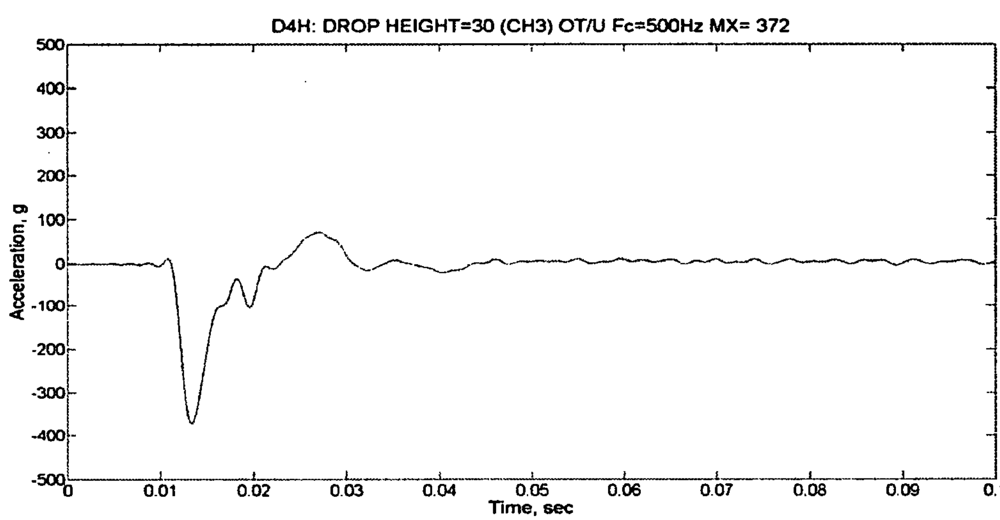
D4H: DROP HEIGHT=30 (CH3) OT/U Fc=500Hz MX= 372
Acceleration, g
Time, sec

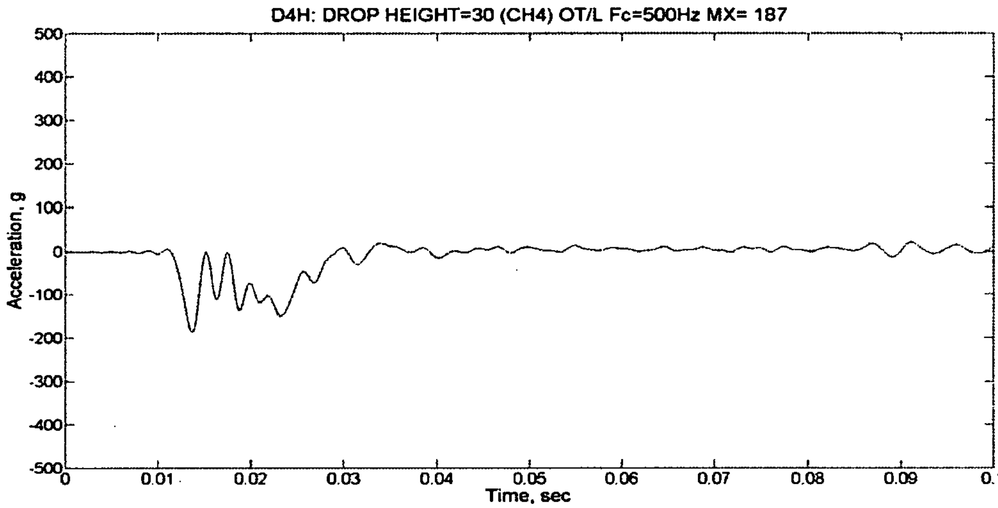

2.12.3.7 References

1. Title 10, Code of Federal Regulations, Part 71 (10 CFR Part 71), *Packaging and Transportation of Radioactive Material*, 01-01-11 Edition.
2. 435-B Certification Test Report, PKG-TR-SPC-011, AREVA Federal Services LLC.
3. ANSI N14.5-1997, *American National Standard for Radioactive Materials – Leakage Tests on Packages for Shipment*, American National Standards Institute (ANSI), Inc.
4. International Atomic Energy Agency, *Regulations for the Safe Transport of Radioactive Material*, TS-R-1.

two distinct drop events. The purpose of applying this simulation method is to limit the number of necessary simulations, thereby decreasing the total calculation computer run time, required data storage space, and post-processing labor while producing reasonable simulation results. The benchmark simulation results in Section 2.12.4.5.1, *Benchmark Results* justify the applicability of this method by comparison with the certification test results. Additionally, one benchmark orientation is simulated with sequential and cumulative, NCT and HAC drops for comparative information.

See Figure 2.12.4-2 through Figure 2.12.4-12 for the FEA model components and mesh. See Table 2.12.4-5 and Table 2.12.4-6 for a summary of the benchmark cases and their respective parameters.

2.12.4.3.1.2 Slapdown (Prototypic) Model

The second phase of the work in this calculation is to take the benchmarked FEA model and perform a series of slapdown free drops to demonstrate the certification test orientations are appropriate for the license application. The benchmark model is slightly adjusted for the slapdown simulations. The primary differences include 1) Weight. The benchmark model uses the as-tested LTSS weight of 4,460 lb, from Table 2.12.3-2, and the slapdown model uses the estimated design gross weight of 4,650 lb, essentially equal to the maximum weight of 4,660 lb from Table 2.1-2, 2) The bell shell and upper torispherical head strength. The benchmark model uses 45 ksi yield strength from the CTU CMTR, while the slapdown model uses 40 ksi yield strength from the SAR drawings in Appendix 1.3.3, *Packaging General Arrangement Drawings*, and 3) The aluminum plate thickness. The benchmark model uses 0.53 inch thick main lodgment plates and internal impact limiter base plates from the CTU fabrication, while the slapdown model uses 0.50 inch thick from the SAR drawings. All the slapdown simulations have the CTU side thermal shield and upper torispherical head thermal shield like the D3 benchmark simulation, i.e., D3_benchmark_302_6JN0.

The different FEA models are grouped in Table 2.12.4-7 with their respective component weights. Note that the "Loaded Package" weight for the slapdown simulations of 9,935 lb is only 1.6% less than the maximum weight of 10,100 lb given in Table 2.1-2. A complete summary of the FEA model components and descriptions is in Table 2.12.4-8, and a complete summary of the FEA model component parameters (material and thickness) is in Table 2.12.4-9. The material references in Table 2.12.4-9 are from Section 2.12.4.2.3, *Material Properties* where the ID # refers to the curves in Section 2.12.4.2.3.2, *Type 304 Stainless Steel (*mat_piecewise_linear plasticity)* and 304 PK refers to the Plastic Kinematic material in Section 2.12.4.2.3.1, *Type 304 Stainless Steel (*mat_plastic_kinematic)*. The foam densities refer to the material curves in Section 2.12.4.2.3.4, *Polyurethane Foam (*mat_crushable_foam)*.

2.12.4.4 Acceptance Criteria

The objective of simulations performed in this calculation is to demonstrate that the certification test orientations performed are appropriate for the licensing basis. The primary method by which this will be demonstrated is comparison of the package free drop accelerations and package impact surface dimensions ("impact patch") between the simulations and the certification test results. The certification test orientations are the worst case and conservatively demonstrate the structural NCT and HAC free drop safety effectiveness of the package. If a governing